



**POLITECNICO DI TORINO**

---

**DEGREE COURSE IN BIOMEDICAL ENGINEERING**  
Master Thesis in BIOPRINTING and TISSUE ENGINEERING

## **Development of Multi-Nozzle Inkjet BioPrinting of Living Cells**

Tutor:

Prof. Dott. Ing. **DEMARCHI DANILO**

Co-Tutor:

Prof. Dott. **NUSSBAUMER ROSELINE**

Student:

**PALMA ADRIANA**

---

ACADEMIC YEAR 2017-2018

***“Science is but a perversion of itself  
unless it has as its ultimate goal  
the betterment of humanity.”***

*Nikola Tesla*



## Abstract

In the field of human health, animal experimentation is the most widespread model used for the development of new drugs, diseases and for risk assessment. Anyway, the in-vitro alternatives regarding these trials are preferable for the following three factors: firstly, the pressures to ban animal testing and to reduce costs in drug development, finally concerns about the significance of animal experiments to model human health.

Nowadays various cell culture models have already produced, however, there is still a significant inter-laboratory variability since the techniques are complex. BioPrinting technology has emerged recently driving innovations in many areas such as medicine by generation of several tissues in a laboratory environment. Although it is stated that bioprinters could revolutionise medical practice, there is a large knowledge gap on the definition of standard protocols and how cells have to be printed for an optimal result.

BioPrinting is expected to provide the means to produce tissues and organs for both research in the pharmaceutical industry and grafts on patients in the future. One drawback of all current printing technologies is their low throughput: it takes several minutes to fill a 6-Well Plate with a single layer of cells using a single-nozzle printhead. iPrint developed a new platform for the printing of living cells using industrial inkjet multi-nozzle drop-on-demand technologies, allowing to reduce that time to seconds.

The aim of this multi-disciplinary project is to start the living cells printing activities on this platform, performing the bioink formulations, based on hydrogel and cell-culture medium, and investigating cells viability after printing on several substrates in different biomaterial, to find the best one and the best printing process to apply with this multi-nozzle technology.

It is a project with high interdisciplinary, based on cells culture, hydrogel fabrication and chemical study for dissolving after printing, improvements of the printing platform and inkjet, dropwatching trials to optimize the drop jetting for different materials, sedimentation velocity study to understand the maximum printing time for each type of cells and viability tests after printing by several different approaches.

## Index

<b>Abstract .....</b>	<b>3</b>
<b>1 Introduction.....</b>	<b>7</b>
<b>2 State of Art .....</b>	<b>9</b>
<b>2.1 Tissue Engineering.....</b>	<b>9</b>
2.1.1 Mimic the Native ECM via Synthetic and Natural Hydrogels .....	12
2.1.1.1 Extracellular Matrix .....	12
2.1.1.2 Hydrogels .....	17
2.1.2 Arranging Tissue Elements by 3D BioPrinting .....	20
<b>2.2 BioPrinting.....</b>	<b>23</b>
2.2.1 Available Commercial Technology .....	25
2.2.2 Fundamentals of Inkjet Printing .....	27
2.2.2.1 Microfluidic .....	31
2.2.2.2 Inkjet Process, DOD Generations.....	40
2.2.2.3 Inkjet Printheads.....	42
2.2.3 Polymers in Inkjet Printing.....	45
2.2.3.1 Polymer Solutions .....	50
2.2.3.2 Van der Waals Attractive Force .....	52
2.2.3.3 Electrostatic Repulsive Force.....	53
<b>3 Cell Culture .....</b>	<b>56</b>
<b>3.1 Working under Laminar Flow .....</b>	<b>58</b>
<b>3.2 Taking Care of Cells .....</b>	<b>65</b>
3.2.1 Medium Change.....	65
3.2.2 Difficulties in Cell Culture .....	67
3.2.3 Cell Passage.....	67
<b>3.3 Trypan Blue and Live/Dead Assay .....</b>	<b>70</b>
<b>3.4 Cells Preparation for Printing.....</b>	<b>71</b>
<b>4 BioPrinting Platform.....</b>	<b>73</b>
<b>4.1 Cleaning Procedure of Printhead.....</b>	<b>78</b>
4.1.1 Pipet Test.....	79
4.1.2 Capillarity Test .....	87
4.1.3 Recirculation Test .....	90
4.1.3 Printhead Test.....	91
<b>4.2 Automatic Pressure Regulation .....</b>	<b>93</b>

<b>4.3 Printing Procedure.....</b>	<b>97</b>
<b>4.4 Stability Nozzle Process and Waveform Optimisation.....</b>	<b>98</b>
<b>5 Preparation of Bioink.....</b>	<b>103</b>
<b>5.1 Viability test with pipet and hydrogel for Rat2 with Trypan Blue method.....</b>	<b>104</b>
5.1.1 First Viability Test for Rat2 .....	105
5.1.2 Second Viability Test for Rat2 .....	106
5.1.3 Third Viability Test for Rat2 .....	108
<b>5.2 Test for different Types of Hydrogel remaining in Viscosity Range for Fibroblast 3T3 ...</b>	<b>110</b>
5.2.1 Viability Tests with Fluorescent Microscope .....	111
5.2.2 Viability Tests with Trypan Blue.....	114
<b>5.3 Viability Tests for Lung Epithelial Cells A549 with Trypan Blue Method .....</b>	<b>117</b>
<b>5.4 Sedimentation Tests for Cells .....</b>	<b>119</b>
5.4.1 Sedimentation Theory .....	119
5.4.2 Aggregation .....	122
5.4.3 LDVO Theory.....	123
5.4.4 Sedimentation Velocity .....	124
5.4.5 Neutral Buoyancy .....	124
5.4.6 RLCA aggregation .....	125
5.4.7 Algorithm Development and Test with PMMA and results .....	126
5.3.8 Sedimentation Tests with only DMEM and Hydrogel .....	129
5.4.9 Sedimentation Test for Rat2 .....	130
5.4.10 Sedimentation Test for Fibroblast 3T3.....	133
5.4.11 Sedimentation Test for Lung Epithelial Cells A549 .....	135
<b>5.5 Test and Optimization of the Best Printing Process for Cells.....</b>	<b>136</b>
<b>6 Results of Viability and Reliability .....</b>	<b>138</b>
<b>6.1 Printing Fibroblast 3T3 and Viability Tests.....</b>	<b>138</b>
6.1.1 Print in DMEM.....	139
6.1.2 Print in Hydrogel .....	142
6.1.2.1 Viability Tests with Trypan Blue and Confocal Microscope .....	143
6.1.2.1 Viability Tests with LIVE/DEAD ASSAY and Fluorescent Microscope.....	146
<b>6.2 Printing Lung Epithelial Cells A549 in DMEM and Viability Tests .....</b>	<b>149</b>
6.2.1 Print in DMEM on Petri Dish.....	149
6.2.1 Print in DMEM on Different Substrates.....	151
6.2.1.1 Viability Tests with Trypan Blue and Confocal Microscope .....	152
6.2.1.2 LDH Tests.....	154

<b>7 Conclusions and Future Perspectives .....</b>	<b>160</b>
<b>8 Figure Index .....</b>	<b>162</b>
<b>9 Bibliography .....</b>	<b>167</b>
<b>10 Appendix.....</b>	<b>172</b>
<b>10.1 Pressure Regulation Arduino.....</b>	<b>172</b>
<b>10.2 Final Code with Pressure Regulation Matlab .....</b>	<b>176</b>
<b>10.3 Sedimentation Test.....</b>	<b>181</b>
<b>10.4 Sedimentation Test Tables .....</b>	<b>183</b>
<b>10.4 Materials used in This Master Thesis.....</b>	<b>186</b>
<b>11 Acknowledgments.....</b>	<b>187</b>

# 1 Introduction

Biorpinting is a multidisciplinary field based mainly on the printing of materials related to life: this broad sector, in fact, concerns the printing of natural or biocompatible polymers, and of cells, DNA, RNA, proteins or elements inherent to the biological sphere.

The aim of the present project is to investigate its possible use in industries; the high-throughput multi-nozzle printhead would allow to create or manufacture 3D or 2D tissues models in a reliable and fast way.

Before being able to find the actual formulation of the bioink for each type of cell used, it was necessary to investigate different fundamental aspects of BioPrinting.

In this project, it was decided to formulate two different types of bioink based on different materials and mammalian cells, in particular a type of mouse fibroblast and a type of human tumour epithelial cell.

First of all, since the BioPrinting Platform needed improvements, an automatic pressure regulator was designed and implemented to regulate the pressure inside the multi-nozzle printhead automatically, by setting different values for each type of bioink used. Furthermore, an automatic algorithm to calculate cell sedimentation rate in different bioinks has been implemented and optimised through different simulations and tested using a camera already positioned on the BioPrinting Platform to perform Dropwatching.

Chemical tests were required to simulate the printing process to investigate the hydrogels used and their dissolution to ensure that they will not block the printhead nozzles during the printing process.

In this study, therefore, for each type of cells, first of all a study of viability was made looking for the suitable matrix or hydrogel, in which the cells survived in greater number, simulating by pipet the printing process.

Once the bioink has been found, which gives the best percentage of cellular viability, tests have been performed for each cell type and scaffold material, related to the speed of cell sedimentation in each material and dropwatching, optimising the parameters and finding the waveform standard, to be sent to the transducer in the printhead, for each material used.

Finally, thanks to the parameters found in the printing simulation tests, it was possible to define a printing protocol for two types of cells in two different materials, on different substrates designed specifically for the multi-nozzle inkjet platform developed at the iPrint Institute. Cell viability tests have been made following the printing process in three different ways: Trypan Blue, Fluorescence and LDH test.

## 2 State of Art

### 2.1 Tissue Engineering

Tissue Engineering is an interdisciplinary field of research and clinical applications whose purpose is the reparation and/or regeneration of organs/tissues in order to restore their lost functionality due to diseases, trauma and aging. [1]

The essential principle is collecting cells from the patient: it is possible to take either cells that are already differentiated and belong to the tissue that needs to be repaired, or stem cells. Then, they are usually grow into a culture flask, increasing them in number and proliferating. Eventually, seeding cells on a three-dimensional construct brings them to colonize it, only if it is well-formed: if it happens at the end of the process, this will result in a bio-hybrid tissue. The bio-hybrid tissue looks like a real tissue and is obtained with an engineering approach that has implicated the choice of suitable cells and the construction of a good scaffold to let them grow. [2]

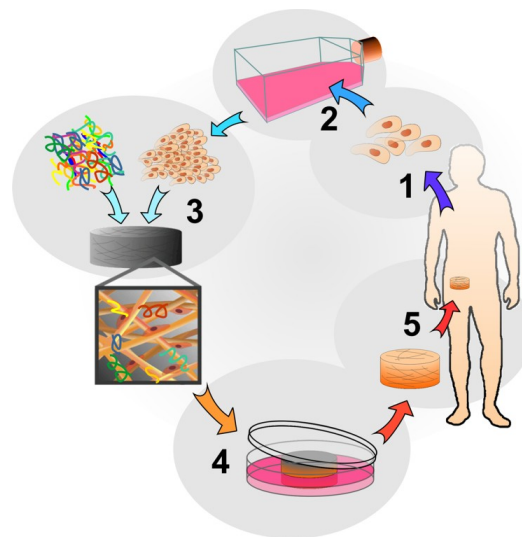


**Figure 1: Tissue Engineering Concept:** The classic TE approach (1) harvests cells from the patient and (2) expand them in-vitro. Upon sufficient expansion (3) cells are seeded on a scaffold contingently with growth factors. (4) The construct is then matured in-vitro before (5) being implanted in the patient. [3]

Tissue engineering consists in merging the cells with a scaffold, a bioreabsorbable porous three-dimensional support capable of guiding their behaviour. It is necessary to use these scaffolds

because not all tissues have regenerative capacity (reconstitute parts of an injured or lost organism) even though stem cells exist within the tissues. In fact, for example, the nervous tissue and the myocardium, if damaged, do not regenerate but repair (restore a damaged part of a tissue) themselves. **Figure 1**

In conclusion, tissue engineering is useful for those tissues that have a very low regenerative capacity but can also be good for tissues that renew spontaneously with a large amount of damage that can compromise regenerative tissue capacity.

The help that tissue engineering can give is a porous scaffold, made up of bioactive materials. A bioactive material is different from an inert one because an inert material has no communication with the biological environment, although it is not toxic due to the fact that it is always maintained without physical or chemical alterations. A bioactive material communicates with cells, adhering to them, allows their differentiation guiding their behaviour and it could also have alterations after being implanted: in this sense, it is a temporary support because cells colonize the scaffold and then gradually the scaffold disappears. [4]

There are two approaches to tissue engineering: *in vitro* and *in vivo*. In *in vitro* used scaffolds are seeded with cells and are cultured either statically, without any stimulation, or in a bioreactor, i.e. in a biomimetic stimulation system, without the proper tissues stimulation. Then, in the bioreactor, cells colonize the scaffold as it gradually degrades. These types of tissues can then be used in two ways: one consists in the creation of *in vitro* tissue models with pathologies for the study of new therapies, the other in the fabrication of tissues that can be subsequently implanted.

In the *in vivo* strategy, there are various possible approaches to act within the body. There are two fundamentals for which a cell-free scaffold or one with cell can be implanted. If a scaffold with cells is installed, there are many steps to follow: to design the scaffold, to seed it with the cells and then to implant it. So, on a practical level, there are two methods: in one, a scaffold is designed then seeded and implanted, in the other the scaffold is designed, implanted and kept in the bioreactor so that cells can penetrate and begin to create the extracellular matrix which should be subsequently implanted. In both cases, what is technically called "CONSTRUCT", scaffolds and cells, with or without preculture, is implanted.



To create a bioengineered tissue, it is necessary to make it as close as possible to the original one, from the histological, morphological and biochemical point of view. There are three variables to consider:

- **SCAFFOLD:** to choose the material, the architecture, the porosity and the shape;
- **CELLS:** in-vitro or in-vivo approach, which cell-type use;
- **REGULATOR ELEMENTS:** Everything used to guide cell behavior, which can be introduced into the scaffold, for instance as molecules that induce recruitment, adhesion or differentiation of cells into a bioreactor by introducing mechanical stimulation or in vitro using a culture medium enriched with growth factors.

Subsequently it is important to consider the tissue to regenerate: some of them have spontaneous regenerative capacity, such as skin and bones, while others have very scarce regenerative capacity, such as the heart and nervous tissue. So, the approaches are different and they depend on the tissue chosen to regenerate.

The features, that a **scaffold** must have, are:

- **POROSITY:** the correct choice of the porosity is important to let cells penetrate inside the scaffold, to let them reach the nutrients and to remove the waste materials. Moreover, it must have dimensions comparable to those of the original tissue and it also serves to ensure angiogenesis (blood vessel formation process), which is simplified if a bimodal porosity (porosity that allows the exchange of substances in the two directions of entry and exit through the wall of the vessel) is introduced, because smaller pores are reserved for the aforesaid process: for example, vessel cells are very small, so they easily penetrate;
- **MECHANICAL PROPERTIES** are influenced by porosity, but also by material and architecture. They are important because cells are affected by the mechanics of the substrate on which they are placed, so as to differentiate cells as desired;
- **BIODEGRADABLE AND RELIABLE:** the rate of degradation must be equal to the essential to the reformation of the tissue;
- **SUPERFICIAL CHEMISTRY:** the entire surface where cells come into contact, because through it, cells communicate with the scaffold and therefore they tend to make it functional to make cells, as they want, and to adhere to them;
- **SIMILAR TO REALIZE AND REPRODUCTIVE;**

- **BIOCOMPATIBILITY** should not induce an inflammatory response and also the materials of degradation must be well tolerated by the body.

Biomaterials in which the scaffold is made must be biocompatible, biodegradable or bio-reabsorbable and bioactive. The choice of biomaterials usually falls on polymeric or ceramic materials; ceramics, or polymer-ceramic composites are used when the scaffold should have strong mechanical properties such as resistant to compression or rigidity, as for bone.

The polymers that can be used are natural ones, proteins or polysaccharides, or biocompatible and biodegradable synthetic polymers. [5]

### 2.1.1 Mimic the Native ECM via Synthetic and Natural Hydrogels

Tissues are formed by cells and extracellular matrix (ECM), which has not only common characteristics between various tissues, but also distinctive features. It is necessary to know main components of the ECM to mimic its features and thus to create interactions between the cells or between cells and the ECM. Depending on its composition, the ECM can perform different functions such as cell support and their anchorage to the matrix and differentiation between different tissues.

#### 2.1.1.1 *Extracellular Matrix*

The Extracellular Matrix or ECM is the most complex unit of tissues structural organization in living organisms. Tissues, in fact, are not only made up of cells: a significant part of their volume is formed by extracellular space, occupied by an intricate network of macromolecules, the three-dimensional organization, precisely the ECM. Biochemical analysis of the ECM reveals that it is made up of proteins and polysaccharides plethora, which organises in a compactly arranged reticulum and connects to the cells surface, that produced it, and surrounds cells.

Cell anchorage occurs through interactions between the ECM and membrane proteins, called glycol-receptors, belonging to the integrin family. Through these molecular bridges, ECM

variations can transmit mechanical stimulation and affect the organization of the cytoskeleton; likewise, the cytoskeleton may induce changes in the ECM.

Often, the ECM plays a role in the intercellular recognition regulation process, allowing cellular receptors to function properly, such as neuron and molecules adhesion.

It has two types of functions depending on the type of tissue: in the connective tissue, the matrix abounds and the cells distribute them scattered; in the epithelial one, the ECM is poor and most of the volume is occupied by the cells.

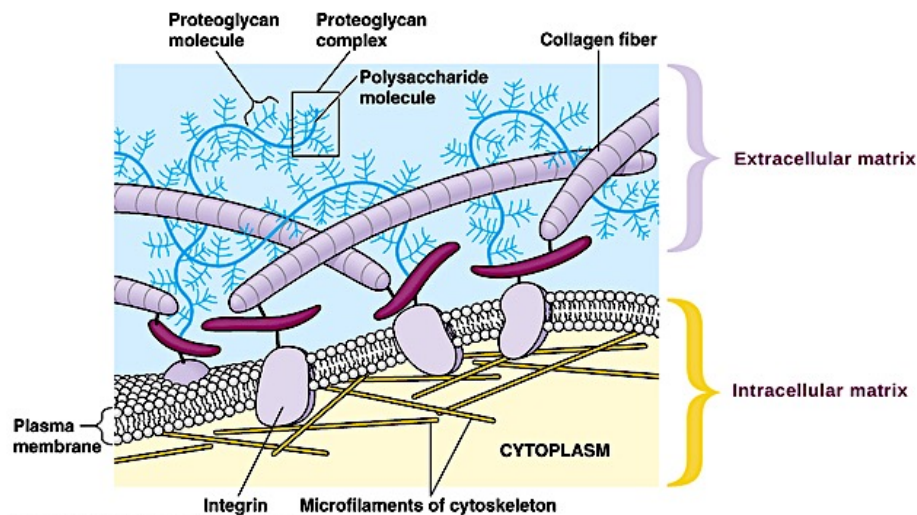


Figure 2: Schematic of various components of ECM. [6]

Some proteins located in the membrane of the cells emerge outside them, preserving a portion inside, so they are internally linked to cytoplasmic proteins: these proteins, that communicate with the outside of the cell, are called *extra-membrane proteins*. Because they come out of the membrane, they do not have a purely chemical protein composition (poly-amino acid) but they are also formed by oligosaccharide portions. **Figure 2**

These protein portions, coming out of the cell membrane outwardly, are used as *receptors* because they exchange signals with the rest of the surrounding world.

ECM is composed of proteins and polysaccharides. Part of it has the structural task, consisting of proteoglycans that are large molecules mixed protein-polysaccharide, which give a viscous/viscoelastic characteristic to the ECM. Another part of the ECM contains proteins; it takes on a functional task thanks to extracellular matrix proteins.

Extracellular matrix proteins can be grouped into 3 groups [3]:

- structural proteins like collagen and elastin;
- specialized proteins like fibronectin, laminin and fibrillin that play a role in interaction and cell communication;
- glycosaminoglycans and proteoglycans. [7]

The structural proteins are:

- **COLLAGEN**: it gives traction resistance to the matrix. It is a protein made up of amino acids, especially there are three repeated regularly in collagen, glycine, proline and hydroxyl-proline, so there is a constant chemical structure. At the 3D level structure, there is a left-handed propeller stabilized by hydrogen bonds. Three propellers of this type tend to combine themselves, composing a super-straight right structure, called super-helix and formed by three  $\alpha$ -propellers that interweave triple helix or tropo-collagen equally; after the aforesaid process the three propellers are stabilized and there are sometimes covalent bonds, ionic interactions, hydrogen bonds. **Figure 3** Tropo-collagen molecules have a subsequent organization, they create fibrils, where the various triple propellers are arranged in parallel rows with a spacing between them, then the successive propellers will maintain the same spacing and in addition to they will be offset from the first series.

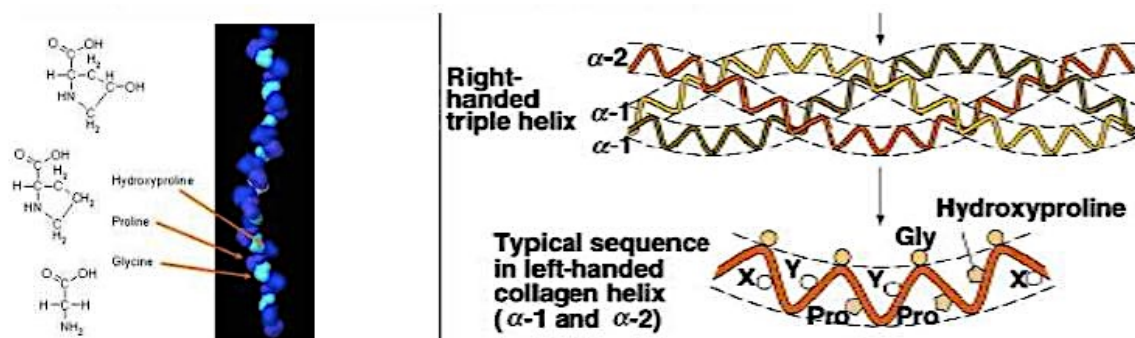


Figure 3: Collagen chain [3]

This arrangement is typical for collagen molecules and the spacing is typical for the tropocollagen, with precise dimensions between one row and the other. This structure is set by crosslinking, covalent bonds. Collagen fibrils have a nanometric diameter: more fibrils organize themselves by creating collagen fibers. If there are no fibrils in the

collagen it is because it has been denatured by malignant treatments, aggressive solvents, etc.

- **ELASTIN:** it gives elasticity and deformability characteristics to the tissue and it is therefore typical of very elastic tissues such as blood vessels, skin and lungs. As a protein, it is made up of amino acid chains, the most abundant amino acids are always proline and glycine. Elastin, which has hydrophobic characteristics, has a relaxed structure based on transverse chains of amino acids linked by bridges. When elastin is in relaxed form, the chains have a statistical elbow structure, instead when they are stretched they tend to roll out and undergo orientation. The various chains do not slip on each other because they are blocked by transverse ties.

The specialized proteins are [3]:

- **FIBRONECTIN:** It is one of those proteins that serve to establish the communication between the extracellular matrix and cells. It is made up of two chains (a dimer) tied to one end. These chains have different regions, each of which interacts with something, some with collagen, others with heparin, others with cells.
  - **LAMININE:** It has a different structure but a similar role to that of fibronectin. It is made up of three chains: there is an area where they are enveloped to form a triple helix and a central part where they are tied covalently with one another. Even if these chains have different regions with different peptide sequences, they interact with molecules or cells. The laminin is abundant in the laminate baseline.
  - **FIBRILLIN:** High molecular weight protein constituting 10 nm of diameter of microfibrils, which play an important role in the aggregation of the extracellular matrix of the elastic fibres: they appear before elastin, during development, to form a skeleton on which secreted elastin molecules are deposited. Subsequently, the microfibrils are moved to the periphery of the growing fibre and form a sheath around the resin elastin.
- [8]

Collagen and elastin have not only a structural function, but they can also bind cells: in this case, they are under the name of structural proteins because they are the primary responsible for the mechanical properties of the matrix.

- **GLYCOSAMINOGLYCAN (GAGs):** The basic units are disaccharide and they have a linear structure with common elements: di-acid base unit, whose one of the two has amino groups, so it is an amine. Another characteristic feature of the GAGs is that they have a negative charge, which gives them a linear conformation, generally due to the presence of carboxyl or sulphate groups. Therefore, GAGs are linear amine polymers negative and hydrophilic. Generally, they do not live on their own but are bound to proteins to form proteoglycans.
- **PROTEOGLICANS:** They are the real hetero-polysaccharides because they have disaccharide units from GAGs and a protein portion, which they bind to. The structure is similar to a tree: at the centre, there is the protein connected to GAGs, structured in a linear way for their charge. They are hydrophilic molecules, so they absorb water to hydrate the matrix, where there are many proteoglycans which, interwoven with each other, keep the matrix very well hydrated thanks to pores and their wall inside negative charged for the presence of the GAGs. For all these reasons, the proteoglycans have the function of sieve, that is, they make just pass some molecules or some cells depending on the size of the pores and the charge of molecules or cells. Another function of proteoglycans is that these very high molecules tend to interact with signal molecules that are secreted by cells, such as growth factors or enzymes. *Figure 4*

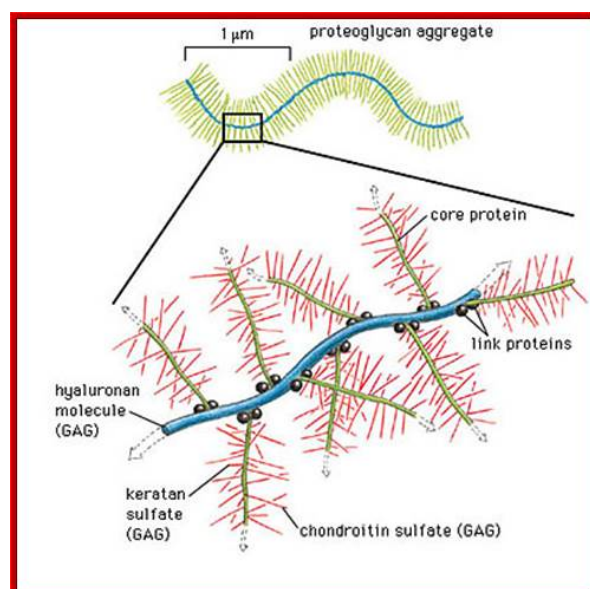


*Figure 4: Proteoglycans [3]*

### 2.1.1.2 Hydrogels

Hydrogels represent 3D hydrophilic polymer networks that, in contact with water, undergo a swelling: they are able to absorb water and hold it within their reticulum, so they increase their size but maintain their shape. The amount of water absorbed is quite variable and can reach up to 99%; this property gives to hydrogels biomimetic characteristics. They exhibit a high biocompatibility due to their similarity to ECM for both composition and mechanical properties; Particularly, proteoglycans in the ECM are a kind of natural hydrogel, indeed, brought into contact with water, the hydrogel swells gradually to a balance, at which the hydrogel is stable in water, it does not dissolve.

The crosslinked hydrogel structure stability is due to the presence of chemical or physical interactions between the polymer chains.

Polymeric chains, that form the hydrogel grid, may have chemical junction points or covalent bonds that give to the hydrogel a permanent gel configuration. In this case, as a characteristic parameter of the hydrogel structure, it is possible to calculate the molecular weight between two subsequent chemical junctions.

Polymeric chains, that form the hydrogel grid, may have physical junction points, i.e. secondary links such as hydrogen bonds, ion interactions or hydrophobic interactions may exist between polymeric chains, which give the hydrogel a temporary structure (non-permanent gel).

The stability of the hydrogel shell structure is, in fact, caused by the presence of other types of physical junctions called entanglements, corresponding to the petty twisting between polymeric chains.

According to the definition of hydrogel, it is possible to identify three fundamental characteristics of hydrogels [9]:

- Water content: The amount of water, retained within the hydrogel grid, can be calculated as the difference between the weight of the bubbling hydrogel, i.e. once it is in contact with water and absorb it to reach a balance situation, the hydrogel lose weight, or vacuum-packed are released to absorb water.
- Mesh Size: hydrogels are very commonly used as carriers, i.e. cell or medicine carriers, it is important to know the size of the hydrogel reticulum mesh to see if it is possible to spread the nutrients and therefore whether the cells, eventually contained within it,

remain vital, or to see if the crosslinked hydrogel structure can provide a good kinetic of drug released possibly loaded within the hydrogel.

- Character of water: a hydrogel can hold two different types of water:
  - Water-free: represents water which, being not linked to the hydrogel structure, is able to evaporate.
  - water-linked: represents water which, being strongly bound to the hydrogel structure (mainly via hydrogen bonds), cannot evaporate and remain within the hydrogel. The amount of water bound is the difference between the amount of water retained within the hydrogel and the amount of free water.

There are several classifications of hydrogels, the most interesting is the one that classifies the hydrogels based on the crosslinks, i.e. the intercutaneous crosslinking bonds which can be of chemical crosslinks or of the physical one, providing the hydrogel with a permanent or temporary structure respectively, and thus distinguishing chemical and physical hydrogels.

The latter ones are used more in BioPrinting applications.

Physical hydrogels are hydrogels whose smoothness is stabilized by secondary interactions and represent “intelligent hydrogels”. They are susceptible to stimuli, able to undergo a SOL/GEL or GEL/SOL phase (sol means solution) in response to signals (as variations in pH or temperature and even the presence of a certain analyte) and this makes them very useful as injectable gels.

A subclass of physical hydrogels is represented by ionic crosslinking hydrogels. These are particular pH-sensitive hydrogels within the structure composed of weakly acidic or weakly basic groups are present, which, depending on the pH, may ionize by assuming a negative or positive charge respectively, and therefore cause such hydrogels to be crosslinked by exploiting ion interactions exerted by cations or multivalent anions, respectively.

A classic ion-sensitive polymer exemplary is Alginate. It is a polysaccharide of natural origin, rich of weakly acidic COOH groups which in physiological pH, i.e. basal pH (7.3), deprotonate by becoming COO<sup>-</sup> anions and transform the Alginate into a poly-anion, which can then be crosslinked by multivalent calcium Ca<sup>2+</sup> cations. From a structural point of view, the Alginate consists of blocks of poly-mannuronic acid, which have a linear and exudate conformation, and blocks of poly-glycolic acid, which, on the other hand, exhibit a linear and shorter conformation. For this reason, at poly-glycolic acid blocks, COO<sup>-</sup> anions are more accessible than Ca<sup>2+</sup> cations



and hence it is only in such blocks that crosslinking is determined by ionic interactions between the various Alginate chains.

In particular, the crosslinking model is the “egg-box model”, within polymeric Alginate, chains are represented as "accordion", while multivalent calcium cations are represented as "balls": at low concentration of  $\text{Ca}^{2+}$  cations, the polymeric chains of Alginate are actually coupled to two to two by  $\text{Ca}^{2+}$  cations; high concentrations of  $\text{Ca}^{2+}$  cations show a true crosslinking of the Alginate polymer chains induced by  $\text{Ca}^{2+}$  cations [9]. **Figure 5**

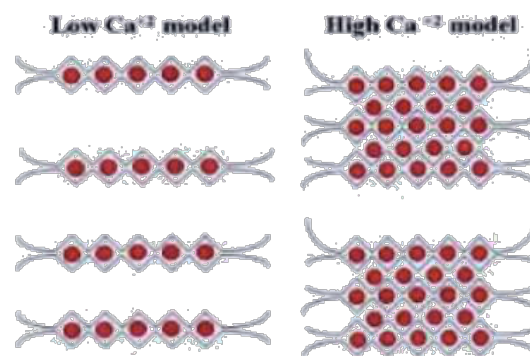


*Figure 5: Alginate models [9]*

As it is a physical crosslinking, the advantage is that Alginate can be used as an injectable gel; in particular, it is possible to inject a biocompatible solution of Alginate (possibly containing cells or drugs) in specific inflammatory areas of the body, where there is a high concentration of  $\text{Ca}^{2+}$  ions, and thus it is reasonable to run the crosslinking of the Alginate inside the organism, holding the cells or drugs in the area.

More generally, gels have a similar soft tissue stiffness. They aim to mimic natural ECM. Gels produced from mixtures of natural ECM, such as collagen and alginate, have been used as substrates for 3D cell culture for several years. The best known gel is Matrigel <sup>TM</sup>. It was first documented in 1972 by Hynda Kleinman [10]. Matrigel is a preparation based on reconstituted basal membrane extracted from the mouse sarcoma Engelbreth-Holm-Swarm, a tumor rich in ECM proteins, such as laminin and collagen, in addition to growth factors and enzymes [11].

The development of synthetic gels arose from the desire to impart controllability in gels, such as polyethylene glycol (PEG) hydrogels from QGel <sup>TM</sup>, which are modified to achieve the desired characteristics. The modification of the bulk material can be performed through the hybridization

of natural and synthetic materials, the incorporation of different types of proteins or molecules within the matrix and the hybridization of biomaterials with functional nanomaterials [12].

Many 3D gels have as their drawback their difficulty of use due to their gelling mechanism. Matrigel, for example, is a type of gel that must be kept in ice. Other types of hydrogels instead use the pH variation to jellify: this mechanism can be doubly favorable because it could be used to expose sensitive cells to adverse conditions.

Their soft-like properties and the ease of converting planar cultures into 3D have made hydrogels quite popular and used. Furthermore, 3D cell cultures in gels have led to significant results, for example in cancer research.

Finally, gels can be combined with other methods, such as spheroidal cultures, scaffolds and microchips [6].

### 2.1.2 Arranging Tissue Elements by 3D BioPrinting

There is a hybrid technique, the BIOPRINTING one, that uses both cells and biomaterials. An image of the tissue is created, that it is need to design the form; cells and polymers are chosen, and also the most suitable printing technique, such as micro-extrusion, inkjet, or laser-assisted printing.

Thermal Printheads can be used for inkjet printing owing to they can operate with a thermal impulse, which causes a temperature rise inside the printer head within a very short period of time, by the way it does not rise to extreme value, in the printer head, indeed it ups to 10°C, so cells are not affected by this temperature variation and drops can be printed. Then, there is the possibility to use a piezoelectric mechanism that generates a force, pushing the ink out of the nozzles, and the piezoelectric crystal can be stimulated in order to emit acoustic waves that exhale the ink from the printer head. Generally, to use these systems, the liquid must be non-aggressive to avoid damaging cells and clogging phenomena.

In the micro-extrusion approaches, there is a small dispenser that compresses the liquid through pneumatic compression, a piston or screw, usually not used because the cutting efforts could damage cells. In these systems, it is necessary to create cutting efforts due to a needle too thin and to have the possibility to use larger needles with a lower resolution. This method compared to the other two is the only one that allows to get a continuous filament. These procedures usually

use hydrogels such as Alginate: for instance, a solution, obtained by modifying an Alginate with an adhesive peptide, is inserted into a printer head, while the plate on which it will deposit is immersed in a calcium bath. The crosslinking is done after it is deposited in the bath, so the structure may not have an optimal resolution.

In the present project, it has been selected to work with the following hydrogels.

Natural polymers are very important because they are the ones through which cell communicates in tissues, natural components of the extracellular matrix.

Signals, arriving to the cell, are sent by these natural polymers in the matrix. Integrating all these signals, cell knows how to behave.

It is possible to have a matrix, like the extracellularly one, very moisturized and it is noticeable to underline that the easily gelling substances using the Alginate. These algae-derived materials are not adhesive to the cells and do not allow protein adsorption. Alginate is easily ionized in ice where calcium ions bind the Alginate chains with reversible physical cross-linking due to calcium ions concentration.

This polymer is a polysaccharide formed by various units of guluronic acid and mannuronic acid, which are saccharide units, containing OH groups, but also COOH. The structure of the polymer is made to have units of maleic acid open, while the guluronic acid units have a more contracted structure. **Figure 6**

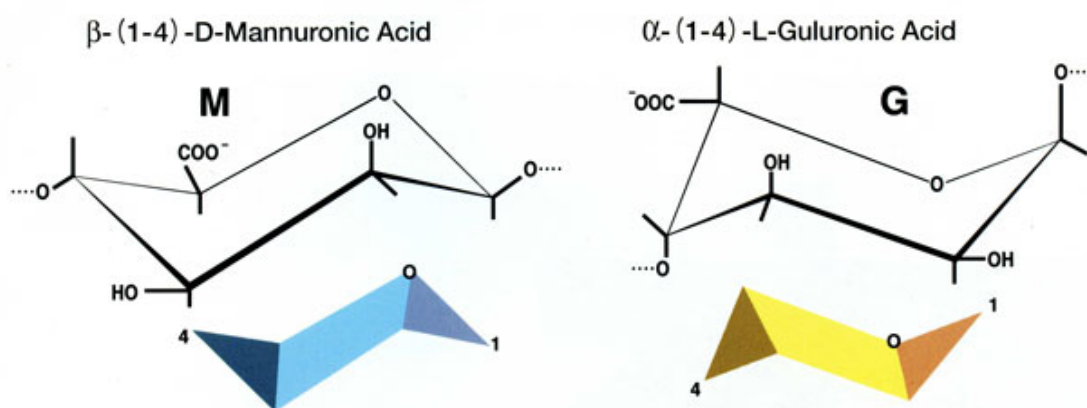


*Figure 6: Alginate components [13]*

Alginate is a natural product that melts in water; it is possible to create a phase reversal by contacting a film of Alginate with a calcium chloride clot bath. Calcium ions are bound to the

polymeric chains of the Alginate which have negative charges, and they tend to retrieve various chains at the ionic level.

This cross-linking is also called egg-box. Since guluronic acid is more compact, it exposes the carboxylic acid to the outside, where there are the units that interact with calcium ions. Putting a few ions calcium is the way to have a low cross-link, otherwise it is possible to create some cross-linking blocks. This is an ionic cross-linking that dampens the polymer.

Another used polymer is PEG (polyethylene glycol) ( $\text{HO-CH}_2\text{-CH}_2\text{-O-(-CH}_2\text{-CH}_2\text{-O-)}_n\text{-H}$ ) has a molecular weight below 40000, otherwise it is called PEO (polyethylene oxide) if it has a weight molecular major. **Figure 7**

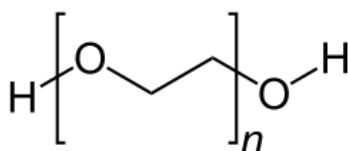


*Figure 7: Polyethylene glycol [3]*

This type of material can degrade oxidatively by initiating an inflammation process and generally has long degradation times. PEG can be found in anti-fouling coatings, i.e. it is in particles that need to avoid protein adhesion, to carry bioactive drugs and molecules such as peptides, proteins and nucleic acids, protecting them from recognition through the immune system and the enzymatic attack (in this case, the agent is embedded in PEG-coated particles, or the agent is conjugated, covalently bound to PEG). It can also be found on vascular prostheses and stents to prevent adsorption proteins and then then ligated the platelets and form a clot. This is because the polymer is very hydrophilic and water adsorption on the polymer limits protein adsorption and recognition through the macrophage-mediated immune system. In these applications, PEG the one called "brush like" because combs out the particle surface almost perpendicularly. PEG is also a component of hydrogels because it is very hydrophilic and creates crosslinked and bioactive hydrogels (for the presence of alanine). This use of PEG in peptide hydrogels also makes it possible to exploit its anti-fouling feature by allowing the peptide to be always exposed to degradation enzymes or cells.

## 2.2 BioPrinting

While 3D Printing, which allows DDM, direct digital manufacture, of a great variety of plastic and metal items, is driving a manufacturing revolution, its application in the biological field is the most surprising one: BioPrinting is the most recent and promising tissue engineering technique.

A definition of BioPrinting was given in 2009 at the International Conference on BioPrinting and Biofabrication held in Bordeaux:

*"BioPrinting can be defined as the use of computer-aided transfer systems for modeling and assembling living and non-living materials with a prescribed 2D or 3D organization in order to produce bio-engineered structures serving in regenerative medicine, pharmacokinetic and basic cell biology studies."* [14]

BioPrinting, therefore, consists of a technique that, through the use of software and hardware dedicated to 2D and 3D schemes and structures design, aims to produce an engineered structure that can be used directly on the man to repair or replace damaged tissues or as material for biological and pharmacological tests and studies.

For simpler organs or for cartilaginous structures such as ears or trachea, 3D BioPrinting uses "scaffolds" drawn in CAD and printed in 3D using biocompatible materials, on which will be then implanted the cells that will form the tissues and the organ.

For the most complex organs made up of many different cells, such as the liver, the heart or the kidneys, this method is not applicable and it is necessary to print both tissues and scaffolds directly. In this case, a similar process to 2D inkjet printing is adopted, where many 2D "sheets" will be printed one on top of the other (layer-by-layer) **Figure 8** to form a complex 3D structure.

The basic elements of BioPrinting are the following:

- Bioprinter: the device for dispensing and depositing "drop-on-demand" bio-ink, i.e. only where and when the computer says to print in order to recreate the desired model as faithfully as possible;
- Bioink: drops of single cells or cell aggregates that are printed "layer-by-layer" on the bio-paper;
- Biopaper: the base on which to deposit the bioink layer by layer, with which it will then merge to form the desired construct;

- Bioreactor: environment in which to build and grow the constructs and keep them alive.

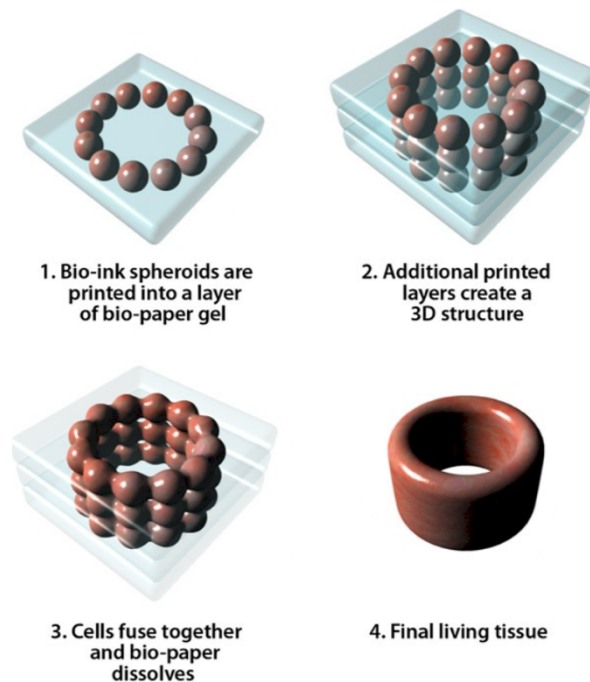


*Figure 8: Process scheme of engineered tissue using layer by layer method [15]*

On the 3<sup>rd</sup> March 2011, surgeons and regenerative medicine pioneer Anthony Atala gave a talk at the annual TED conference in California. [16] In his presentation, Atala explained the increasing health crisis that is arising as people live longer and organ failure become more common. In the United States alone, up to 100.000 patients are always waiting for an organ transplant, with less than a third of these people ever receiving one. BioPrinting therefore has the potential to deliver humanity into a new medical age in which damaged or diseased body parts will be routinely replaced with fully organic and “natural” alternatives. One day BioPrinting could allow doctors to heal wounds and replace organs by BioPrinting new cells directly onto and into their patients. In response to this situation, Atala is one of the pioneers who are working to create living, artificial human organs in the laboratory. Atala demonstrated on stage a special 3D printer that was building a prototype human kidney: he held a complete kidney that he had “printed out earlier”. [15]

### 2.2.1 Available Commercial Technology

A Japanese pediatrician, Makoto Nakamura started to investigate to create mechanical, inorganic prosthesis; he also realized that the droplets of ink emitted from the printhead in a standard inkjet photo printer are about the same size as the human cells ( $\sim 10\text{-}30\text{ }\mu\text{m}$ ). [17] In 2002 Nakamura began his first experiments with a standard Epson photo printer and, with the Epson assistance, he modified the photo printer to successfully output cells that survived the inkjet printing process. This was achieved by encasing cells in a sodium Alginate hydrogel to stop them from drying out, and by jetting them into a calcium-chloride solution.

Between April 2005 and March 2008, Nakamura guided a team that scratch-built an experimental bioprinter, then used to create a “biotubing” from layers of two different types of cells, with 15 mm of 1 mm diameter material output every minute.

In addition to Professor Nakamura, other researchers built bioprinters; like in Russia, Vladimir Mironov built a bioprinter called “FABION”. [18] Also, advancing BioPrinting frontiers with their own hardware are a team lead by Anthony Atala at the Wake Forest Institute for Regenerative Medicine in the United States [19]; Will Shu and a team at Heriot-Watt University in Scotland [20]; and Ibrahim Ozbolat at Penn State University in the United States [21]. Over in China, a company called Regenovo has developed three bioprinter models called the Bio-Printer-Lite, Bio-Printer-Pro and Bio-Printer-WS [22].

Principal vendors are Switzerland-based RegenHU, who market two models called the BioFactory and the 3DDiscovery [23], and EnvisionTEC from Germany with their 3D-Bioplotter [24]. Meanwhile, over in South Korea, 3Dison market a “Hybrid Bio 3D Printer” known as the Rokit Invivo, while the Japanese company Cyfuse Biomedical offer their CyFuse Vision 2020.

A final leading player that has both developed a bioprinter, and which is now using it to produce commercial bioprinted materials, is Organovo [25], based in California in the United States. Organovo has the distinction of being the only pure play BioPrinting company to have floated on a stock market. Organovo is bringing to market the work of BioPrinting pioneer Gabor Forgacs from the University of Missouri. In 1996, he recognized cells, from chicken embryos, aggregate and then later re-arrange during embryonic development in a manner that could greatly assist in artificial tissue fabrication. By 2004, Forgacs had used his insight to start developing

his own BioPrinting technology. This builds tissues not from individually jetted cells, but from “clumps” of many thousands of cells called “bio-ink spheroids” and injected into a water-based “biopaper” by a tiny, needle-like print head.

Organovo, founded by Forgacs in 2007, was the first company to enter the 3D BioPrinting space by printing functional blood vessels in 2010. The company now offers 3D printed kidney and liver tissue models for in-vitro tests. There have been a number of other notable attempts to create fully functional 3D bioprinted tissues. For instance, in 2015, 3D BioPrinting Solutions became the first company to print and transplant a thyroid gland in a mouse [26]. Subsequently, in the same year, Aspect Biosystems developed and commercialized 3D printed human respiratory tissue for clinical testing [27]. In addition to these, other companies with commercialized tissue products include MEDPRIN, Poietis, and Sirris.

The current applications of 3D bioprinted products cater to various requirements within the pharmaceutical industry for clinical testing of therapeutic drugs. Owing to the evident interspecies differences, drug candidates that are shown to be efficacious in animal models often fail in humans. For such purposes, 3D BioPrinting can be used to develop more accurate, human specific disease models. Due to the severe unmet need related to organ transplants, the ability to synthetically create organs for transplantation purposes is expected to generate a lot of interest amongst pharmaceutical/biotechnology players in the coming years.

The current market landscape is characterized by the presence of nearly equal number of industry/non-industry players, featuring a number of start-ups and university spin-offs. Although several 3D BioPrinting technologies are available, active efforts are being made to add to the intellectual property portfolio. [28]

The field has witnessed growing partnering activity and has managed to capture the interest of both public and private sector investors. Despite certain challenges, several technical advancements and high unmet need of current patients waiting for organ transplants is anticipated to significantly drive future growth.

The BioPrinting approach chosen in this Master Thesis work is the use of multi-nozzle inkjet technology. The goal is to see if cells, after the printing process in hydrogel and in the water-based Dulbecco's Modified Eagle Medium (DMEM), can survive to the process using a commercially available printhead (Dimatix Fujifilm Sapphire QS-256 AAA Printhead Family)



based on 256 piezoelectric nozzles which can work all together in the same time. The main advantage of the use of multi-nozzle printheads is to reduce the printing process time from hours to 1-2 minutes: for example, to cover a rectangular surface with a multi-nozzle printhead it is not necessary to move the printhead in two direction, but only in one; for this reason, the process time is significantly reduced and the solvent attach to the surface at the same time per each printed line. With this kind of printhead there is much more throughput: it could be also possible to have several printheads in parallel with different bioinks and print bigger liquid volume/time than the others actual BioPrinting systems on the market. Multi-nozzle inkjet printheads permit to drastically reduce the printing time, thus reducing the cost of BioPrinting.

Multi-nozzle technology has been already used in photo/electro-printing applications, but it is not-commercially available for BioPrinting applications. This kind of technology, in the BioPrinting world, could be used in a near future towards the industrialization of the 3D BioPrinting, to create a tissue and maybe an organ in a fast, economically, reproducible and user-friendly way. A multi-nozzle inkjet BioPrinting process would reduce also the use of animal testing during tissues manufacturing for drug testing in the pharmaceutical/cosmetic industry, which is very expensive and ethically controverted.

The most important characteristics for a deposition process of a cell-loaded hydrogels are:

- Drop formation: straight drops without satellites are the best for a high-quality printing;
- Stability over time: cells might clog nozzles as they sediment and/or aggregate; the drying hydrogel might also be problematic;
- Cells viability: the shear stress induced by the printing process and the prolonged change of extracellular components might have a negative influence on the cells viability.

### 2.2.2 Fundamentals of Inkjet Printing

Inkjet BioPrinting is a printing process that involves the precise on-demand (digital) deposition of bioink drops, varying in size from nanoliter to picoliter, on the biopaper according to a precise digital model. It is an adaptation of the traditional inkjet printing process and in most cases, it is achieved by partially modifying desktop printers on the market. [29]

The inkjet printing methods are basically two:

- CIJ (Continuous Inkjet): a continuous flow of droplets is produced by forcing the ink through microscopic nozzles under pressure and deflected on the substrate by an electric field. Where, in the digital model, bioink deposition is not required, the droplets are guided in a sort of gutter and collected to be reused, shown in 2.2.2.2 *Inkjet Process, DOD Generations*;
- DOD (Drop-on-Demand): the droplets of ink are emitted through nozzles by an impulsive pressure only when required by the model.

In BioPrinting, the DOD approach is preferable due to its impulsive nature and to the risk of contamination due to bioink recycling in the CIJ technique. Drop-on-demand printing can be further subdivided according to the drop formation mechanism **Figure 9**: [29]

- Thermal Effect (Thermal DOD): a thin resistive element is heated by Joule effect from an impulsive current. The increase in temperature causes the ink to evaporate adjacent to the resistance, forming a bubble which expands to expel the drop of bioink from the nozzle;
- Piezoelectric Effect (Piezoelectric DOD): a piezoelectric transducer is used which, subjected to voltage variations, expands, causing bioink escape.

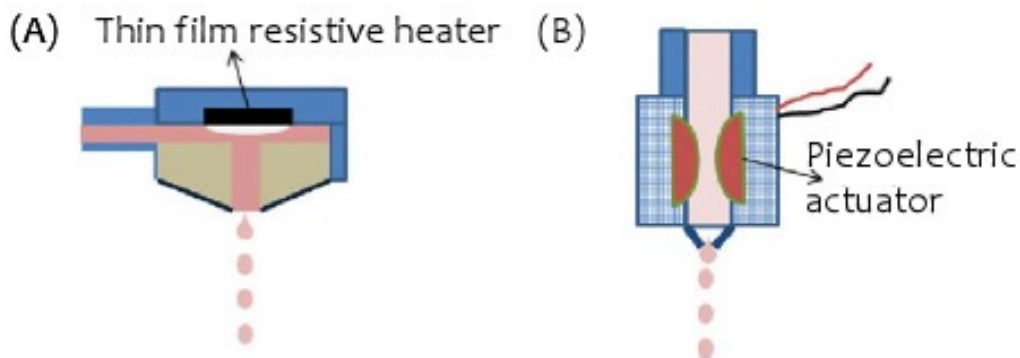


**Figure 9:** (A) Resistive heater and (B) Piezoelectric actuator [29]

The size of the drops and the spatial resolution in inkjet printing are determined by various factors: the viscosity of the bioink, the size of the nozzles, the distance between these and the substrate, the frequency of the current impulse in the Thermal-DOD and the frequency voltage pulse in the Piezoelectric-DOD. The inkjet technique offers the

possibility to print different cell species, biomaterials or combinations thereof through different print heads in a single manufacturing process, allowing the realization of complex multicellular constructs.

- Solenoid valve printing, **Figure 10**, uses electromagnetically controlled valves. A complete system consists of a fluid reservoir, a solenoid valve-based delivery device with bioink volumes between 1 nl and 5 pl, heating elements for controlling the nozzle head temperature, connections to the control system and a source of inert gas. The operation of the solenoid valve is similar to an electrically controlled faucet; it consists of a mechanical opening and closing device very similar to a membrane, which is raised or lowered allowing or preventing the leakage of bioink. This membrane is actuated by a solenoid which, when traversed by current, generates a magnetic field capable of lifting the occluding mechanical element (typically metallic), thus determining the opening or closing of the valve. The control system establishes the frequency and duration of the electrical impulses sent thus allowing the Drop-On-Demand printing. In a multiple nozzle system, multiple materials can be printed simultaneously, each taken from the respective tank, allowing the construction of a complex heterogeneous construction. The system does not involve problems related to overheating and it is able to accept viscous polymers such as collagen and 1-2% sodium Alginate. [29]

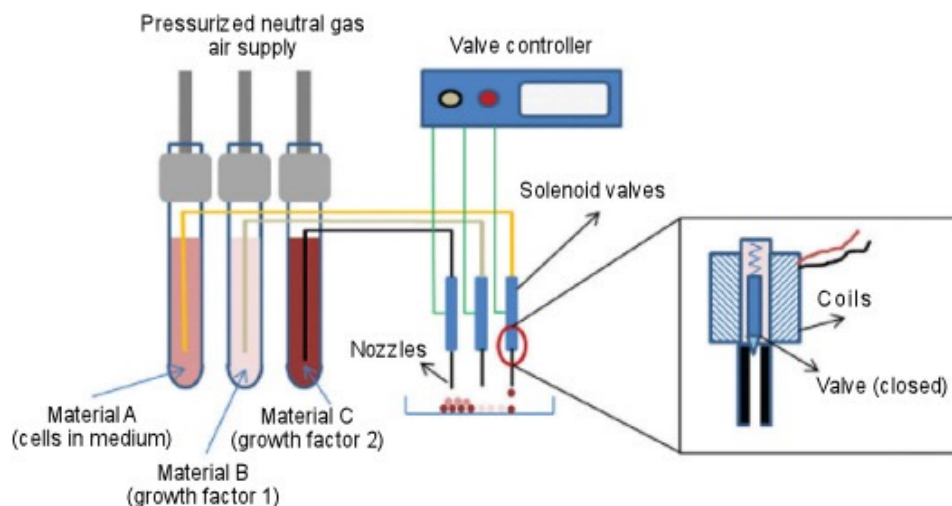


*Figure 10: Solenoid Valve Based BioPrinting Single Nozzle [29]*

The inkjet and solenoid valve systems are versatile and low cost, they favor the encapsulation of cells and moreover, through the use of multiple printheads, they allow a simpler realization of cellular hetero constructs. However, these types of technologies are subject to drawbacks such as sedimentation and cellular aggregation in the nozzle orifice, with consequent clogging of the latter. It is therefore necessary that the construction process of the construct be of short duration, since the material is sedimented in static conditions. Furthermore, the nozzle diameter must be designed appropriately in order not to damage the cell during deposition. In conclusion, therefore, the parameters to be optimized in order to make this functional technique are the nozzle diameter, the viscosity of the biological material and the time of delivery of the bioink.

The ultimate goal of the printing process is to make "vital" tissues, so special attention must be paid to aspects that could cause cell damage or death: temperature variations imposed by resistors, too small nozzles or excessive pressure in the expulsion of the drops.

In a study conducted by researchers Xiaofeng Cui and Thomas Boland, it has been demonstrated that, respecting the optimal parameters, the BioPrinting allows to preserve the viability of cells and not to alter their properties, evaluating two parameters: cell viability and the apoptotic average. [30] The first is the relationship between the number of live cells and the sum of living and dead cells. Apoptosis, on the other hand, is defined as programmed cell death and contributes to the maintenance of the number of cells in an organism; it is therefore a process that normally happens in tissues, but the purpose of the study is to evaluate if the BioPrinting can alter it. As a printing technique, thermal inkjet printing was chosen. Twelve hours after printing, the live cells were highlighted using a green marker, while the dead cells with a red marker were counted by means of a microscope, thus calculating cell viability.

The test was also repeated with various cell concentrations to find the ideal one: 8 million cells per mL, which corresponds to an average viability of 89%.

### 2.2.2.1 Microfluidic

Fluids have many different properties that describe their kinematic, thermodynamic behaviors.

Most of their properties depend on various factors such as the nature of the molecules and the operating conditions imposed on the fluid. The properties examined are: density, surface tension and viscosity [29].

The density  $\rho$  of a fluid is defined as its mass per unit volume. Its unit, in the SI system, is kilogram per cubic meter. The density of a material depends on the mass of the molecules and on the number of molecules per unit of volume. In addition, other factors, such as intermolecular spacing, such as temperature and pressure. In fact, if the temperature increases, the fluid molecules become more energetic and tend to separate. this phenomenon leads to a decrease in the number of molecules per unit of volume and consequently the density will be lower. The density of a liquid depends mainly on its molecular content in measurement of the lowest temperature. A liquid does not change state.

This phenomenon is different for a gas. For an ideal gas,  $pV = nRT$ , where  $p$  is the pressure,  $V$  is the volume of the gas,  $n$  is the number of moles,  $R$  is the gas constant and  $T$  is the absolute temperature. The density of the gas is given by:  $\rho = M_w p / RT$ , where  $M_w$  is the molecular weight.

**VISCOSITY:** Viscosity is the property of a fluid that defines its resistance to deformation under the shear flow. Resistance to deformation is caused by a cohesive intermolecular force that generates friction between adjacent layers of volumes of fluids that are in relative motion. They glide over each other.

Viscosity depends on three factors: the attractive force between the molecules, the frequency of interchange of the moment between the molecules positioned in the adjacent layers, and the temperature (the effect is different for liquids and gases). In a liquid, molecular cohesion dominates viscosity [29].

The molecules in a liquid become more energetic and separate as the temperature increases. The viscosity of a gas, on the other hand, increases with temperature because of the increase in the frequency of intermolecular collisions and intermolecular forces.

The system, shown in **Figure 11**, represent the graphic way to calculate the li represents two parallel plates close together with fluid between them. Both plate A, and the top plate moves sideways to the right with a speed  $U$  due to an appli the bottom plate is stationary. Since the fluid molecules adhere to both walls velocity  $u$  of the fluid is the velocity of the wall at each interface.

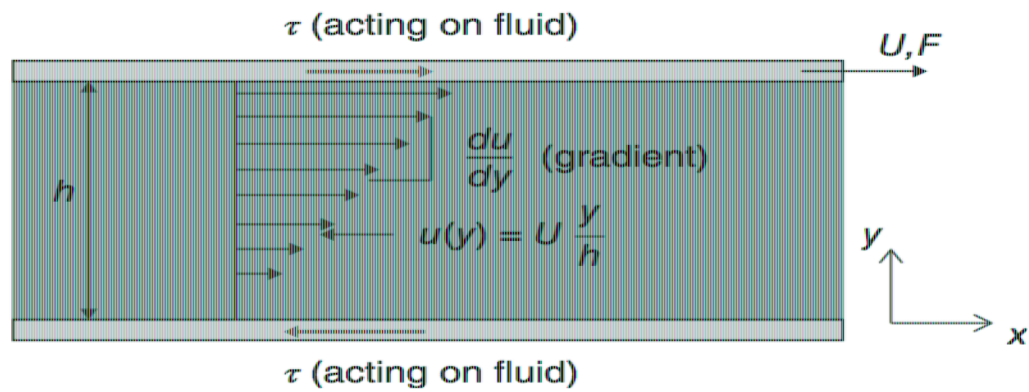


**Figure 11:** Illustration of a viscosity measurement showing a cross section of a thin layer of fluid subjected to a shear stress between two plates that are in relative linear motion [29].

This phenomenon is called a *no-slip boundary condition*. The velocity of the fluid has been considered:  $u=U$  at the upper boundary and  $u=0$  at the lower boundary. The velocity varies due to the distance  $y$  between plates. For example, the velocity profile is linear if plates are closely spaced,  $U$  is low and there is no fluid flow between plates.

The applied shear stress  $\tau = F/A$  is proportional to the velocity gradient (in all fluids)

$$\tau = \mu \cdot \frac{du}{dy}$$

where the constant of proportionality  $\mu$  is called the *coefficient of viscosity* (or *dynamic viscosity*) [29]. This equation is called the *Newton's law of viscosity*. Kinematic viscosity is the ratio of the dynamic viscosity  $\mu$  to the density  $\rho$  and is usually denoted by  $\nu$ .

$$\nu = \mu / \rho \quad [29].$$

The ratio  $U/h$  is the *rate of shear deformation* or *shear velocity*, and the gradient  $du/dy$  is the *local shear velocity* or *strain rate*, which has the unit of per second and is often denoted by  $\dot{\gamma}$  [29]. Fluids that obey Newton's law of viscosity, for which  $\mu$  is a constant independent of shear velocity, are known as *Newtonian fluids* [29].

Fluids for which  $\mu$  varies with the shear velocity are known as non-Newtonian fluids. There are three main classes of non-Newtonian liquids: time-independent, time-dependent, and viscoelastic fluids. In the first ones, the rate of shear at a point is determined only by the value of the shear stress at that point at that instant (*purely viscous, inelastic, or general non-Newtonian fluid*) [29]. In the second ones, the relation between the shear stress and the shear rate depends on the duration of shearing and on the kinematic history of the fluids [29]. These fluids show characteristics of both ideal fluids and elastic solids and show partial elastic behavior under deformation [29]. **Figure 12** is a list of different non-Newtonian fluid categories.

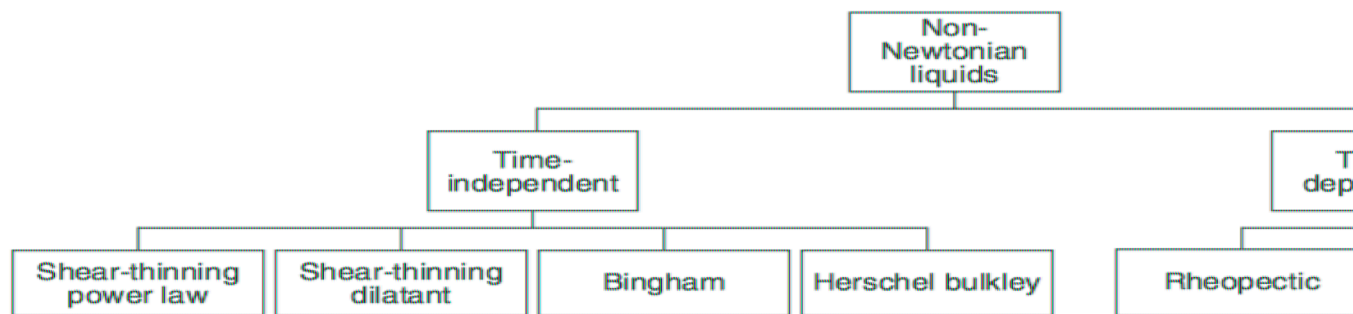


**Figure 12:** Non-Newtonian Liquids [29]

- *Plastic*: the shear stress must reach a minimum value before flow starts;
- *Bingham Plastic*: similarly to plastic, a minimum shear stress must be achieved before flow starts;
- *Pseudoplastic*: the viscosity decreases with the rate of shear;
- *Dilatant Substances*: viscosity increases with the rate of shear;
- *Viscoelastic Materials*: similar to Newtonian fluids, but when a sudden big velocity gradient is applied, their behavior is similar to that of plastic [29].



**Figure 13** shows an example, which represents the basis for the definition of viscosity of liquid is defined by two parallel surfaces a distance  $d$  apart [29]. The lower surface is stationary, and the upper surface moves relative to it at a constant velocity  $v$ .

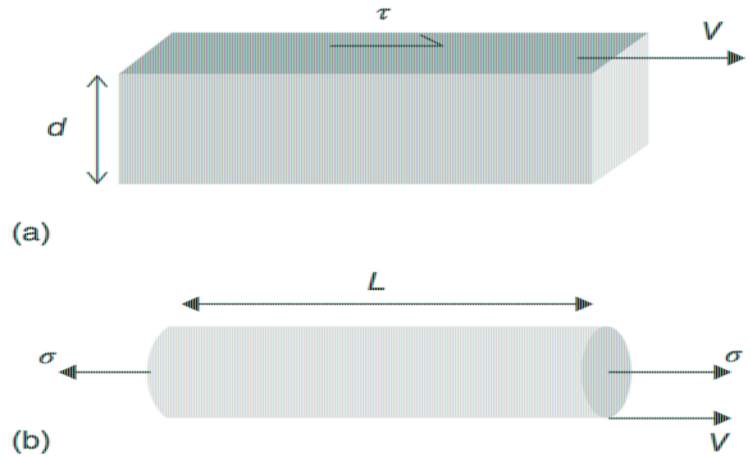


**Figure 13:** Geometry used to define (a) shear flow and (b) extensional flow [29]

This movement generates a linear gradient of velocity through the liquid, from the upper and lower surfaces. The shear strain rate  $\dot{\gamma}$  is given by:

$$\dot{\gamma} = V/d$$

and the shear stress  $\tau$  acting on the upper and lower surfaces is proportional to

$$\tau = \eta \cdot \dot{\gamma}$$

The constant  $\eta$  is the *dynamic viscosity* ( $\text{Pa}\cdot\text{s}$  in SI or poise P in c.g.s.:  $1\text{mPa}\cdot\text{s}=10^{-3}\text{Pa}\cdot\text{s}$ ). If  $\eta$  is independent from  $\dot{\gamma}$ , it is *linear* or *Newtonian*. The term “viscosity” means dynamic viscosity as defined for a shear flow [29].

For example, water has a viscosity of  $1\text{mPa}\cdot\text{s}$  at  $20^\circ\text{C}$ , while fluids used in inkjet printing typically have viscosities in the range from  $\sim 2$  to  $\sim 50\text{mPa}\cdot\text{s}$ . The viscosity of most fluids decreases rapidly with increasing temperature. This is often appreciated in inkjet printing: by varying the temperature of the printhead, it is possible to change the viscosity of the ink and thus control the droplet formation [29].

The shear flow shown in **Figure 13a** represents a particular pattern of liquid flow



represent well the flow that occurs in the formation or collapse of a jet. It is important to consider the extensional flow, which is shown in **Figure 13b** [29]. If a cylindrical column of length  $L$  is stretched along its axis at a velocity  $V$ , the uniaxial strain rate  $\dot{\epsilon}$  is given by

$$\dot{\epsilon} = V/L$$

and the axial stress  $\sigma$  is linearly proportional to the strain rate:

$$\sigma = \eta_T \dot{\epsilon}$$

The constant of proportionality  $\eta_T$  is called the *extensional viscosity*, and for a Newtonian fluid,  $\eta_T$  is three times the shear viscosity  $\eta$  [29]. The ratio  $\eta_T/\eta$  is the *Trouton ratio*. Values greater than 3 for viscoelastic liquids, that are non-Newtonian fluids. They exhibit a time-dependent response as well as viscosity due, for example, to the presence of polymer molecules in solution [29]. Organic solvents are usually Newtonian, but practical inkjet inks often exhibit some degree of viscoelasticity. [29]

**SURFACE TENSION:** The intermolecular attractive force exhibited by the molecules of a liquid is called cohesion. At the interface between a liquid and a gas (surface tension) or between two non-mixable, immiscible liquids), the attractive force on the molecules in the liquid creates a tension on the surface, i.e. a surface tension as shown **Figure 14**. The range of values covered by the surface tension of liquids is large: most of these values tend to decrease with increasing temperature [29]. The molecules of a liquid have the characteristics of both cohesion and adhesion. Cohesion is the attractive force between the different molecules of the liquid, and adhesion is the force that causes the liquid to adhere to another body. When a liquid is placed on a plane, the form it takes is determined by the relative strength of these forces. If the strength of the adhesive dominates, the liquid will spread out (wet) on the substrate. If the cohesive force dominates, the liquid will "pull up" on the surface [29].

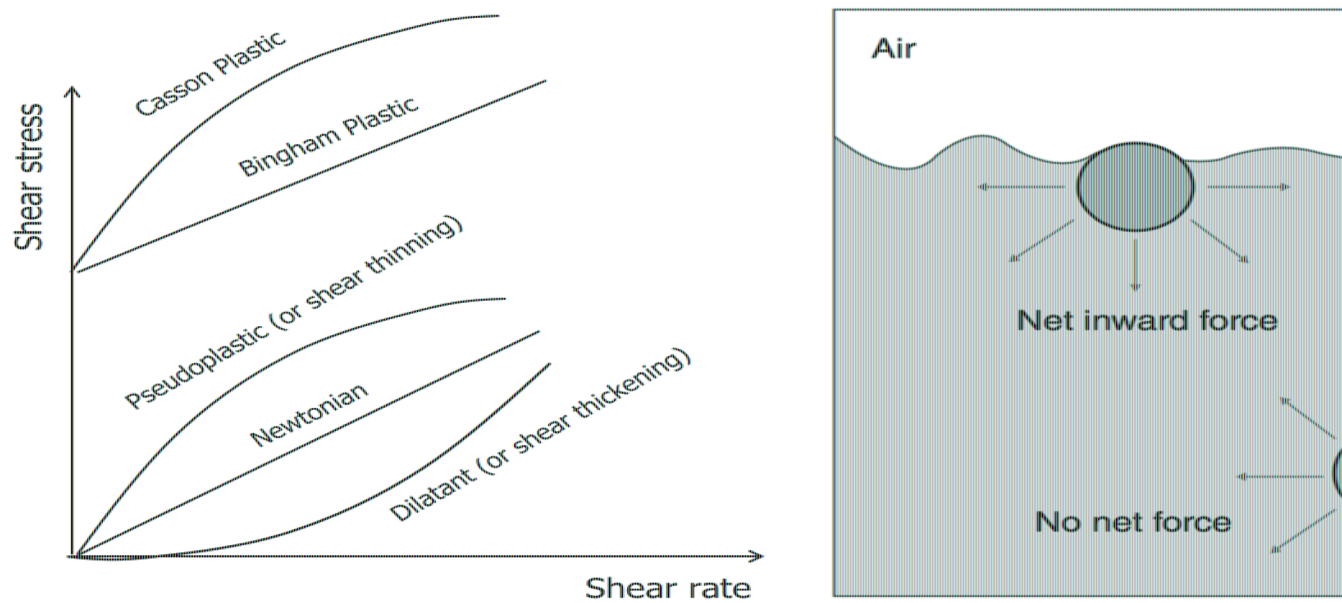


**Figure 14:** Graph of different non-Newtonian fluid categories and illustration of intermolecular forces and surface tension [29]

Capillarity is the property of exerting forces on fluids by fine tubes or porous materials. It manifests itself when the force coexisting inside a liquid dominates the adhesive force. If the cohesive force is greater, the surface of the liquid will form a concave shape downwards in order to reduce its contact with the wall. Nonetheless, when the adhesive force predominates, the liquid will rise. The attraction of the wall is greater than its interior and its surface will assume a concave shape. The curved liquid surface that forms is called a *meniscus* [29].

Surface tension and viscosity are two physical properties that dominate the liquid behavior in the inkjet printing system, considering the liquid jets and the drops formations.

The liquid surface tension reflects the fact that atoms or molecules at a free surface have higher energy than those in the bulk. Creating a new surface area costs in terms of energy. The shape with the lowest surface area, and therefore the lowest surface energy, is a sphere. When a drop is in contact with a solid surface, for example after it has been printed on to a substrate, it is necessary to consider the energy of its free surface and the energy of the interface between the liquid and the solid substrate. In that case, the equilibrium shape of the drop becomes a spherical cap. The liquid surface tension causes a force to act in the plane of the surface, perpendicular to a free edge in that surface [29].

The force is proportional to the length of the edge. The surface tension  $\gamma$  can be defined as the force per unit length. Since by moving the edge in the direction of the force the surface will increase and also does work on the system against the surface tension, it is possible to treat the force per unit length as a *surface energy*: the work done in creating a unit area of new surface. These two definitions are equivalent, as are the SI units of  $\text{N} \cdot \text{m}^{-1}$  and  $\text{J} \cdot \text{m}^{-2}$ . Most liquids of practical interest for inkjet printing have surface tensions,  $\gamma$ , of the order of  $\text{mN} \cdot \text{m}^{-1}$  (or  $\text{mJ} \cdot \text{m}^{-2}$ ). For pure water at  $20^\circ\text{C}$ ,  $\gamma = 72.5 \text{ mN} \cdot \text{m}^{-1}$ , while for organic liquids (which have smaller intermolecular energies than water),  $\gamma$  is in the range  $10\text{--}30 \text{ mN} \cdot \text{m}^{-1}$ . [29]

The tendency of a liquid to form the shape with the lowest total energy is responsible for the breakup of the stream in CIJ printing and for the formation of the main drop and satellite drops in DOD printing.

**FORCES:** Forces that resist the contraction of a liquid jet through the action of surface tension have two origins: the inertia of the liquid and its viscosity. Inertial forces are associated with a change in a body's momentum: in the case of a moving liquid, they are proportional to the density and the rate of change of velocity. Viscous forces arise from the interaction between the molecules of the liquid and act between regions of liquid moving relative to each other.

Forces drive the motion of fluids. Two different types of force are encountered in fluid mechanics: surface forces, which are proportional to area, and body forces, which are proportional to volume. Surface forces are usually expressed in terms of stress. Surface forces constitute pressure  $p$ , which always acts normal to a surface, and shear stresses  $\sigma_{ij}$ , which develop within a fluid when its molecules are in relative motion with respect to one another.

Pressure is a normal stress that equals  $F_n/A$ , where  $F_n$  is the force acting normal to an area  $A$ . Pressure is referred to as *tensile* or *compressive*, depending on whether it tends to stretch or compress a fluid, respectively. Standard atmospheric pressure is  $1\text{ atm} = 101325 \text{ Pa}$  and is equivalent to  $760\text{ mm Hg (torr)}$  or  $14.696\text{ psi}$ . The amount by which the pressure exceeds the ambient atmosphere pressure is called the *gauge pressure*. Most pressure gauges report the gauge pressure, not the absolute pressure, which equals the gauge pressure plus the ambient pressure.

the atmospheric pressure.

A flowing fluid is described by a velocity field  $\vec{v}$ , that is, a vector-valued function of time that typically varies in both magnitude and direction from point to point within the fluid.

$$\vec{v}(x, y, z) = u(x, y, z)\hat{x} + v(x, y, z)\hat{y} + w(x, y, z)\hat{z}$$

The fluid velocity field  $\vec{v}$  for practical applications is often very complicated and difficult to be predicted using numerical analysis. The volumetric flow rate  $Q$  through a surface with unit normal  $\hat{n}$  is:

$$Q = \int \vec{v} \cdot \hat{n} \, dA. \quad [29]$$

If  $U_{\text{ave}}$  is the average velocity normal to a planar area  $A$ , then  $Q = U_{\text{ave}} \cdot A$  ( $\text{m}^3/\text{s}$ ).

The corresponding mass flow rate is

$$\dot{m} = \rho U_{\text{ave}} \cdot A (\text{kg s}^{-1})$$

where  $\rho$  is the fluid density. The momentum flow rate  $\dot{M}$  is obtained by multiplying the mass flow rate by the fluid velocity, that is,  $\dot{M} = \rho U^2 \cdot A$ . These expressions are useful for estimating momentum transport for relatively simple applications.

In conclusion, surface tension, inertia, and viscosity play key roles in the formation of liquid jets and drops. [29] Two dimensionless numbers can be used to characterize the relative importance of these: the Reynolds and Weber numbers. The Reynolds number is a dimensionless ratio between inertial and viscous forces in a moving fluid and is defined by eq (30):

$$Re = \frac{\rho V d}{\eta}$$

where  $\rho$  is the density of the fluid,  $V$  is its velocity,  $\eta$  is its viscosity, and  $d$  is a characteristic length: typically, the diameter of the jet, nozzle, or drop. It gives a good tip on whether the flow is laminar or turbulent.

The Weber number  $We$  depends on the ratio between inertia and surface tension

$$We = \frac{\rho V^2 d}{\gamma}$$

where  $\gamma$  is the surface tension. For a spherical drop traveling at velocity  $V$ , the kinetic energy and the energy of its free surface is  $We/6$ .

The influence of velocity in these two dimensionless groups can be removed by the second group, the Ohnesorge number  $Oh$  defined by:

$$Oh = \frac{\sqrt{We}}{Re} = \frac{\eta}{\sqrt{\gamma \rho d}} \sim \frac{\text{viscous forces}}{\sqrt{\text{inertia} \cdot \text{surface tension}}}$$

The value of the Ohnesorge number, which reflects only the physical properties of the fluid and the size scale of the jet or drop, but is independent of the driving conditions (velocity), turns out to be closely related to the behavior of a jet emerging from a nozzle, thus, to the conditions in DOD printing. If the Ohnesorge number is too high, viscous forces will prevent the separation of a drop, while if it is too low ( $Oh < 0.1$ ), it will form a large number of satellite droplets.

Satisfactory performance of a fluid in DOD inkjet printing thus requires a certain combination of physical properties, which will also depend on the droplet size (through the value of the Reynolds or Weber number) as shown in **Figure 15**.

Some authors use the symbol  $Z$  for the inverse of the Ohnesorge number ( $Z = 1/Oh$ ). The range over which liquids can be printed is often quoted as  $10 > Z > 1$ , although other works suggest that  $14 < Z < 4$  may be more appropriate. [29]



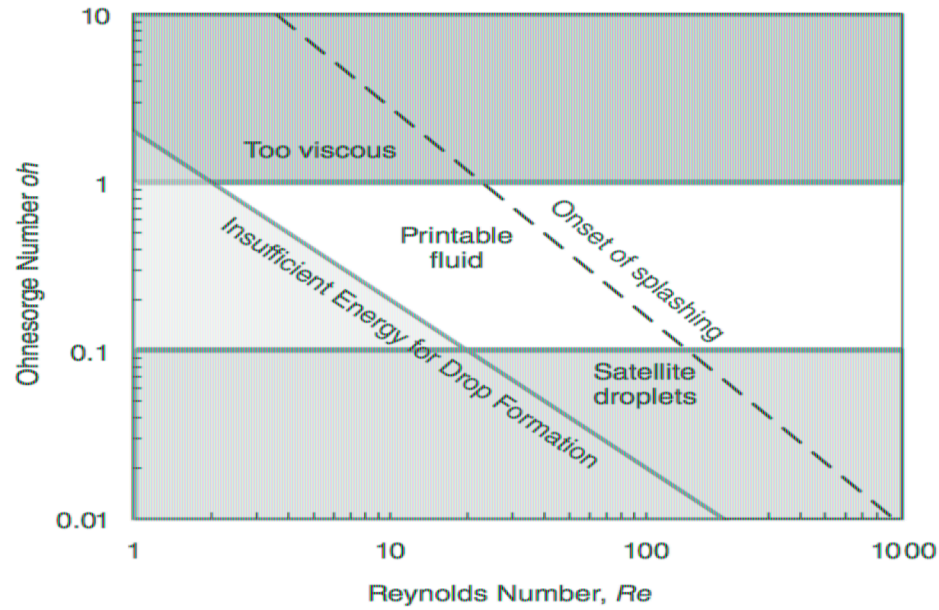


**Figure 15:** Schematic diagram showing the operating regime for stable operation of drop-on-demand inkjet printing as a function of the Ohnesorge and Reynolds numbers [29]

These ranges of Ohnesorge number provide some bounds to the “printability” of a fluid. However, other factors must also be considered: the jet must possess enough kinetic energy to overcome the surface tension from the nozzle (leading to the solid diagonal line, corresponding to  $Re = 2/C$ ), and the drop must be desirable to avoid splashing of the drop on impact with the substrate (which leads to the dashed diagonal line for which  $OhRe^{5/4} = 50$ ). Enough kinetic energy is also necessary for the drop to accurately reach the substrates and doesn't evaporate.

#### 2.2.2.2 Inkjet Process, DOD Generations

An inkjet system basically consists of three fundamental components: inks, a printhead, and an imaging medium (e.g., paper or substrate). Inks produce color by absorbing and scattering light. Inks can be broadly categorized into three groups: colorant, that is, organic dyes, polymeric dyes, and pigments. Organic dyes consist of dye molecules, polymeric dyes consist of dye polymers, and pigmented inks consist of inorganic pigment particles. The printhead operates under digital control and

of ink, typically 10–100  $\mu\text{m}$  in diameter depending on the technology, onto the to form an image. Modern inkjet systems utilize microfabricated printheads with hundreds to thousands of integrated micronozzles. A printhead can produce millions of ink per second with remarkable uniformity in both volume and velocity. The ink is projected onto the imaging medium with precision placement to render high resolution. While traditional printing has been the dominant impetus for the advancement of this technology is rapidly evolving toward applications in emerging fields such as functional materials, deposition of biomaterials, production of pharmaceuticals, and prototyping. [29]

Inkjet systems broadly fall into two categories, continuous inkjet (CIJ) and drop-on-demand (DOD) inkjet as shown in **Figure 16**. In CIJ, continuous jets of ink are produced by applying pressure in a common ink reservoir. The jets are inherently unstable (due to Rayleigh instability) and can be modulated using a periodic stimulus to break up into a stream of equally spaced droplets.

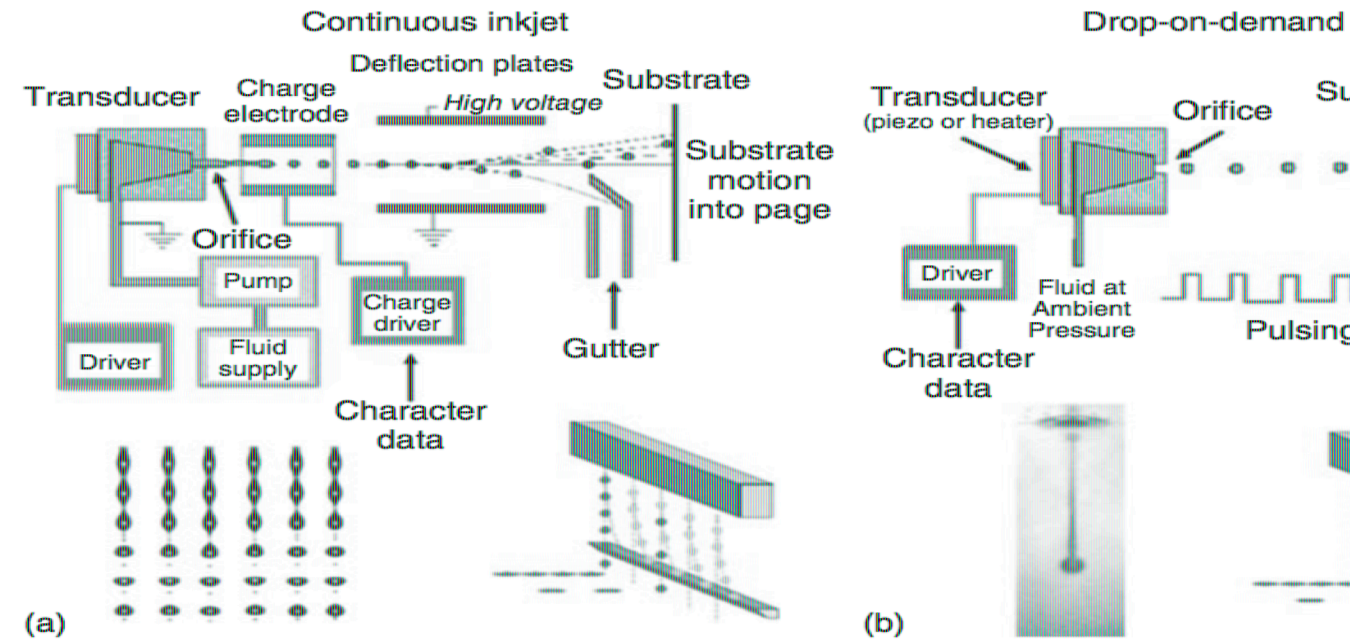


**Figure 16:** Inkjet printing methods: (a) continuous inkjet and (b) drop-on-demand inkjet.

When the jets are properly modulated, the droplets will have a well-defined volume ( $10 - 20 \text{ m} \cdot \text{s}^{-1}$ ) and will form at a consistent distance downstream from the nozzle.

A CIJ printhead can produce hundreds of thousands of droplets per second from a single nozzle; however, only select droplets are allowed to reach the imaging medium to form the image. Unused droplets are deflected in flight and recycled to the ink reservoir that feeds the printhead.

In DOD systems, droplets are produced as needed (on demand) to form an image. Droplets are generated by applying a raised pressure pulse within an ejection chamber through a nozzle [29].

#### 2.2.2.3 Inkjet Printheads

The vast majority of commercial DOD printers utilize either piezoelectric or thermal droplet generation. Piezo DOD printheads use a voltage-induced deformation of a piezoelectric transducer to produce the pressure pulse needed to eject a droplet. In thermal inkjet (also referred to as *bubble jet*), a resistive heating element is used to super-heat the ejection chamber to generate a homogenous vapour bubble that expands rapidly, creating the pressure needed to eject a droplet.

In piezoelectric DOD **Figure 17**, a voltage-driven piezoelectric transducer mechanically deforms the walls of the ejection chamber to eject a droplet. Each nozzle is driven by a separate transducer, and when a voltage is applied, it produces an electric field in a thin layer of piezoelectric material that causes the transducer to deform. The deformation of the volume of the ejection chamber to contract or expand depending on the polarity of the voltage. This controls the pressure within the chamber, that is, higher pressure when it contracts and lower pressure when it expands. A custom voltage waveform is applied to create a desired time-dependent pressure within the chamber to optimize both droplet ejection and the volume of the chamber. [29]

Here the general principles are presented, but later in this work, the attention is focused on Piezoelectric DOD technology, the one that has been used in this Master Thesis.



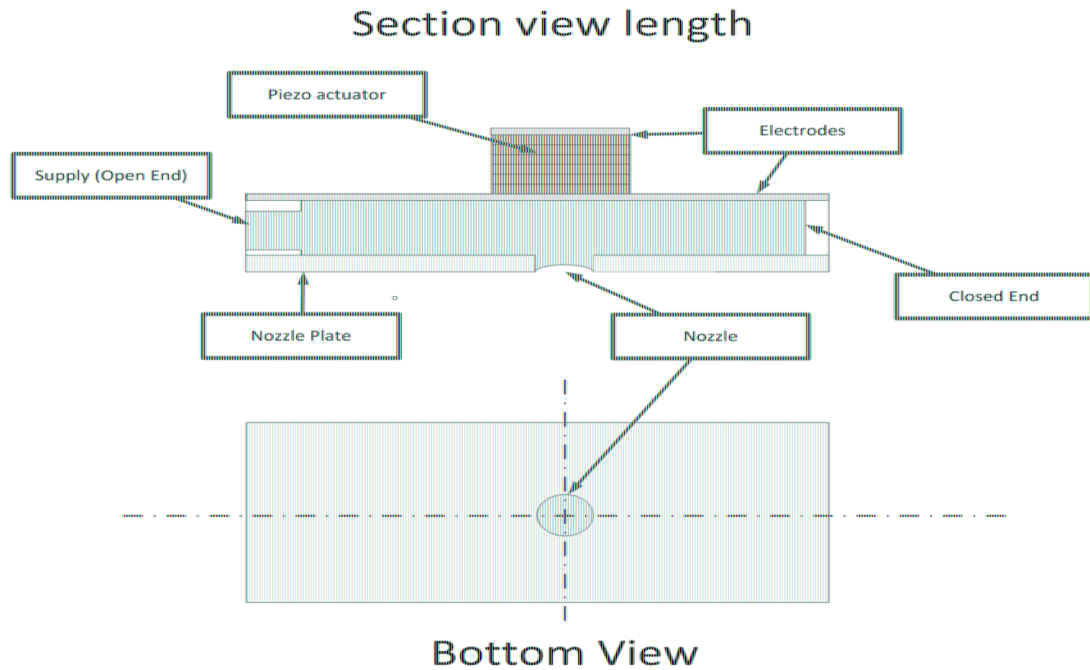


*Figure 17: Piezoelectric actuator [31]*

Viscosity in piezoelectric printheads are related to the frequency [31]:

- High performance range usually 4 - 20 mPa · s;
- Theoretical viscosities of up to 500 mPa · s possible;
- Viscosities out of the nominal range are usually only possible with frequency

Z-Number of the ink [31]:

- Often used as simple aid to estimate jettability;
- Inverse of the Ohnesorgenumber ( $Oh = \sqrt{We/Re}$ );
- Droplet formation process is a function of viscosity, surface tension, nozzle diameter, and shear rate.

Meniscus Pressure (Vacuum at nozzle level) is [31]:

- Usually 0 to - 25 mBar;
- Typical tolerance  $\pm 0.5$  mBar;
- Tighter tolerances for larger nozzle diameters;
- Positive pressures possible, but impractical;
- Affects engaging behavior.

A TIJ, thermal ink jet, printhead can also contain hundreds to thousands of micronozzles, each with its own ejection chamber. [31] A thin-film resistive heater is embedded into a wall of the ejection chamber. When a droplet is desired, the heater is activated by a short (microsecond)-duration voltage pulse. The voltage is of sufficient magnitude to raise the temperature of a thin layer of ink in contact with the wall (above the heater) to its boiling temperature, approximately  $300^{\circ}\text{C}$  for water under atmospheric pressure. Once this temperature is reached, the ink evaporates explosively and forms a homogeneous vapor bubble with a high initial pressure ( $>100$  bar). Given this pressure, the bubble expands rapidly into the ink chamber and ejects ink through the nozzle with enough momentum to form a droplet of a desired volume and velocity. The bubble subsequently collapses and the chamber is refilled with ink from a reservoir due to capillary pressure provided by surface tension. **Figure 18:**

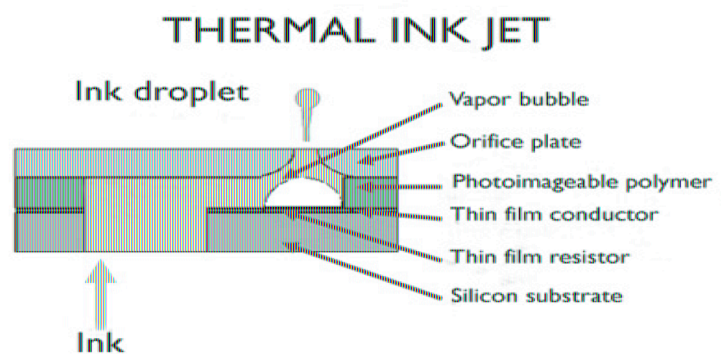


*Figure 18: Thermal Ink Jet [31]*

Characteristics of the Thermal Ink Jet printhead are [31]:

- Frequencies  $5 \sim 25$  kHz (Typically lower than Piezo DoD);
- Drop size  $1 \sim 50$  pl;
- Drop speeds  $\sim 5 - 10$  m/s.

Ink properties should be [31]:

- Typical viscosity  $1\text{--}5$  mPa  $\cdot$  s;
- Surface tensions  $18 - 60$  mPa  $\cdot$  s;

- Typically limited to aqueous or solvent inks;
- Life expectancy  $\sim 4 \cdot 10^8$  drops / nozzle.

For this reason, among the technologies of inkjet printers, piezoelectric technology was chosen in this work because, for tissue engineering, it must be considered that cells cannot survive at a temperature of 300°, being their maximum temperature of 37°.

### 2.2.3 Polymers in Inkjet Printing

Polymers fulfil many different roles both in formulation and end-use applications. The use of polymeric additives in both aqueous and solvent-based ink formulations is widely reported in both CIJ and DOD systems.

The formulation of polymer-based fluids presents a number of challenges. Foremost is the fact that polymer solutions can show significant non-Newtonian behaviour due to the shear rates experienced in inkjet printing, which impacts directly upon both jetting and drop formation behaviours and potential degradation of the polymer during the printing process. [29]

Polymers are long-chain molecules formed of small repeating units (monomers) and are ubiquitous in modern life, both in industrial and consumer goods. Polymers can be divided into two broad classes: thermoplastics and thermosets. Thermosets are cross-linked, and cannot be solution processed or recycled. Thermoplastics are polymers that are not cross-linked and can usually be dissolved in a solvent, and in most instances, will melt and flow.

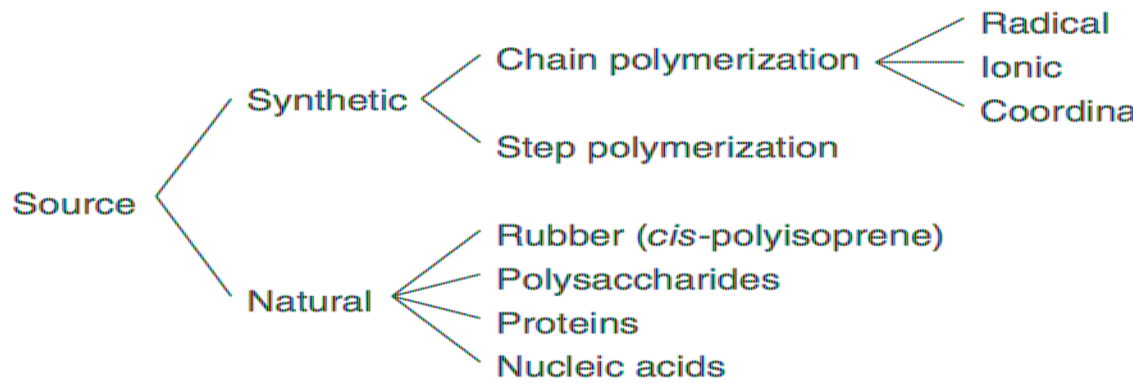


*Figure 19: Different types of polymers [29]*

The properties of polymer solutions are determined by both the molecular weight of the polymeric solute and the interactions between the polymer and the solvent. Both molecular weight and solution properties are determined by the nature of the monomer and the synthetic method used to produce the polymer. Polymers can be split into two categories: synthetic and natural, with synthetic polymers further characterized by either chain growth or step-growth polymerization.

Chain growth is a polymerization technique where unsaturated monomer molecules add to the active site of a growing polymer chain one at a time. Addition of each monomer occurs at the active site, which is radical, anionic, or cationic. Step-growth polymerization is a polymerization mechanism in which bifunctional or multifunctional monomers react to form first dimers, then trimers, longer oligomers, and eventually long-chain polymers. The resulting polymer is not limited to a linear configuration. By utilizing different synthetic methodologies, it is possible to generate widely varying polymer architecture, which can be used to control the physical and chemical properties. Several examples of different polymer architectures are listed in *Table 1*. The most fundamental questions that need to be answered about any polymer are: what are the sizes of the molecules of which it is composed, since all of the properties of a polymer solution, and thus to inkjet performance are critically dependent on the molar mass of the polymer.

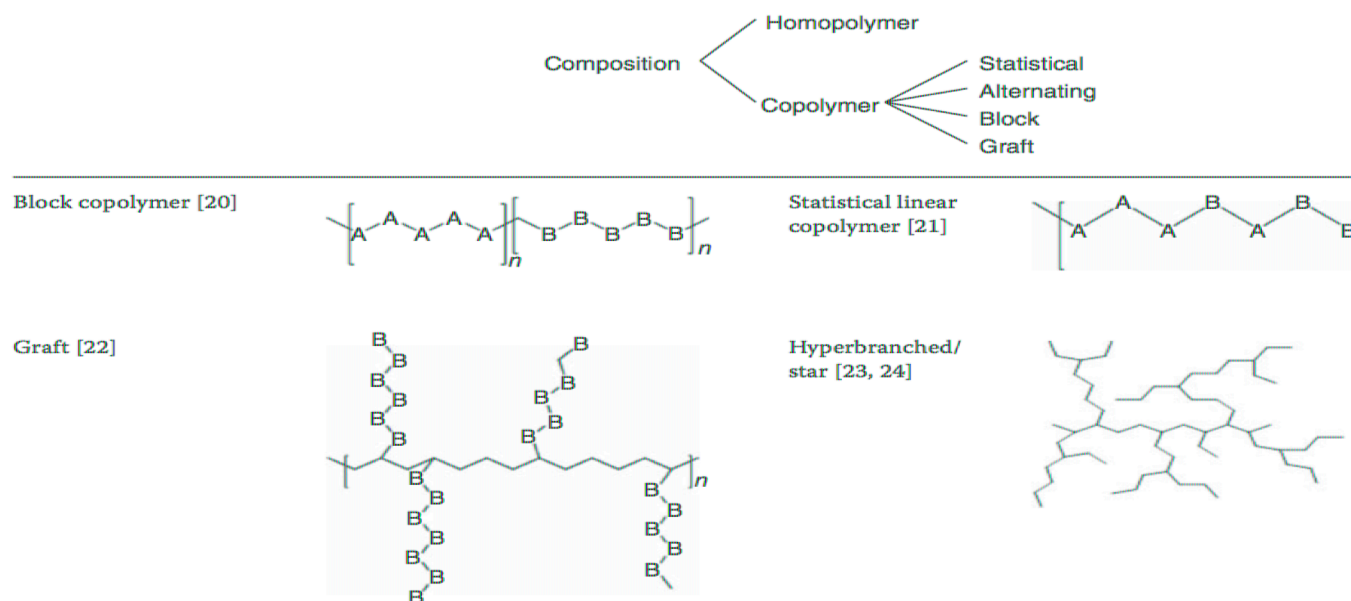


*Figure 20: Different polymer architectures [29]*

Molar mass,  $M$ , is expressed in units of  $\text{g} \cdot \text{mol}^{-1}$  or daltons ( $1 \text{ Da} = 1 \text{ g} \cdot \text{mol}^{-1}$ ). borne in mind that if SI units are used in the calculations, then it is appropriate to use  $\text{kg} \cdot \text{mol}^{-1}$  or kDa. Also, the “relative molecular mass” has the numerical value expressed in  $\text{g} \cdot \text{mol}^{-1}$ . The term “molecular weight” is traditionally used in polymer science, but some workers treat “molecular weight” as synonymous with “relative molecular mass,” but some workers treat “molecular weight” as synonymous with “molar mass.” When using molar masses from experimental data in any calculation, it is important that appropriate units are used [29].

For a small molecule,  $M$  is easily calculable from the chemical formula, but for a polymer, the situation is more complex apart from some naturally occurring polymers, which have a single molecular weight value, that is, they are monodisperse. Virtually all samples of synthetic polymers, and of many natural polymers such as polysaccharides, comprise a variety of species differing in  $M$ , that is, they are polydisperse. This is due to the nature of the polymerization process in which monomers add on to the growing chains with varying probabilities. Therefore, it is necessary to consider how the amount of polymer with a particular molar mass varies with  $\sum M_i$ , that is, the distribution of molar mass. Polymer molar mass is not a continuous variable, but for a high polymer, the number of species becomes very large, and the distribution can be represented as continuous curves, **Figure 21**.

In the continuous number-fraction distribution,  $n(M)$  versus  $M$ , the area of a slice  $n(M)dM$ , is the number fraction with molar mass in the range from  $M$  to  $M + dM$ . In the continuous weight-fraction distribution,  $w(M)$  versus  $M$ , the area of a slice  $w(M)dM$ , is the weight fraction with molar mass in the range from  $M$  to  $M + dM$ . The most probable distribution is an example of the “most probable” distribution, which is predicted by theory for step-growth polymerization or linear condensation polymerization in certain situations. Analytical techniques available for the determination of molar mass provide a single value for a polydisperse polymer sample, must therefore be an average value [29].

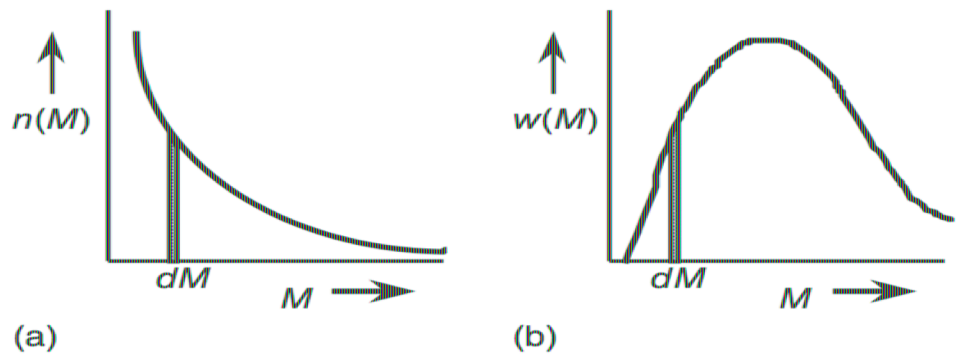


**Figure 21:** Illustration of (a) a number-fraction distribution and (b) the equivalent weight fraction distribution

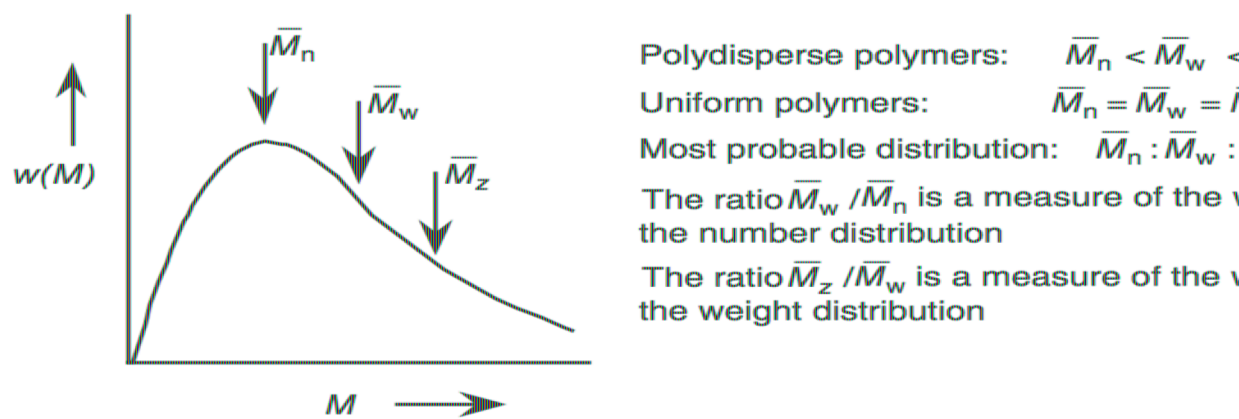


**Figure 22:** Representative molecular weight distribution showing the most probable distribution with the weight averages shown [29]



Important averages are:

$$\text{number average } (\overline{M}_n) \quad \overline{M}_n = \frac{\sum_i n_i M_i}{\sum_i n_i}$$

$$\text{weight average } (\overline{M}_w) \quad \overline{M}_w = \frac{\sum_i W_i M_i}{\sum_i W_i} = \frac{\sum_i n_i M_i^2}{\sum_i n_i M_i}$$

$$z - \text{average } (\overline{M}_z) \quad \overline{M}_z = \frac{\sum_i W_i M_i^2}{\sum_i W_i M_i} = \frac{\sum_i n_i M_i^3}{\sum_i n_i M_i^2}$$

and the relative positions of these on the molecular weight distribution are shown in Figure 1.

The techniques used to determine molecular weight can give different results depending on the physical basis of the experiment. Many of the techniques for the determination of molar mass provide a single value, which, for a polymer that is polydisperse, must be an average value.

Some techniques for the determination of molar masses of polymers may be regarded as absolute methods, in that they can be used to determine an absolute value for an average without calibration against samples of known molecular weight. Second-order moments of molecular weight determination require calibration against standards of known molecular weight [29].

Methods to determine the molecular weight based on colligative properties of polymers (such as membrane osmometry or end-group analysis) give  $\overline{M}_n$ , as these techniques are based on counting the number of polymer chains irrespective of the size. If the measurement is more responsive to polymer molecules of greater size, then a higher molecular weight is determined. An example of this is the determination of  $\overline{M}_n$  by static light scattering. Static light scattering was used in this project to calculate, given the molecular weights taken from the manufacturers of purchased elements, the amount of quantity of the various chemical compounds used in the solutions or as solvents.

A larger polymer molecule will scatter incident radiation to a greater extent than a smaller one, provided the polymer molecules are of the same size order of magnitude to the wavelength of the incident radiation. These primary methods require experimentally taxing

dilute polymer solutions and have generally been replaced by chromatography [29].

### 2.2.3.1 Polymer Solutions

A polymer solution, that is, polymer dissolved in a solvent, can be described in different solvent regimes. In a poor solvent, a polymer will occupy a tight, contracted conformation because polymer-polymer interactions are energetically favourable as compared to polymer-solvent interactions. In a good solvent, the polymer-solvent interactions are favourable and the polymer adopts an expanded self-avoiding walk conformation. In a solvent of intermediate quality, at a certain temperature and pressure, the polymer occupies its ideal random walk/ideal coil conformation. When this condition is met, it is possible to measure the physical properties of the polymer without the influence of solvent effects [29].

When considering polymer solutions in the context of inkjet printing, it is important to understand the fundamental nature of the polymer-solvent interaction, and this information can be obtained from the determination of the intrinsic viscosity,  $[\eta]$ . The intrinsic viscosity is defined as the volume occupied in solution by a unit mass of polymer in a specific solvent, commonly used in polymer sciences using the unit  $\text{g} \cdot \text{dl}^{-1}$ . Depending on the nature of the interaction between the polymer and the solvent, the intrinsic viscosity can vary widely for a specific polymer-solvent system. The relationship between the intrinsic viscosity and the molecular weight is expressed by the phenomenological Mark-Houwink-Sakurada:

$$[\eta] = KM^a$$

where  $M$  is the molecular weight and  $K$  and  $a$  are the empirical constants, which are determined experimentally for the most linear polymers in common solvent systems or determined experimentally.  $K$  and  $a$  are dependent upon the specific polymer-solvent system while  $a$  gives additional information about the polymer architecture. For  $a = 0,5$ , the polymer is either in its  $\theta$  state or highly branched; for  $a = 0,6 - 0,8$  for a coil conformation in a good solvent, and  $a = 1$  for a rigid-rod-type polymer. It is common to see  $\alpha$  used interchangeably with  $a$ , but  $a$  is the correct notation for the exponent.



Printability of inkjet fluids can be predicted to a first approximation by considering the Weber number ( $We$ ) and the Reynolds number ( $Re$ ). The Weber number is important in the early stages of drop generation/ejection where the interplay of forward inertia and surface tension is most important and the Reynolds number in the middle to latter stages (while the drop is still in flight) where the interplay with the viscoelasticity of the ligament is critical.

$$We = \frac{\rho(v^2)L}{\sigma}$$

$$Re = \frac{\rho v L}{\eta} = \frac{v L}{\nu} \quad \text{as} \quad \nu = \frac{\eta}{\rho}$$

where  $\rho$  is the density,  $\sigma$  is the surface tension,  $v$  is the drop velocity,  $\eta$  is the dynamic viscosity,  $\nu$  is the kinematic viscosity, and  $L$  is a characteristic length (often drop length). Early on, out a simulation work that predicted inkjet drop behavior and drop morphology for  $Re/We > 2$ , but did not explicitly state printability conditions or printing ranges. This work was expanded by Reis and Derby, using the Ohnesorge number ( $Oh$ ) to predict printability during flight and give a range of values of  $Oh$  for which inkjet printing is possible. Using  $Oh$  has the advantage that the drop velocity dependence is removed [29]:

$$Oh = \frac{\sqrt{We}}{Re} = \frac{\eta}{\sqrt{\rho \sigma L}}$$

It was found through fluid dynamics simulations and printing studies of fluids with various physical properties that, within the range  $0.1 < Oh < 1$ , DOD printing is possible. If  $Oh > 1$ , viscous dissipation within the liquid prevents drop formation, and if  $Oh < 0.1$ , the balance between surface tension and viscosity results in the liquid breaking into a series of droplets rather than a single drop as desired. In some publications, the inverse of the Ohnesorge number ( $Z$ ) is used to describe printability ranges. In practice, systems in which  $Oh$  is in the range 0.1 to 1 are printable so long as the satellites merge with the main droplet.

The majority constituent of the ink is the solvent, and the density of the ink is not significantly affected by polymeric or other additives [29]. The generally recognized surface tension range for inkjet formulation is  $20 - 50 \text{ mN} \cdot \text{m}^{-1}$ . This is in the general range for the surface tension of organic solvents commonly used for ink jet formulations (xylene, toluene,

phthalate (DEP)) with the most linear polymers not being surface-active to Aqueous inkjet fluids are controlled to be within the surface tension limits by small amounts of cosolvent and/or surfactants. The characteristic length ( $L$ ) is by nozzle geometry rather than any physical effects due to polymer concentration

### 2.2.3.2 Van der Waals Attractive Force

Short-range van der Waals (vdW) attractive forces are due to electric dipole fluctuations between neighboring particles and are a sum of all single interactions acting on the cores of the particle cores.

The cell membrane can have positive or negative ions on its surface based on its activity that takes place inside the cell and the suspension medium in which the cell is. Based on this superficial charge that they may or may not present, the cells can be attracted or rejected according to the Van der Waals attractive force. They can be considered as particles with superficial charge.

This attractive interaction is typically effective up to a separation distance,  $h$ , of about  $23\text{ nm}$ . At larger distances, the attractive force decays rapidly due to retardation effects.

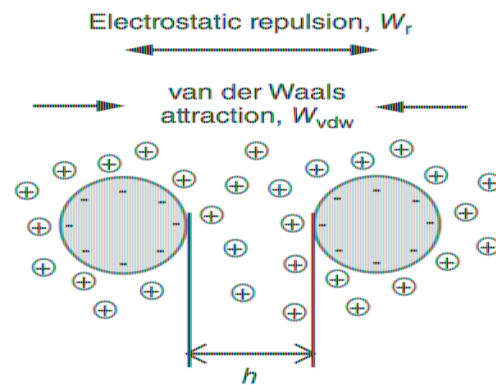


**Figure 23:** Schematic of DLVO interactions experienced by two approaching colloidal particles.

The summation of all the interactions assumes pairwise additivity and is expressed as the total interaction energy,  $W_{vdW}$ , for two spherical particles of radii,  $r_1$  and  $r_2$ , with small surface charges.

$$W_{vdW} = -\frac{A}{6} \left[ \frac{2 r_1 r_2}{a^2 - (r_1 + r_2)^2} + \frac{2 r_1 r_2}{a^2 - (r_1 - r_2)^2} + \ln \left( \frac{a^2 - (r_1 + r_2)^2}{a^2 - (r_1 - r_2)^2} \right) \right]$$

where  $a$  is the centre-to-centre distance between spherical particles,  $r_1$  and  $r_2$  are the radii of the two particles, and  $A$  is the Hamaker constant, which is material-dependent but typically falls in the range of  $10^{-21}$  and  $10^{-19}$  J [29]. Note that, as a result of the aforementioned simplification, the following relationship applies;

$$a = r_1 + h + r_2$$

When the separation distance between particles is significantly smaller than the diameter of the particles (i.e.,  $h \ll r_1$  or  $r_2$ ),  $W_{vdW}$  equation can be simplified to:

$$W_{vdW} = -\frac{A r_1 r_2}{6 h (r_1 + r_2)}$$

For two equally sized spherical particles of radius,  $r$  this becomes:

$$W_{vdW} = -\frac{A r}{12 h}$$

### 2.2.3.3 Electrostatic Repulsive Force

When a particle is dispersed in an aqueous phase (such as aqueous mixtures of water and a typical inkjet ink solvent), the particle may acquire a surface charge, with the aid of dissociation of surface groups or adsorption of charged molecules/ions. The charged particle attracts counterions and co-ions from the surrounding bulk phase to restore the electroneutrality of the system within a specific volume around the particle surface [29]. This is known as the *electrical double layer* and is schematically represented in **Figure 24**. The electrical double layer consists of two regions:

- Counter-ions closest to the particle surface are strongly bound to the surface and are known as the *Stern layer* and corresponds to a volume of liquid that is adjacent to the particle;

- A volume of loosely associated ions form the diffuse layer, which is replenished as the particles undergo Brownian motion.

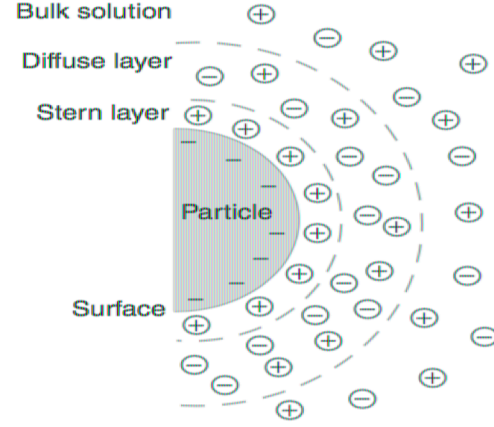


**Figure 24:** Schematic of electrical double layer of a charged particle [29]

When two particles approach one another, the electric double layers of the respective particles will overlap. As the local concentration of ions in the overlap volume increases, the osmotic pressure difference with the bulk phase induces a difference in osmotic pressure, which tends to push the particles apart. Provided the force induced by the electric double layer overlap is high, this process will maintain particle stability against aggregation in the colloidal system. The strength of the repulsive interaction is dependent on the distance between the particles, which is the thickness of the electric double layer [29]. This thickness is known as the Debye length,  $K^{-1}$ , which is defined in:

$$K^{-1} = \left( \frac{F \sum N_i z_i^2}{k_B T \epsilon_0 \epsilon_r} \right)^{1/2}$$

where  $F$  is the Faraday constant;  $N_i$  and  $z_i$  are the number density and valence of ion type  $i$ , respectively;  $k_B$  is the Boltzmann constant;  $T$  is the absolute temperature;  $\epsilon_0$  is the permittivity of vacuum; and  $\epsilon_r$  is the dielectric constant of medium.

Aside from the characteristics of the bulk phase in which the colloidal particles are dispersed,  $K^{-1} = \kappa$  is highly dependent on the type and concentration of electrolytes present.

phase. Indeed, as the concentration of electrolyte in the system increases, the said to “screen” the surface charges of the particles, effectively decreasing the layer thickness and allowing for particles to approach shorter distances before the This may allow for vdW attractive interactions to be strong enough at this distance to overcome the repulsive forces and bring the particles into contact to form aggregates [29]

The long-range electrostatic repulsion interaction energy,  $W_r$ , for two equally sized particles of radius  $r$  is represented by:

$$W_r = \left( \frac{64\pi k_B T N_i \gamma^2}{\kappa^2} \right) \quad \text{with} \quad \gamma = \tanh \frac{ze\Psi}{4k_B T}$$

where  $e$  is the charge of an electron and  $\Psi$  is the particle surface potential.

### 3 Cell Culture

Cell culture is a homogeneous group of eukaryotic cells, in which there are nucleus and other organelles enclosed within membranes, of tissue origin that can grow and multiply in vitro for several generations. Both plant and animal cells can grow in the laboratory. Cell cultures are kept in liquid medium in sterile containers (flasks, bottles or Petri capsules) in particular experimental conditions that reproduce the chemical-physical conditions of the natural cellular environment.

Early studies of the possibility of cultivating animal and human cells in an artificial environment date back to the nineteenth century when W. Roux, in 1885, managed to keep for few days in vitro brain cells of a chicken embryo [32]. Subsequently, several attempts were made to cultivate many types of isolated cells from different living organisms, but decisive progress was made in 1943 when Earle succeeded in cultivating of the first mammalian cell lines [33], and ten years later with Scherer who cultivated the first human tumour cell line, called HeLa cells [34].

HeLa cells are called by the name of Henrietta Lacks, a cancer patient from whom these cells were taken for diagnostic purposes. Even today, HeLa cells, which can be indefinitely divided, are cultivated and are being studied in many laboratories. Thanks to the development of sterility techniques and the use of ever-growing and perfectly balanced crops in their components, the use of animal cell cultures has been greatly expanded and has become an irreplaceable tool since it has made it possible to use a simplified and reproducible "model system" for the study of biochemistry and cellular physiology.

There are numerous applications in many scientific research fields. Cell cultures are currently being used:

- for the production of pharmacologically active substances (antibodies, vaccines, growth factors, etc.);
- in drug toxicity tests before they are tested on animals or humans;
- in ecotoxicity tests, to assess the effect of environmental pollutants;
- in studies of physiology and cellular development mechanisms;
- in oncological studies;
- in the diagnosis of genetic diseases;
- in the creation of transgenic organisms;
- in tissue engineering.



The use of cell cultures, in addition to the many advantages represented above all by the ability to control and standardize the physical and chemical conditions of the environment in which it operates, the relative simplicity of experimental conditions and their reproducibility and rapid response times, but it presents some limitations [35]:

- objectively different conditions from those in vivo;
- possibility to study only acute toxicity, but not chronic toxicity of a substance;
- inability to study complex phenomena of cellular interaction;
- ease of contamination by microorganisms;
- possibilities of alterations and mutations.

Cells that make up cell cultures are obtained from organs removal, biopsies of animal tissues that are surgically removed and mechanically or enzymatically fragmented until a cell suspension is transferred into sterile glass or plastic containers.

In order to recreate the naturally environment in vitro, cells are immersed in an appropriate culture medium, that is, an isotonic solution that contains nutrients, mineral salts, amino acids, growth factors necessary for their growth. Cells are, then, kept at the appropriate temperature within appropriate incubation systems: the temperature should be at 37°C and the gaseous phase at 5% CO<sub>2</sub> and 95% O<sub>2</sub>. In optimal environmental conditions, cells of the connective tissue, epithelial tissues of the nervous system (solid tissues) adhere to the substrate by assuming their characteristic form and begin to multiply giving rise to a primary culture. The cells grow up to occupy the entire surface of the container (Petri dish or flask) thus coming into a single layer. At this stage, normal cells cease to grow because of the phenomenon of contact inhibition and enter the retirement phase, so to keep them alive it is necessary to transplant (or pass them) into other flasks with appropriate dilution liquid. Tumour cells, on the other hand, if environmental conditions allow, continue to grow staggering to each other as they do not suffer from contact inhibition.

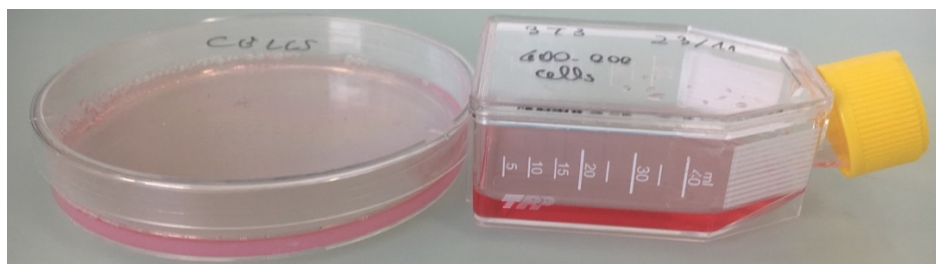


*Figure 25: Petri Dish and 40ml Flask. Image taken from the laboratory [36]*

### 3.1 Working under Laminar Flow

The Laboratory must be an isolated and self-sufficient area. To better separate the environments, it is necessary to create a double area for the entrance of people in the laboratory.

The main tools used in cell culture are:

- Biological Safety Cabinet
- Incubator;
- Centrifuge;
- Confocal microscope.

Basic rules to be applied in a cell culture laboratory are:

- allowing the simultaneous access of a few people in the laboratory
- do not manipulate cells of dubious origin in the main work area or at the same time as other cell lines;
- keep the cells in culture for no more than 25 steps, 2/3 months depending on the type of cell line;
- keep the cells for a short time at the confluence.

The Biological Safety Cabinets (Laminar Flow) are distinguished by the level of containment in three classes (I, II and III), the microbiological protection (II and III), the various degrees of protection for the operator and the types of HEPA filters (High Efficiency Particulate Air) within them. **Figure 26**

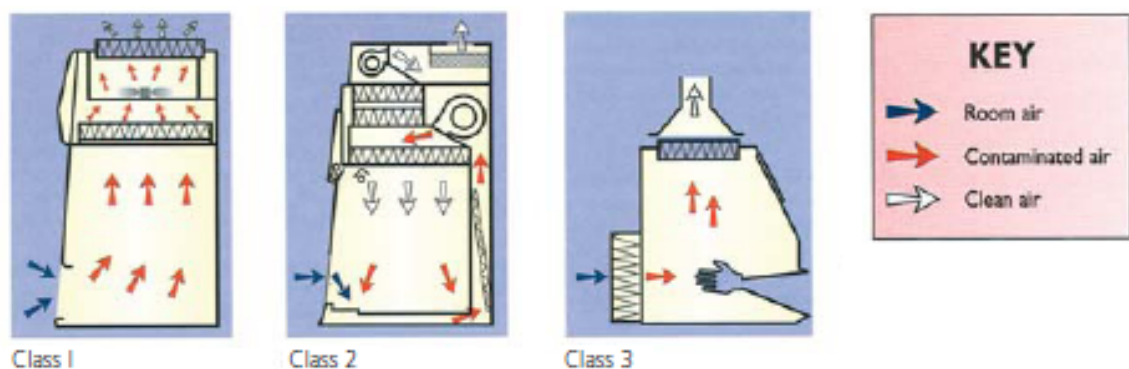


*Figure 26: Biological Safety Cabinet: Class I, Class II and Class III [37]*



In the laboratory at the iPrint Institute, the Biological Safety Cabinet Class II is present.

**Figure 27**



*Figure 27: Biological Safety Cabinet Class II [36]*

Horizontal Biological Safety Cabinet has microbiological protection for crops, but no protection for the operator because it is open from the front; HEPA filters are placed on entry. **Figure 28**

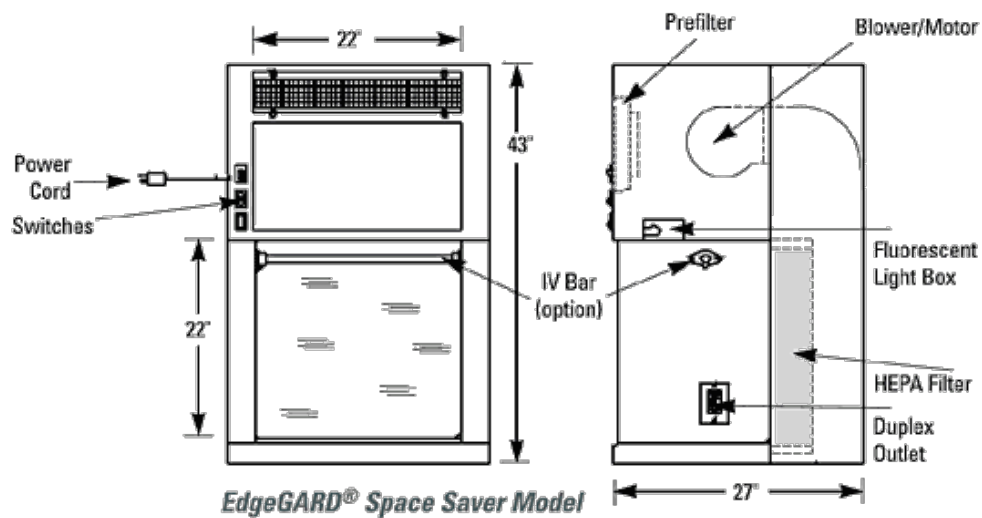


*Figure 28: Schematic of Horizontal Biological Safety Cabinet [38]*

The incubator maintains the optimal environmental conditions for cell culture, that is the temperature at 37 °C, the humidity (about 98%) and the pH at 7,4 (CO<sub>2</sub> bicarbonate buffer system). It is necessary to carry out a regular cleaning and control of the parameters before and after use. At the bottom of the incubator there must be water with disinfectant, copper sulphate and antifungal agents.

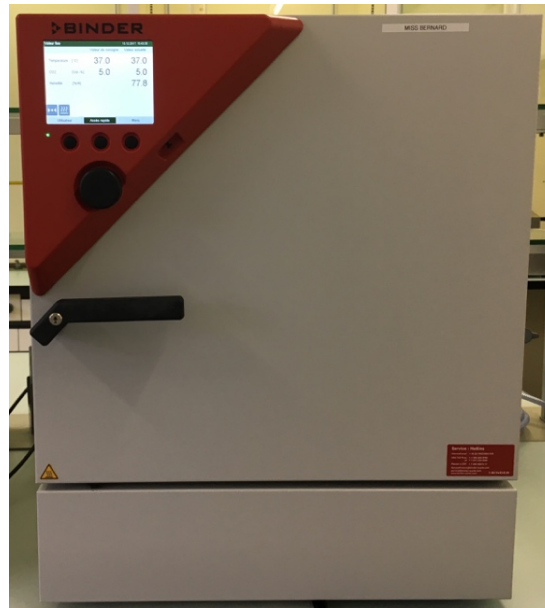


*Figure 29: Incubator [36]*

The centrifuge, **Figure 30**, avails to separate cells from the liquid in which they are found.



*Figure 30: Centrifuge [36]*

To determine the number of RPM and minutes needed to separate cells from the solution they are in, a viability test was performed with three different spin settings in the following way. Fibroblast 3T3 cells were used in the concentration of  $3 \cdot 10^6$  cells/ml as these cells will be selected and used for hydrogel printing. Since with centrifugation in DMEM there should not be any mortality problems, and that this type of cells is printed in Alginate-based hydrogel, the centrifugation test was done by using a possible simulation through pipet of the printing process. The Alginate particles present in the hydrogel could cause cell death in the centrifugation process because they would create a higher pressure based on the speed and on the time. Subsequently the cells viability was tested with Trypan Blue Solution.

Cells were counted in the right concentration, placed in a hydrogel solution, mixed and crosslinked with a Calcium Chloride based solution and subsequently dissolved with the Sodium Citrate Solution (procedure to mimic the simplest printing process with Alginate-based hydrogel). At this point three different centrifugation parameters have been chosen and tested to separate cells from the solution obtained because to carry out the viability test it is necessary to separate the cells from the solution, remove the liquid and insert the DMEM in the same amount of hydrogel in which cells were insert.

Results, shown in **Figure 31**, show that there is not a particular incidence of cell mortality at the increase in the number of revolutions per minute and the minutes set in the centrifuge. Acceleration chosen, to sediment cells without damaging them, is 1200 revolutions per minute (RPM) x 7 minutes. Centrifugation is an operation that must always be done by balancing the liquids inside flacon tubes, 2 or 6 tubes each time.

### 3T3 Viability Tests after Centrifugation

Trypan Blue Method with Confocal Microscope					
3/4 N27 + 1/4 PBS/EDTA	Alive Cells (cells/ml)	Dead Cells (cells/ml)	Total Cells (cells/ml)	Alive Cells Percentage %	Dead Cells Percentage %
1000 RPM x 5 min	470000	30000	500000	94,0	6,0
1200 RPM x 5 min	850000	60000	910000	93,4	6,6
1200 RPM x 7 min	1060000	50000	1110000	95,5	4,5

*Figure 31: Centrifugation Test with Fibroblast 3T3 Cells [36]*

**Figure 32** shows an example of cells separated from the DMEM after centrifugation.

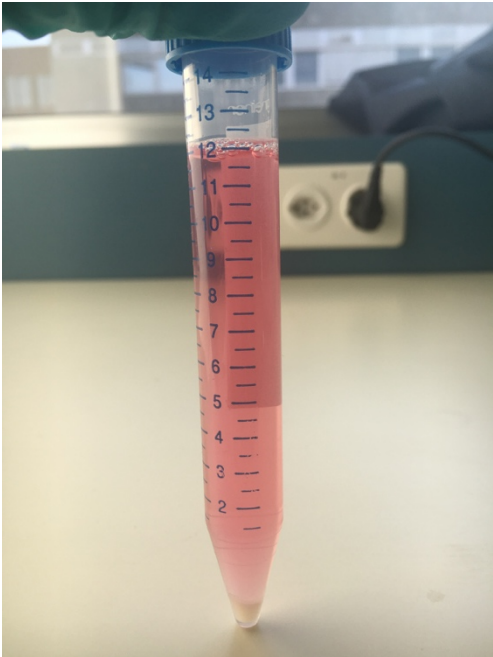


*Figure 32: Lung Epithelial Cells A549 separated from the DMEM 10%FBS*

The confocal microscope, **Figure 33**, is an optical microscope, a scientific instrument that is based on a technology aimed at significantly increasing the spatial resolution of the sample, eliminating the halos due to the light diffused by the out-of-focus planes of the preparation. It is schematically constituted by a normal transmission microscope to which is superimposed an apparatus that deals with illuminating and detecting the image of an illuminated sample with a point-to-point scan. The method of image formation in a confocal microscope differs from that of a conventional compound microscope due to the fact that, while in the second the illumination beam invests the entire sample and instantaneously forms the image on the detector, in the first the light coming from the source it illuminates the object only one point at a time and a scan is needed to form the final image. The use of this technique allows to achieve very small axial resolutions. In fact, an image thus obtained is commonly called "optical section", in reference to the fact that it is possible to investigate the sample in the three spatial dimensions with a non-invasive method.

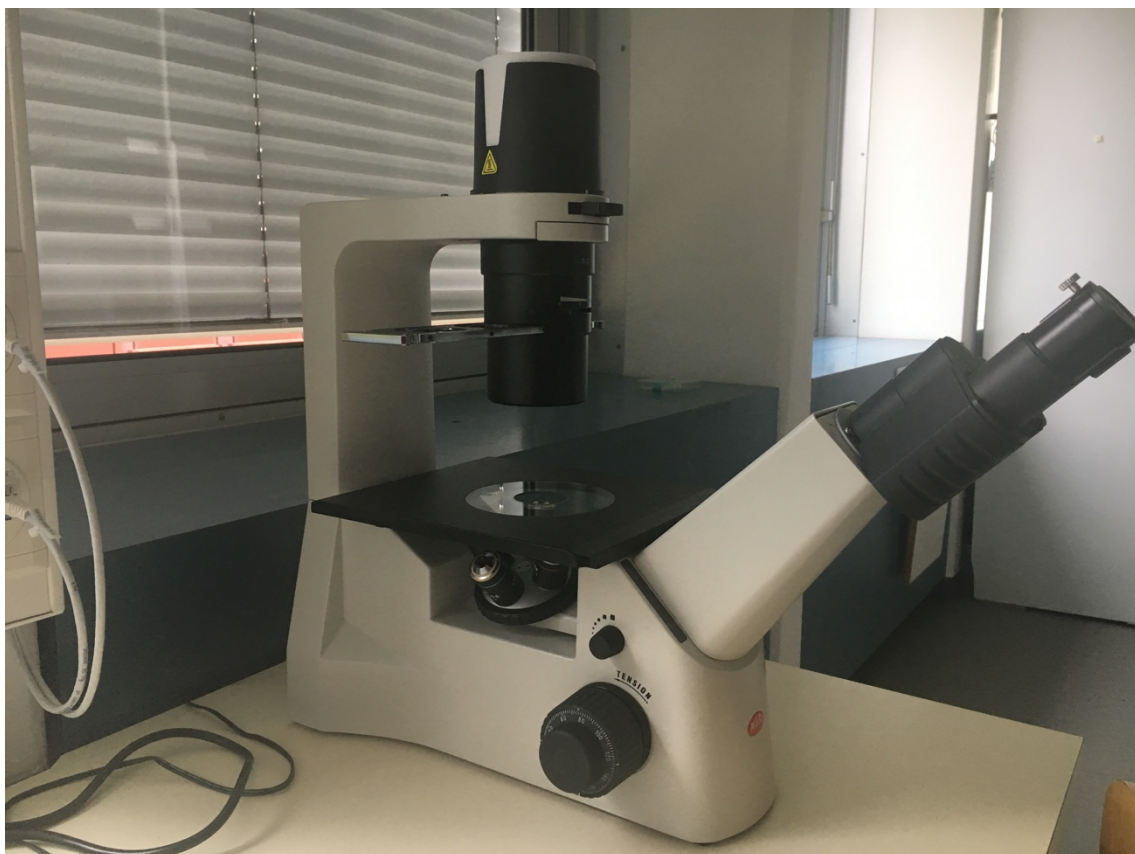


*Figure 33: Confocal Microscope [36]*

In confocal microscopy **Figure 34**, the spot light spot is produced by a pinhole placed in front of the source, that is to say replacing the field diaphragm, which is so fixed is very small. The light is then focused by the collector and by the condenser (or by the lens, in the case of configuration in reflected light) on the sample, and then collected by the lens and the possible ocular and focused on a second pinhole. In correspondence to this there is also the image detector, which produces a signal proportional to the intensity of the light that hits it.

The pinhole of illumination and that of revelation belong to conjugated focal planes and are therefore said to be confocal, hence the name of this particular microscopic technique.

Almost all modern confocal systems use the configuration in reflected light, which, as anticipated by Minsky himself [39], increases the symmetry and resolution of the system at the expense of brightness, which is reduced by the presence of the dichroic mirror or beam-splitter.

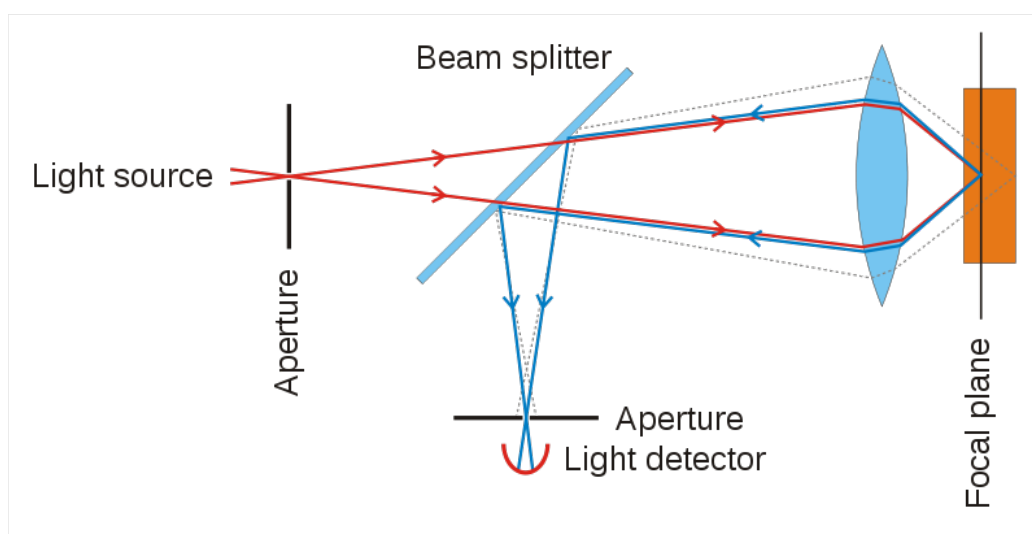


*Figure 34: Schematic of essential structure of a confocal microscope [40]*



## 3.2 Taking Care of Cells

The morphology of cultured cells reflects that of the tissue in vivo. Solid tissue cells grow in monolayer, adhering to the substrate of the container. The fibroblasts, for example, assume the typical fusiform form, epithelial cells (from lung) polygonal. **Figure 35** In this project, rat cells, fibroblast 3T3 and lung epithelial A549 cells are used. Hemopoietic cells (lymphocytes, erythrocytes) are cells that remain suspended in the culture medium and do not adhere to the substrate of the flask: as in vivo circulating in the bloodstream, so in vitro grow in suspension taking on a spherical form. There are also cell lines, such as monoclonal B-monocytes B95-8, which exhibit a heterogeneous cell population, some of which are adherent while others grow in suspension [41].

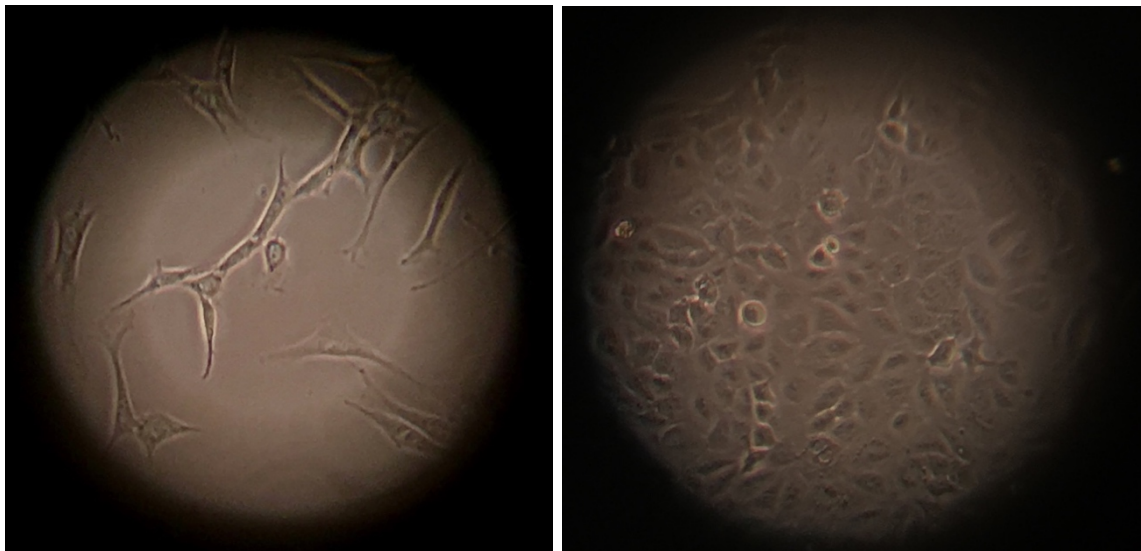


*Figure 35: Fibroblast 3T3 and Lung Epithelial cells A549 [36]*

### 3.2.1 Medium Change

For cells to be cultured in vitro, optimal chemical and physical parameters must reproduce the natural conditions of the organism. As for the fundamental parameters (culture medium, pH, relative humidity, O<sub>2</sub> and CO<sub>2</sub>, temperature requirements), all cells generally have the same basic chemical and physical requirements. The basic culture medium is an isotonic and buffered solution that can provide all the essential substances for survival of the cells.

There are different types, which differ in the concentration of the basic substances listed below:

- water;
- mineral salts ( $\text{Na}^+$ ,  $\text{K}^+$ ,  $\text{Mg}^{++}$ ,  $\text{Ca}^{++}$ ,  $\text{Cl}^-$ ,  $\text{HCO}_3^-$  etc.) that help to determine the osmotic pressure of the medium and the cell membrane potential.  $\text{Ca}^{++}$  also promotes cell adhesion and  $\text{NaHCO}_3$  is added to a number of soils as a buffer;
- a carbon source (glucose and/or glutamine);
- amino acids;
- vitamins;
- pH indicator (usually red phenol).

In the base culture medium, a variable percentage of 5 to 20% of bovine serum is added.

For the lung epithelial cells, 10% of Foetal Bovine Serum (FBS) is added because it is rich in growth factors and hormones, adhesion factors (fibronectin), mineral salts useful as cofactors of enzymes, lipids, proteins (transferrin, albumin) essential for promoting cell adhesion, development and proliferation. For the fibroblast 3T3, 10% of Calf Serum (CS) is added because it has less growth factor and more iron.

Antibiotics and antifungal drugs are added to this formulation to prevent microbial contamination.

The soil pH should be between 7 and 7.4. In the soil, there is a pH indicator, the red phenol, which in neutral pH conditions is red, in alkaline pH purple and in acidic pH yellow-orange. With the advancement of cell proliferation, the soil tends to acidify because inside it accumulates  $\text{H}^+$  and catabolites (there is a metabolic activity of cells). The soil contains a buffer system that is generally carbonate/bicarbonate, able to guarantee the pH stability at least until excessive variations occur. When the soil turns orange/yellow, the acidity is too high and the soil is replaced. In the thermostat,  $\text{CO}_2$  is suffused until a partial pressure of 5% corresponds to the measured  $\text{CO}_2$  pressure in human tissues and is also used for pH adjustment. Partial oxygen pressure is ensured by the presence of atmospheric air inside the thermostat.

The optimum growth temperature for mammalian cells is 37° C: it is maintained by placing cultures in a specific thermostat that ensures not only maintaining the constant temperature but also the appropriate percentage of relative humidity. In the bottom of the unit water is added, which, by evaporation, avoids the drying of the liquid ground placed in the flasks.



### 3.2.2 Difficulties in Cell Culture

If the working conditions are not completely sterile, it may happen that fungi and bacteria attack the cell lines in culture and kill them. For this reason, first of all, in addition to the serum (Foetal or bovine), antibiotics must be included in DMEM formula and finally, if bacterial infections persist in the culture, directly eliminate the entire cell line and clean all the instruments used and the laboratory. **Figure 36** shows two different types of fungi (both figures on the left) and a type of bacteria (figure on the right) found in cell culture due to an inaccurate initial cleaning of the laboratory. The problem was solved, in a short period, by eliminating the cell culture, thoroughly cleaning and defrosting other cells belonging to the same cell line.

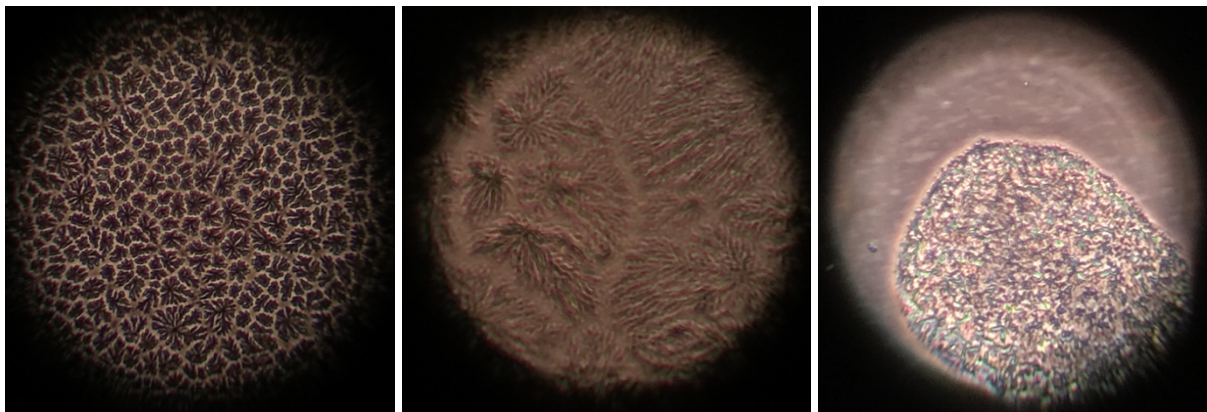


*Figure 36: Fungi and Bacteria (40x) [36]*

### 3.2.3 Cell Passage

Transplants (or passages) are performed by the use of an enzyme, trypsin, which favours the digestion of membrane glycoproteins that anchor cells to the substrate. Technically, this operating phase is called the trypsinization and allows to obtain a cell suspension which, suitably diluted, may be transplanted into new flasks and allow the growth of new cells (culture retention). Primary crops usually take a few steps because cells go to a phenomenon of senescence, state in which the cell is no longer able to proliferate, so they die. Sometimes some cells of a primary culture are subject to spontaneous (or induced) mutations that alter their cellular characteristics: an increase in duplication speed and the disappearance of senescence

may occur. The cells become so immortal, with unlimited growth over time. A stabilized or continuous cell line is formed that can proliferate continuously if maintained under suitable conditions. There are also immortal cell lines that are transformed because they are derived from tumours (such as HeLa cells) or cells that become immortal following genetic manipulation (insertion of oncogenes) or that become viral transformation. These are the case of the fibroblast 3T3 and Lung Epithelial cells, both of them are used in this work.

According to the laboratory procedure, before using the trypsin, it is necessary to aspirate the medium from the flask and to put inside the PBS 1X, Phosphate Buffer Saline, to remove bivalent ions, which would hinder the trypsin action. Subsequently, the PBS 1X is removed and the trypsin 0.25% Ethylenediaminetetraacetic acid (EDTA) is added. It is allowed to act for 3-5 minutes at 37° C, allowing them to act optimally only on these proteins and safeguarding the other cell proteins. Afterwards, to stop the trypsin effect, it is necessary to add fresh ground. After these passages, a volume of this suspension is removed from the mother plate and poured into the new plate where fresh ground is already present. On the new plates, the name of the cells is written, the date of the passage, the number of the passage and the dilution done.

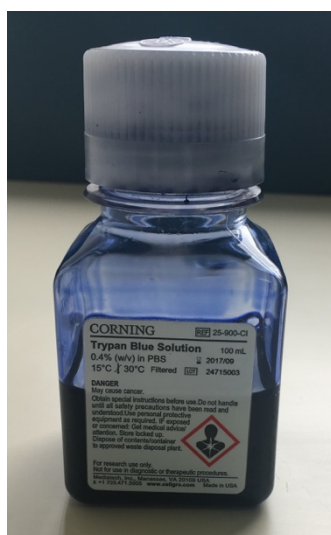


*Figure 37: Trypan Blue Solution [36]*

To count the cells, according to the laboratory procedure, an Eppendorf is taken and 50µl of cells are diluted in 50µl of trypan blue, **Figure 37**.



*Figure 38: Haemocytometer [36]*

After mixing trypan blue and cells, 25µl of this solution is put in the haemocytometer **Figure 38**, in both sides. In this measurement device, there is the Burke Chamber **Figure 39**, a square divided in 25 little squares inside it, that allow to count statistically cells in 1ml under the confocal microscope (focused at 10x). In each side, there is one Burke Chamber, for this reason the calculation of the number of cells/ml is: (number of cells in the first chamber + number of cells in the second chamber) · 10.000.

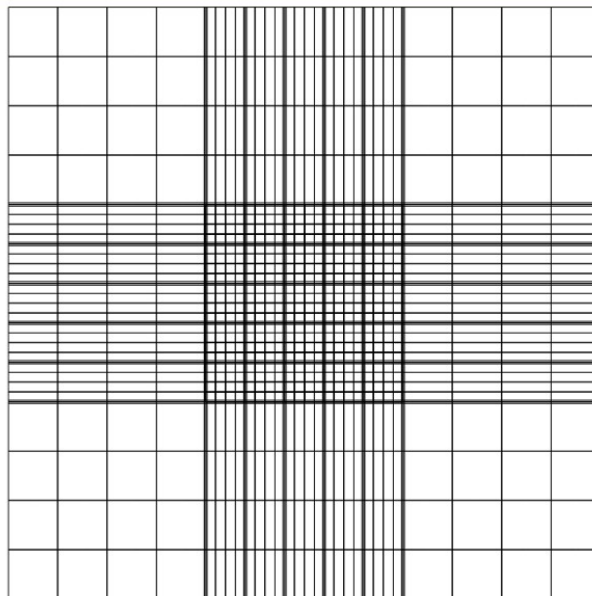


*Figure 39: Burke Chamber [42]*

### 3.3 Trypan Blue and Live/Dead Assay

Every researcher working in cell cultures needs some kind of solution that can count cells, both to determine cell concentration and to evaluate cell viability after different treatments.

Among the well-known vital cell counting methods developed so far, manual counting with a haemocytometer is the most commonly used method for its low cost and versatility.

This method depends on the analyst's ability to evaluate different cellular attributes, regardless of cell type; moreover, it allows to use different colouring techniques according to the purpose of the analyses. Generally, the counting takes place with the aid of a confocal microscope, a haemocytometer, a slide engraved with a counting grid and subjecting an aliquot of the culture by means of vital staining with Trypan blue.

Trypan Blue (Blue Benzamine, Blue Naphthylamine, Blue Niagara) **Figure 40** was synthesized in the early twentieth century as a derivative of toluene, and owes its name to the property of being toxic to the trypanosome parasite. Trypan Blue is commonly used in vital staining with a method defined as exclusion staining. In fact, cell membranes are normally impermeable to this dye, while dead cells, both apoptotic and necrotic, are coloured blue. [43]

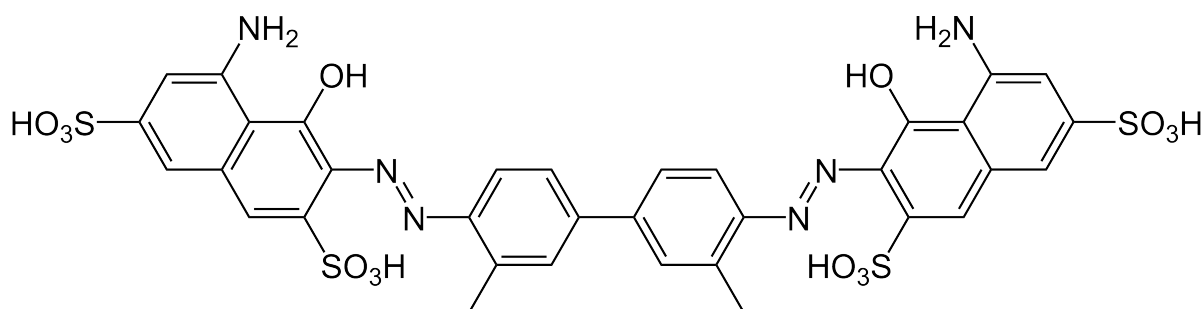


*Figure 40: Trypan Blue [44]*

The procedure for collecting the cells and being able to count them with the Trypan Blue method is the same as described in the paragraph 3.2.3 *Cell Passage*.

Unfortunately, the Trypan Blue procedure cannot be applied in each situation to count live and dead cells. For this reason, another method is described in the Live/Dead Assay, it is more accurate but very expensive and not fast like the first one. The Live/Dead kit is useful in situation in which is very difficult or not possible to put cells in DMEM/Trypan blue solution (or in general

liquid solutions), i.e. if cells are inside a piece of crosslinked hydrogel (Alginate based) on the Agarose (formulated with also  $\text{CaCl}_2$ ) in the petri dish and the operator should count them after printing or pipetting without damage them.

The kit [45] is composed by Calcein AM, 4mM, (= 494/517nm) and Ethidium homodimer-1, 2mM, (EthD-1 in the presence of DNA = 528/617 nm): the EthD-1 stains dead cells in red with fluorescent microscope, the Calcein AM stains live cells in green with fluorescent microscope.

In 0,25-2% Alginate hydrogel, concentrations to use are EtDh-1 100  $\mu\text{M}$  and Calceine 98  $\mu\text{M}$ .

The dye solution is prepared adding sterile PBS under the laminar flow in the following concentration: 1  $\mu\text{l}$  Calcein + 2,5  $\mu\text{l}$  EthD-1 + 40  $\mu\text{l}$  PBS. Then, the dye solution (1  $\mu\text{l}$  diluted with 50  $\mu\text{l}$  of DMEM) is quickly put on the top of the hydrogel (with cells inside) and let acting 30 minutes in the incubator.

After this procedure, it is possible to use the fluorescent microscope to watch live and dead cells: the green optic filter is to see the green fluorescence and indicates live cells, the red optic filter acts at the same way for dead cells.

### 3.4 Cells Preparation for Printing

Cells concentration for printing should be  $3 \cdot 10^6$  cells/ml because the operator needs to be sure that cells come out nozzles every time after a printing process: if cells are not enough, it could be possible to generate drops without cells; otherwise if cells are too much, nozzles can be blocked (cell diameter  $\sim 10\mu\text{m}$  and nozzle diameter  $\sim 30\mu\text{m}$ ) and cells damaged from the sedimentation and the piezoelectric pressure [46].

Cells preparation is the sequent: it is necessary to count the concentration with the trypan blue method and centrifuges them; after the centrifugation, the DMEM is aspired and the right quantity of hydrogel or water solution, like DMEM, (to have  $3 \cdot 10^6$  cells/ml) is added in the tube. If the final solution is not completely mixed, the vortex can be used. Finally, it is possible to put the solution with cells in the tank for the printing process and to print (a little purge is necessary before printing).

It is important for the printing process, shown in **Figure 41**, to use a water base solution to not damage the printhead and a biocompatible/bioactive solution to not kill cells; so, i.e. it is possible to print cells in DMEM or in hydrogel (Alginate and PEG based with 0,25-2% Alginate concentration).

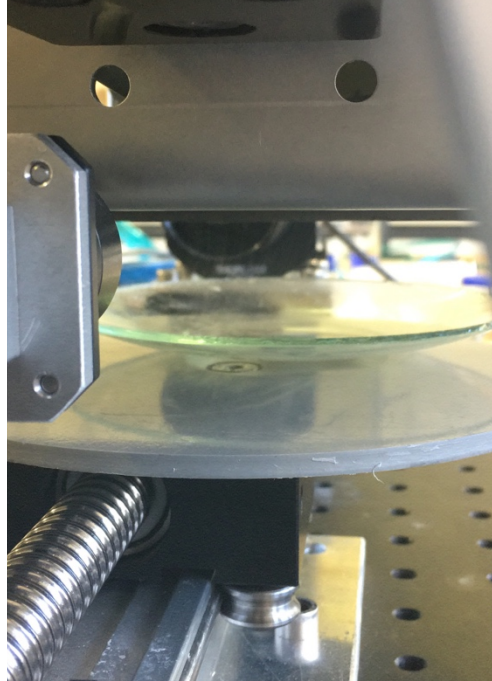


*Figure 41: Back View of the Printing Process [36]*

## 4 BioPrinting Platform

Biowatcher is the name of the experimental 3D inkjet BioPrinting station at the iPrint Institute used for this project.

The printing station is composed by several components already build and assembled **Figure 42**:

- 3-Axis printing system to move the printhead in the XYZ directions for 3D printing;
- Fujifilm Sapphire QS-256 Printhead: water compatible printhead with 256 nozzles which have diameter of 30  $\mu\text{m}$ ;
- Pressure regulation: the ink pressure in the printhead is an important parameter for the drop formation because the Fujifilm Sapphire QS-256 has a piezoelectric technology that needs a negative pressure to eject drops. The system let the operator to adjust the pressure by modifying the height of the cartridge containing the bioink (using the application of Stevino's Law), but this method is not completely precise and reproducible;
- Universal printhead support that permits to easily switch from one printhead to another for the assessment of different models;
- GIS (Global Inkjet Solution) print system is the electronic controller of the printhead, used for the tuning of the pulse (waveform) sent to nozzles for the drops formation. It also converts the 2D-image in drops;
- Dropwatching, implemented by a camera and a stroboscope LED: it consists in recording the drops jetted by the printhead;
- FPGA (Field Programmable Gate Array) is the integrated circuit designed to synchronize axis movements / printing / image acquisition in real time;
- These features are used to implement various processes used: they include multiple software and components controlled by Matlab.

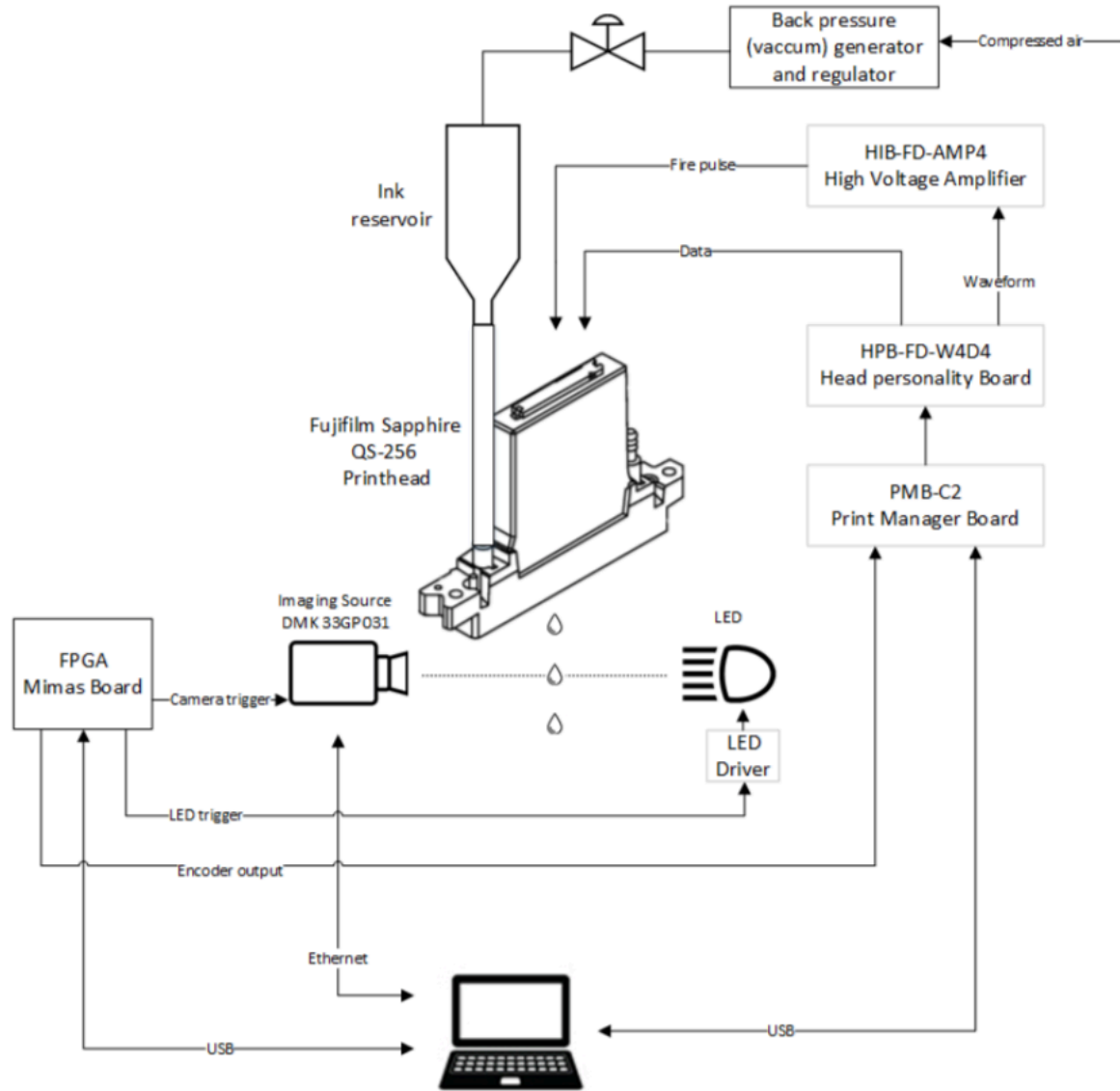


Figure 42: Biowatcher scheme components [36]

Biowatcher, shown in **Figure 43**, as it is composed, is working and ready to perform dropwatching and then printing processes. It was decided to improve the platform both via hardware and software by building an automatic pressure regulator (mechanical and electronic parts) and implementing a fully automatic and user-friendly algorithm for the study of particles and cells sedimentation within the bioink to know, before the printing process, the particles behavior in the bioink.



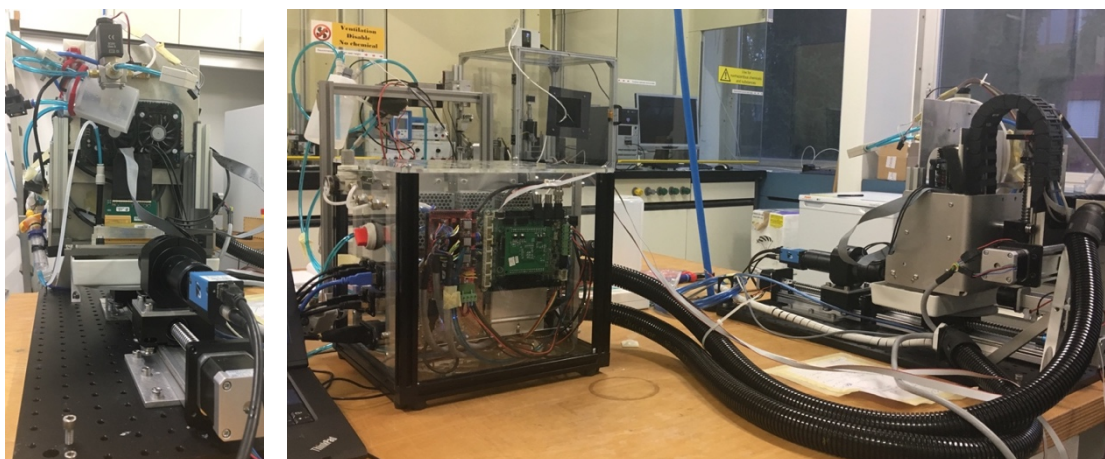


Figure 43: Biowatcher: front and side views [36]

The Sapphire QS-256 module is designed to be stored and operated under the following conditions [47]:

Number of addressable jets	256
Print width	64,77 mm
Nozzle spacing	254 $\mu\text{m}$
Nozzle diameter	30 $\mu\text{m}$
Typical jet straightness	1,5 mrad [0.085°]
Typical drop velocity variability	5%
Ink operating temperature range	Up to 90°C
Fluid optimal viscosity range	8-20 mPa · s
Compatible jetting fluids	UV-curable, organic solvents, aqueous

BINARY OPERATION:	
Adjustment for drop size	80-200 picoliters
Productivity	80 pl $\rightarrow$ maximum 20 kHz
	200 pl $\rightarrow$ maximum 8 kHz

GRAYSCALE OPERATION:	
Number of levels	Up to 4
Fundamental drop size	80 picoliters
Productivity	200 pl $\rightarrow$ 8 kHz
OEM accessible non-volatile memory	Two 256-bit pages, write once

Although the ink viscosity range should be between 8 and 20 mPa·s for optimal printing process, the bioinks, formulated at the iPrint Institute to be suitable for both the printing and the viability and growth of the cells, have a lower viscosity range, measured at a temperature of 37°C.

Alginate/PEG hydrogels were prepared by mixing one type of Alginate (HV or LV) with PEG in distilled water at 60°C until complete dissolution. The concentration of Alginate varied from 0,25% to 1% and the concentration of PEG 8000 from 0,1% to 0,5% w/v (weight/volume).

The most important characteristics for a hydrogel used for BioPrinting are:

- Distinct physical-chemical properties in the liquid state (density, viscosity, surface tension);
- Fast transformation into solid (gelling);
- Necessary bioactive characteristics to guide cells development into a functional tissue.

Hydrogels are based on polyethylene glycol (PEG) and Alginate. Alginate has good properties in the liquid state and has a very fast gelation time in contact with  $\text{Ca}^{2+}$ . It is biocompatible and low toxic, but non-bioactive.

PEG alone is also non-bioactive, but with the adding of the DMEM after the printing process to let cells live inside, it could be crosslinked by enzymes and conjugated with biomolecules (enzymes, proteins, liposomes...) to provide bioactive characteristics to the cells. After crosslinking of the PEG, the Alginate can also be removed by other enzymes to keep only the bio-active part of the hydrogel, without losing the gel properties.

All the bioinks, hydrogel based, formulated contain the 25% of PBS 1x + 1,5 mM EDTA and the 75% of Alginate/PEG hydrogel. PBS 1x is an isotonic solution, so cells can be in contact without problems. Using PBS 1x, cells separation from the surface (from the surface of the tube after centrifugation) is encouraged as the divalent ions are eliminated. These same ions,  $\text{Ca}^{2+}$  and  $\text{Mg}^{2+}$ , are necessary for the adhesion proteins that hold the adherent cells to the plate. They are used in the DMEM formulation and it could be possible that some of them remain after the DMEM removing. For the same reason, to eliminate the ions, EDTA has been added that acts as an ion chelator. The substrate used is 3% w/v Agarose in water containing 50mM  $\text{CaCl}_2$ .

Other experimentats in this project have been done using cells in their DMEM like bioink and different kind of substrates like Alginate 5% and Agarose.

The Material used in the iPrint Institute are:

- PEG: Polyethylene glycol 8000, M=7300-9000g/mol, Roth 0263.2;
- Alginate HV: Alginic Acid Sodium Salt, 15-25cP at 1% in water, Sigma-Aldrich 180947;
- Alginate LV: Alginic Acid Sodium Salt from brown algae, 4-12CP at 1% in water, Sigma-Aldrich A0682;
- CaCl<sub>2</sub>: Calcium Chloride, Roth CN93.1;
- Agarose: Agarose standard, Roth 3810.2;
- PBS/EDTA: Roti-CELL PSB/EDTA, sterile, 0,046% EDTA, Roth 9152.1;
- Rat2 [48];
- Fibroblast 3T3 [49];
- Lung Epithelial Cells A549 [50];
- DMEM [51] 10%CF [52];
- DMEM [51] 10%FBS [53];
- LIVE/DEAD assay: LIVE/DEAD viability/cytotoxicity kit for mammalian cells, Thermo Fischer L3224.

List and formulation of all the hydrogels already prepared at iPrint with their characteristics is in the follow table:

Hydrogel Name	%PEG w/v	%Alginate w/v	Aginate type	Viscosity at 37°C (mPa · s)	Viscosity at 37°C, diluted 25% (v/v) with PBS/EDTA (mPa · s)
N1	0,10	0,250	HV	3,2	
N2	0,50	0,250	HV	3,2	
N3	0,10	1,000	HV	13,0	
N4	0,50	1,000	HV	12,6	
N5	0,10	0,500	HV	5,5	2,4
N6	0,50	0,750	HV	9,4	
N7	0,37	0,250	HV	3,2	
N8	0,23	1,000	HV	13,1	5,8
N9	0,10	0,250	LV	1,9	1,2
N10	0,50	0,250	LV	2,1	
N11	0,10	1,000	LV	4,9	2,8
N12	0,50	1,000	LV	5,6	
N13	0,10	0,750	LV	3,9	
N14	0,50	0,500	LV	2,9	
N15	0,23	0,250	LV	2,0	

N16	0,37	1,000	LV	5,7	
N17	0,30	0,625	LV	3,3	
N18	0,30	0,625	LV	3,3	
N19	0,30	0,625	LV	3,5	
N20	0,30	0,625	LV	3,1	
N22	0,23	0,750	HV	10,7	5,3
N23	0,23	0,500	HV	7,0	3,1
N24	0,23	0,750	LV	5,0	3,0
N25	0,23	0,750	HV	10,2	5,5
N26	0,23	0,750	HV	10,8	5,1
N27	0,20	0,500	HV	5,6	2,5
N28	0,20	0,750	HV	7,8	3,7
N29	0,20	1,000	HV	12,8	6,5

These hydrogel formulations are outside from the optimal working range of the printhead, 8-20mPa\*s. This is the reason why it is difficult to achieve nice drops.

#### 4.1 Cleaning Procedure of Printhead

The investigation of hydrogel dissolving is important to make sure that printhead nozzles are completely unlocked from hydrogel and cells after printing. It is important to be able to clean the printhead and be sure to remove everything after each use of it.

The worst situation, in which the concentration of Alginate in hydrogel solution is the maximum value that it can be printed, 2% Alginate, has been chosen to perform the tests.

It is necessary to find the right combination of Tri-Sodium Citrate and EDTA to dissolve the crosslink between Alginate and Calcium Chloride in the solvent for the cleaning procedure.

The Tri-Sodium Citrate and the EDTA create crosslinks between themselves and the Calcium Chloride, to free the Alginate polymer from Calcium reticulation. EDTA, also, reacts with cells inside the hydrogel because, reacting with the Calcium, helps them to detach from the hydrogel matrix (cells attached better in the presence of Calcium).

The Tri-Sodium Citrate react both with the Alginate and with the Calcium inside the polymer: Sodium react with the Alginate, while the Citrate with the Calcium.

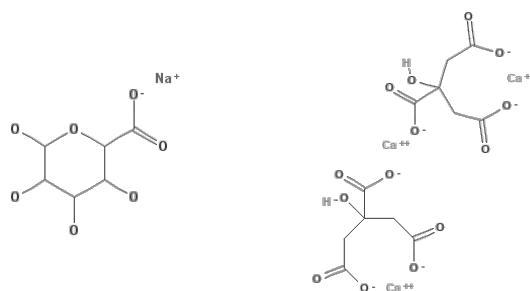


*Figure : Sodium Alginate and Calcium Citrate complexes [54] [55]*

The EDTA react with the Calcium inside the Calcium Alginate and creates the Calcium EDTA (Y) complex showed in **Figure 44**. The reaction equation is  $\text{Ca}^{2+} + \text{H}_2\text{Y}^{2-} \rightarrow \text{CaY}^{2-} + 2\text{H}^+$ . [56]

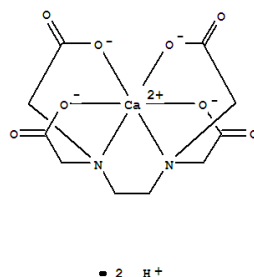


*Figure 44: Calcium EDTA complex [56]*

Three different tests have been done to find the right concentrations of hydrogel and solvent, to simulate a printhead nozzle and to obtain better results with a recirculation system.

#### 4.1.1 Pipet Test

Before printing the bioink with the printhead, it is important to make a cleaning protocol simulating the worst situation that could happen inside the printhead, the nozzles clogging, and to find a safety way (the printhead should not be damaged or broken) to clean and unlock all the nozzles. This type of cleaning procedure has been studied and developed for Alginate-based hydrogels with a maximum concentration of 2% Alginate in demineralized water.

The concentration chosen are: 58,82 g/l (0,2M) of Citrate and 29,2 g/l (0,1M) of EDTA. Thus, for 50 ml of Demineralized Water concentrations are respectively 2,95g and 1,45g.

The investigation in the cleaning procedure has been done in six passages with pipet tests, showed in:

- 1) Creation of the Calcium Chloride solution: a spoon of Calcium Chloride in 25ml of demineralized water, **Figure 45**;

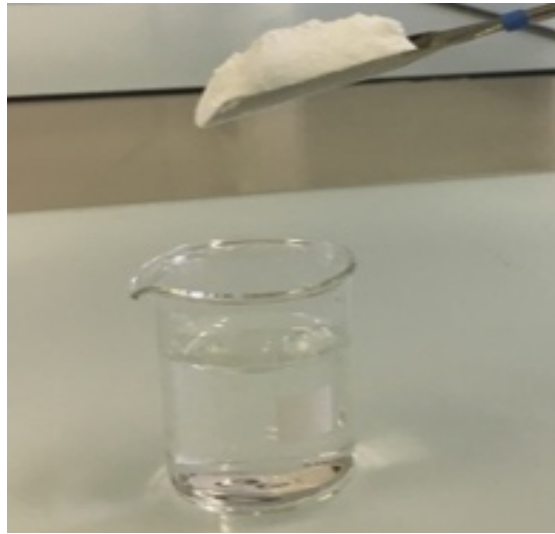


*Figure 45: Creation of the Calcium Chloride Solution [36]*

- 2) 5ml of Hydrogel (2% Alginate HV) coloured with one drop of red food colouring to make it visible, **Figure 46**;

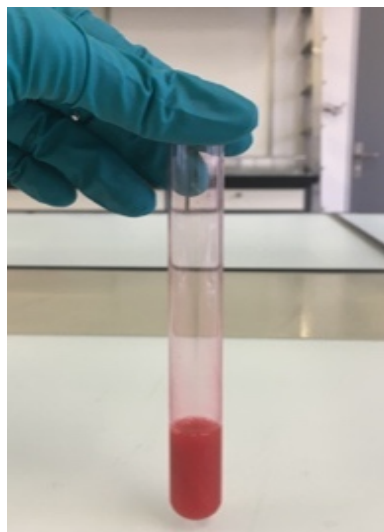


*Figure 46: 2% Alginate HV [36]*

- 3) In the tube with the hydrogel, the Calcium Chloride solution is added and the Alginate reacts with the Calcium molecules to create crosslinks between the Polyguluronic Acid anions and multivalent Calcium cations ( $\text{Ca}^{2+}$ ), **Figure 47**;

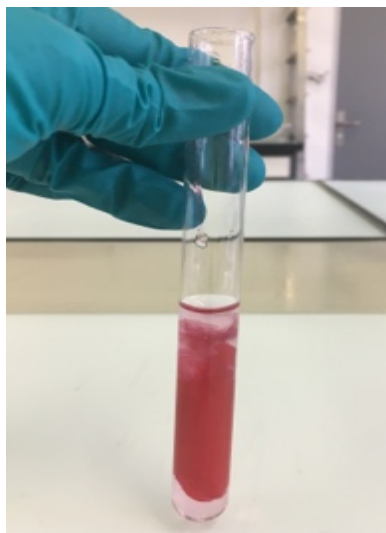


*Figure 47: 2% Alginate HV with Calcium Chloride Solution [36]*

- 4) Measuring the Citrate and the EDTA for the solvent solution and putting them in 50 ml of demineralized water, **Figure 48**;

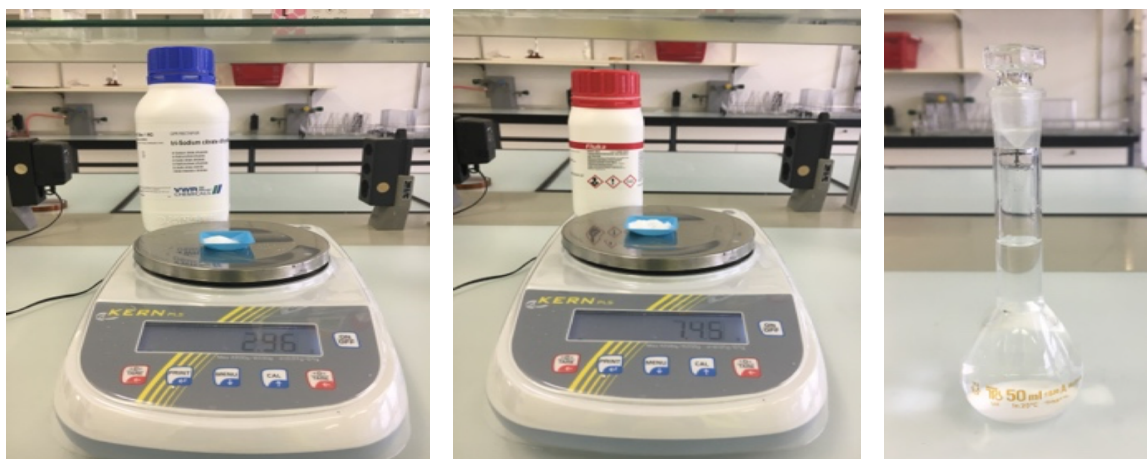


*Figure 48: Trisodium Citrate and EDTA measured and put in demineralized water [36]*

5) The water is removed from the Calcium Alginate, **Figure 49**;

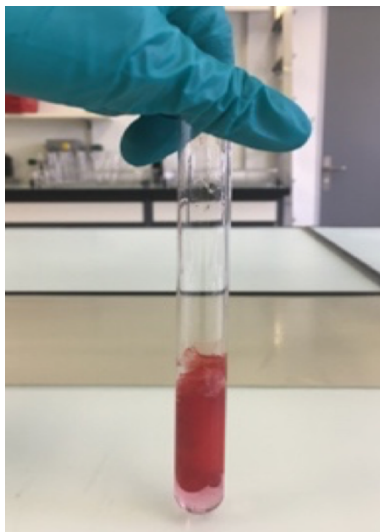


*Figure 49: 2% Alginate HV already crosslinked and without demineralized water [36]*

6) The solvent is added (15ml) into the hydrogel and the solution is mixed (pictures before and after mixing); the hydrogel does not dissolve completely, **Figure 50**;

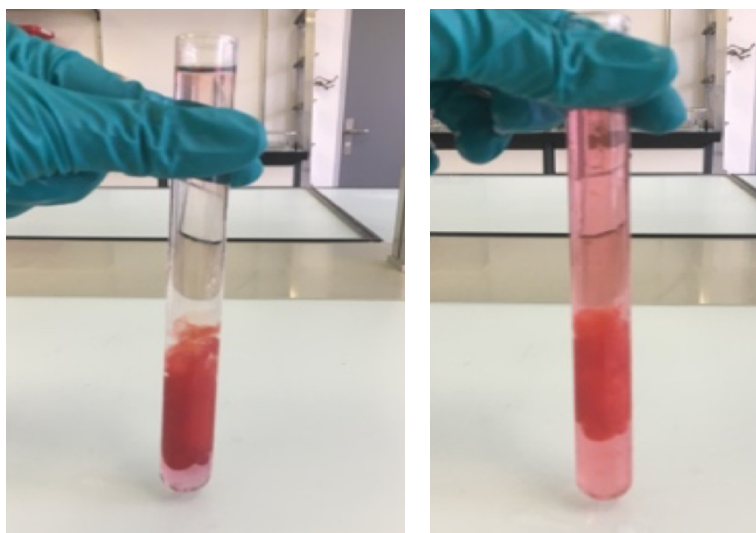


*Figure 50: 15ml of Solvent added to the crosslinked hydrogel [36]*

For a second test, a different concentration of hydrogel in the solvent is tested:



- 1) 2ml of coloured hydrogel and 2ml of Calcium Chloride solution, **Figure 51**:

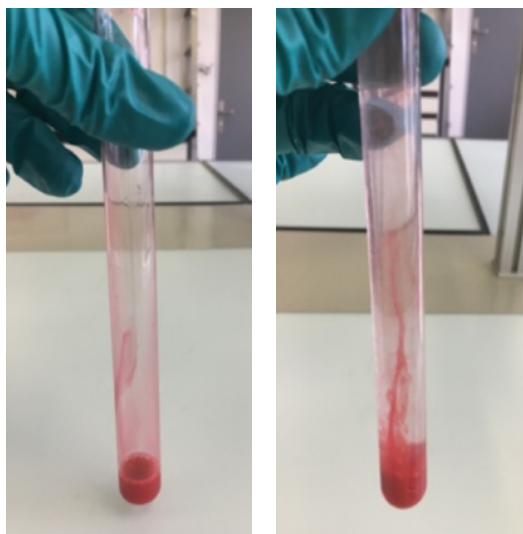


*Figure 51: 2ml of hydrogel and 2ml of Calcium Chloride Solution [36]*

- 2) The solvent is added (20ml) until to the top of the tube and the hydrogel is starting to dissolve without mixing the solution, **Figure 52**;

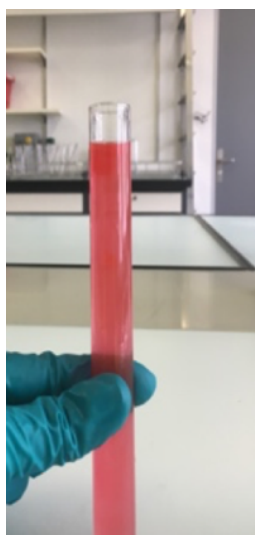


*Figure 52: Addition of the Solvent to the mixture [36]*

- 3) After 15 minutes the first solution of hydrogel and solvent, and after 10 minutes the second one are dissolving like in the pictures: the left picture corresponds at the first test with 5ml of hydrogel in the solution, the right one to the 2ml of hydrogel in the solution, **Figure 53**.

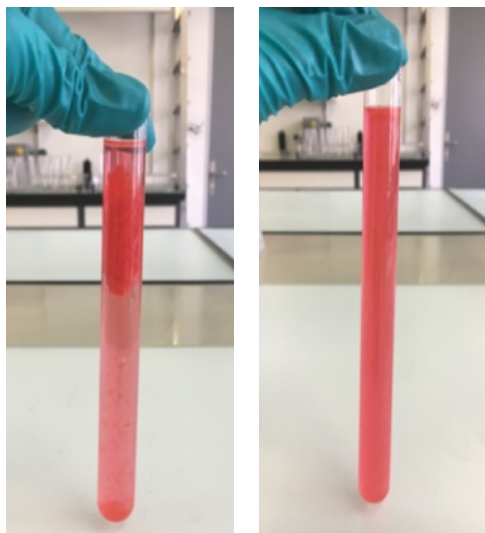


*Figure 53: First and second solutions checked after 15 and 10 minutes respectively [36]*

Because even 2 ml of hydrogel is not completely dissolved after 10 minutes in the solution, a third test has been done:

- 1) 1 ml of coloured hydrogel is put in the tube and then 1 ml of Calcium Chloride solution is added. Then the water is removed, **Figure 54**;

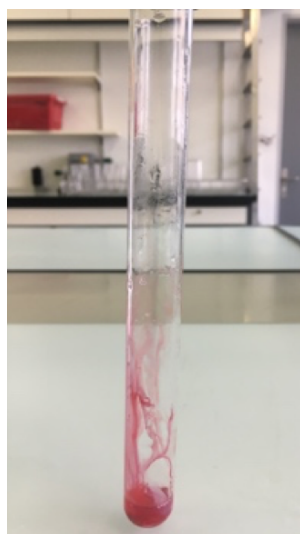


*Figure 54: 1ml of hydrogel and Calcium Chloride Solution, without water [36]*

- 2) The solvent is added until to the top of the tube (around 20ml), **Figure 55**;

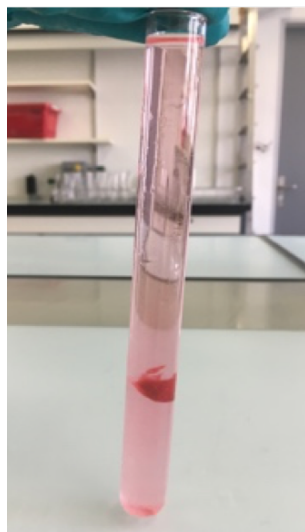


*Figure 55: Addition of 20ml of Solvent [36]*

- 3) The hydrogel is starting to dissolve without mixing the solution and then mixed, **Figure 56**.

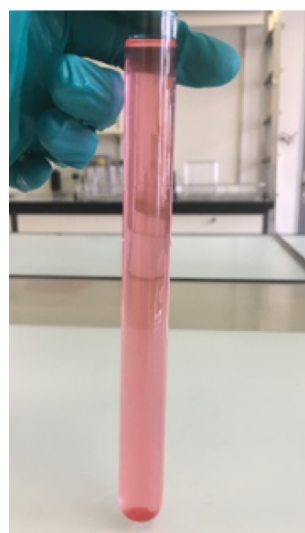


*Figure 56: Dissolution of the hydrogel [36]*

After 30 minutes the first solution, after 25 the second one and after 15 the third one are been checked, **Figure 57**:

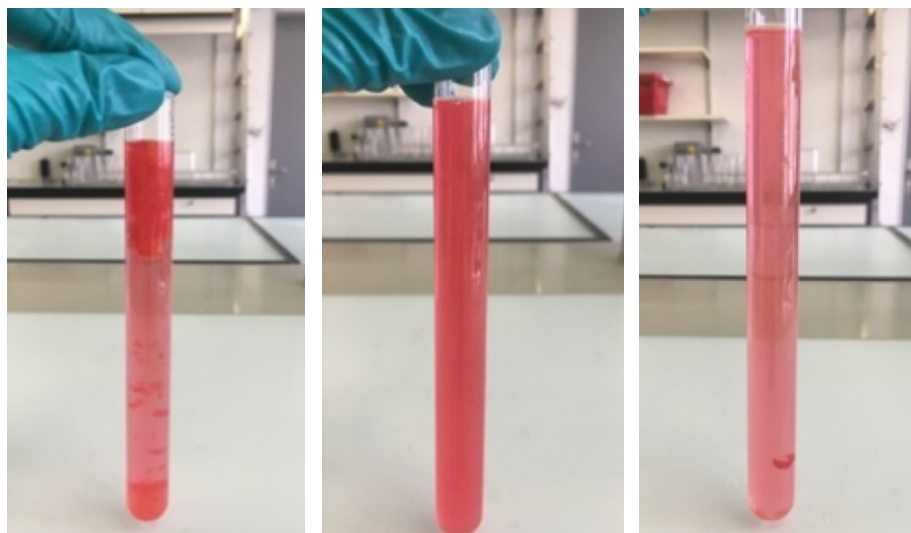


*Figure 57: 5ml, 2ml and 1 ml of hydrogel respectively after 30 minutes [36]*

After 45 minutes the first solution, after 40 the second one and after 30 the third one are been checked, **Figure 58**:

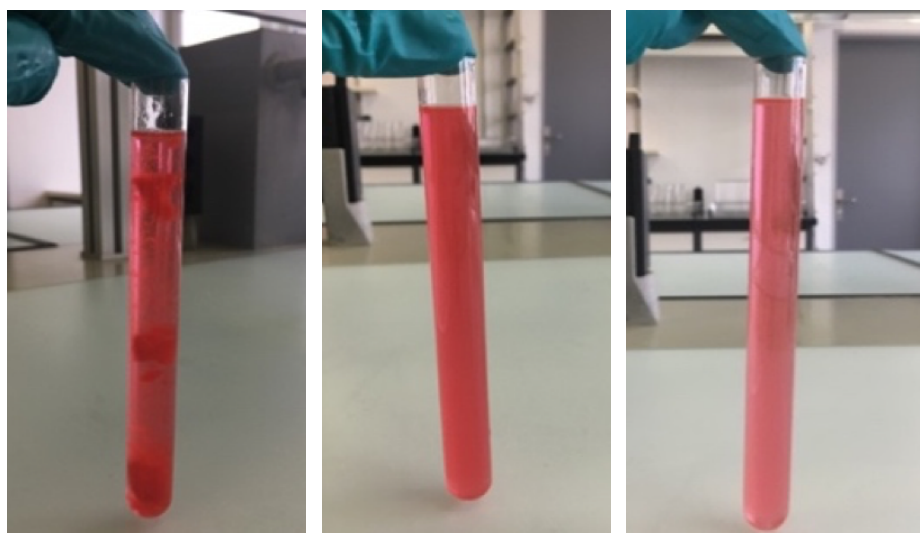


*Figure 58: 5ml, 2ml and 1 ml of hydrogel respectively after 45 minutes [36]*

The second and the third solutions (2ml and 1ml of hydrogel) are completely dissolved after 30 minutes, so it means that the first test with 5ml of hydrogel takes more time to dissolve in the

solution. It is better to use the concentrations of the second and the third experiments (2ml and 1ml of hydrogel).

#### 4.1.2 Capillarity Test

After testing the hydrogel and the solvent concentrations, another kind of test has been taken to simulate in a better way the capillarity phenomena inside the printhead. The goal of this test is to check if it is possible, just with the help of the solvent, to unlock a tube with a small diameter, to mimic what it could happens if a nozzle block after that the hydrogel crosslinked inside it. The tube used for this test has a diameter of 1,90 mm. Capillarity test is described by the following procedures:

- 1) 1ml of Alginate HV 2% is put inside the tube and after, from the same entrance, Calcium Chloride solution is put until the hydrogel became a gel. The gel is moved from the centre of the tube to one extremity and the tube is cut, **Figure 59**;

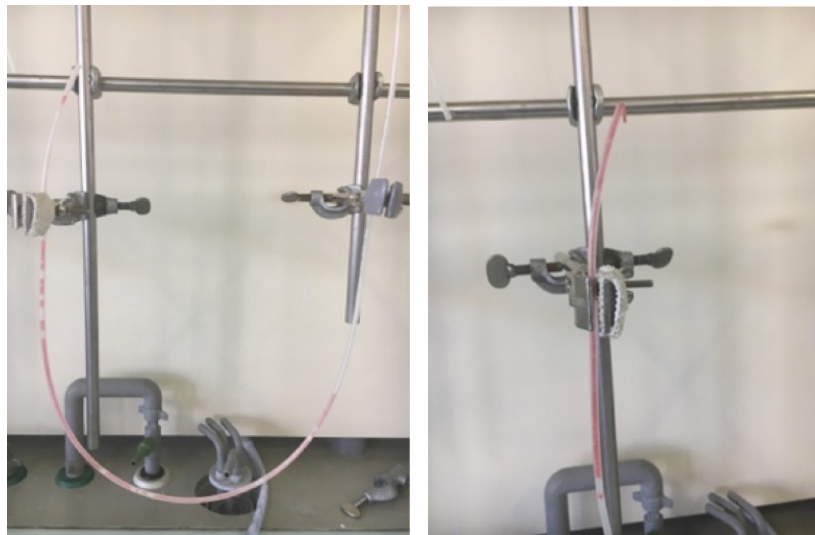


*Figure 59: 1ml of Alginate and 1ml of Alginate with Calcium Chloride Solution [36]*

- 2) The tube has been tilted, and the solvent was inserted from the top of the tube and into the bottom pan to simulate the fact that the printhead is always kept into a water based solution to do not damage the nozzles, **Figure 60**;

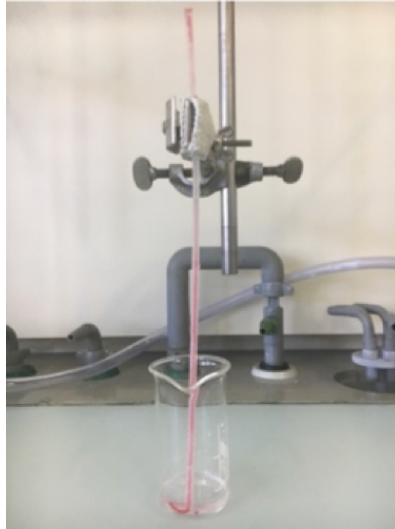


*Figure 60: Addition of the solvent [36]*

- 3) After 30 and 60 minutes and then after 17 hours the hydrogel dissolving is checked,  
*Figure 64;*

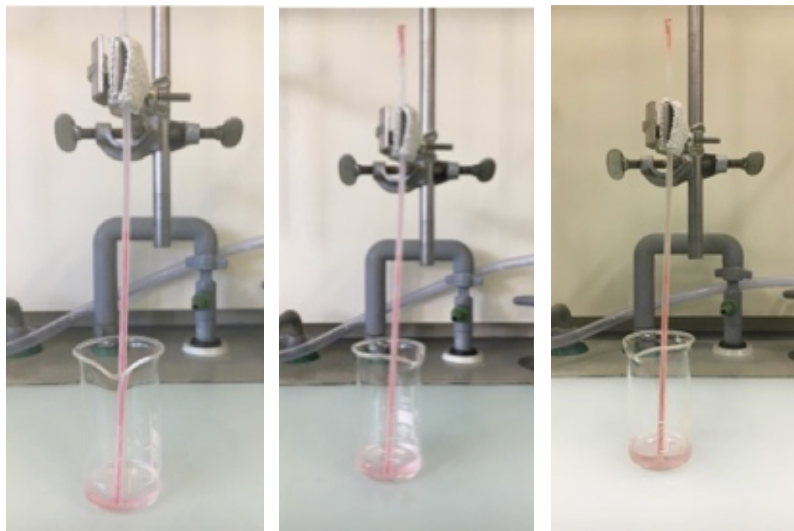


*Figure 61: Capillarity test after 30 and 60 minutes and then after 17 hours [36]*

- 4) The tube has been tilted, and the solvent was inserted from the top of the tube. Black signs indicate the hydrogel level: the first sign is for the beginning level, the second for the level after 30 minutes. The solvent is mixing with the gel and it make the gel slowly dissolve. Pictures are taken every 30 minutes. Everything is pushed out with the help of a positive pressure and the hydrogel is completely dissolved after 10 minutes of mixing, *Figure 62.*

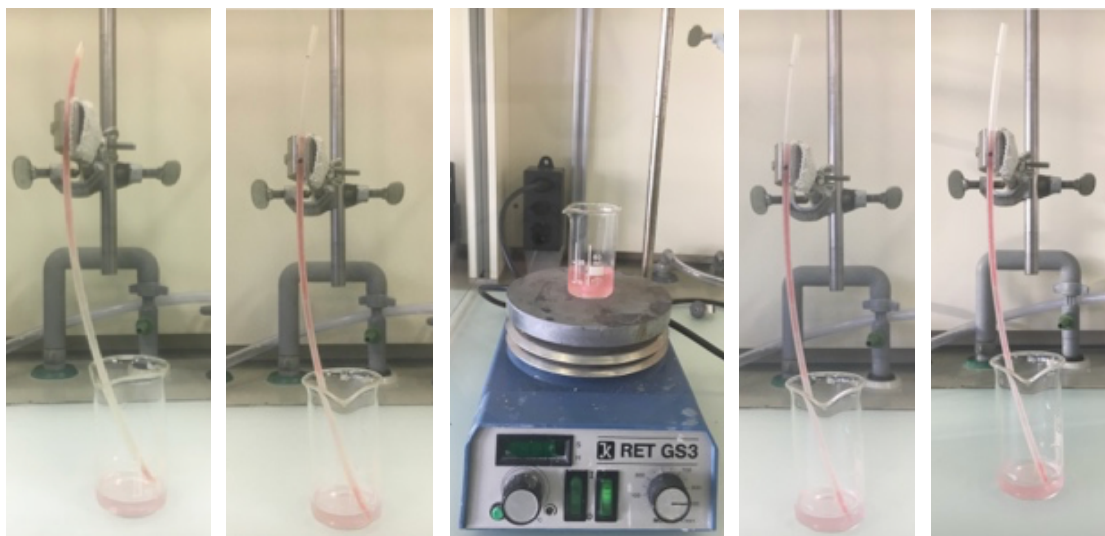


*Figure 62: Final check [36]*

In conclusion, it is not enough to put the solvent inside the tube after that the hydrogel crosslinked because this kind of solvent dissolve slowly the hydrogel, it is not strong enough to dissolve the material in a reasonable time with this formulation. A new solution to the capillarity blocked needs to be find. For this reason, the recirculation test has been done with the same formulation of the solvent and the same hydrogel but with the help of a liquid recirculation system to let the solvent penetrate better inside the hydrogel and dissolve it not only from the outside but also from the inside.



### 4.1.3 Recirculation Test

Because the hydrogel in the tube dissolve well in a reasonable time only if there is a mixing, a recirculation system has been created with the hydrogel into a drop coloured form and demineralized water in a bottle and the solvent (250 ml) in another bottle, **Figure 63**. Applying a positive pressure and with the help of a pump system, the hydrogel completely dissolve after less than 5 minutes.

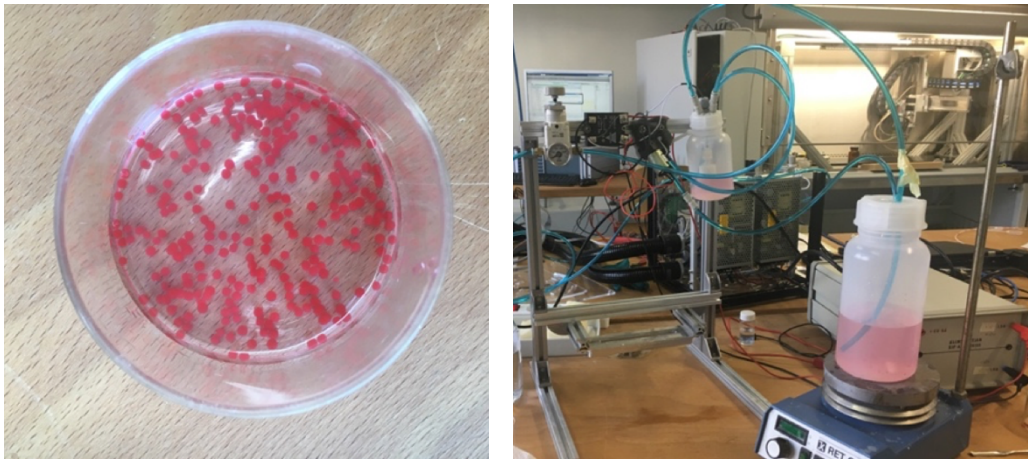


*Figure 63: Creation of Recirculation System [36]*

The fluidic circuit is characterized by the following components, **Figure 64**:

- Precision Regulator: to regulate the pressure inside the Tank1, the positive pressure come from an air compressor;
- Tank 1: in which the solvent is present at the beginning;
- Tank 2: in which the hydrogel drops are present at the beginning;
- Pump: to let the liquid circulate in the system.



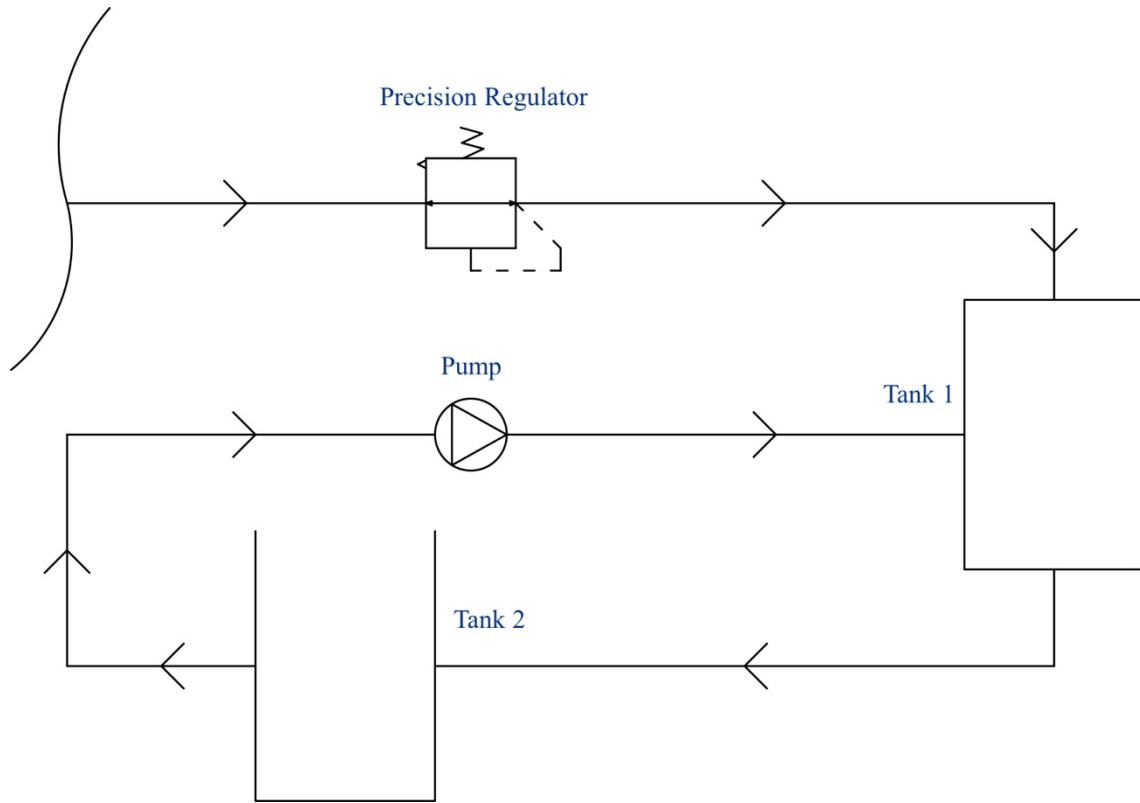


*Figure 64: Recirculation System Scheme [36]*

From these experiments, it can be concluded that the solution created, with the liquid recirculation pumps system, is a good solution for cleaning the printhead after tests containing Alginate (maximum 2%) have been carried out.

#### 4.1.3 Printhead Test

The printhead test has been designed like the recirculation test in the two tanks but with the difference that the hydrogel inside the printhead is not crosslinked. It is still liquid, because, after every printing process, hydrogel jellifies only after the ejection on a calcium ions-based surface, not inside the printhead if nozzles are cleaned. **Figure 65** The hydrogel has been put inside the printhead and pushed out through positive pressure applied on the top of the inlet channel. The hydrogel, in this way, flows outside the nozzles and jellifies in a Calcium Chloride liquid solution. Thanks to the pump and the positive pressure, the hydrogel in the calcium bath has been taken and put in a tank in which the solvent is in it. The liquid obtained, solvent, hydrogel and calcium

solution, has been taken by the tubes in the system designed and put in the inlet part of the printhead. In this way, hydrogels spheres can dissolve fast and the printhead is completely clean. After the cleaning process with the recirculation and the solvent created, the cleaning procedure for the printhead has been concluded with purge of 20 ml of demineralized water and with the positioning of the printhead in a wet container (nozzle have to stay in demineralized water or in contact with a wet material, otherwise they could be blocked). The printhead is completely cleaned after these considerations and the process described should be adopted every time after a general printing process with Alginate-based hydrogels.

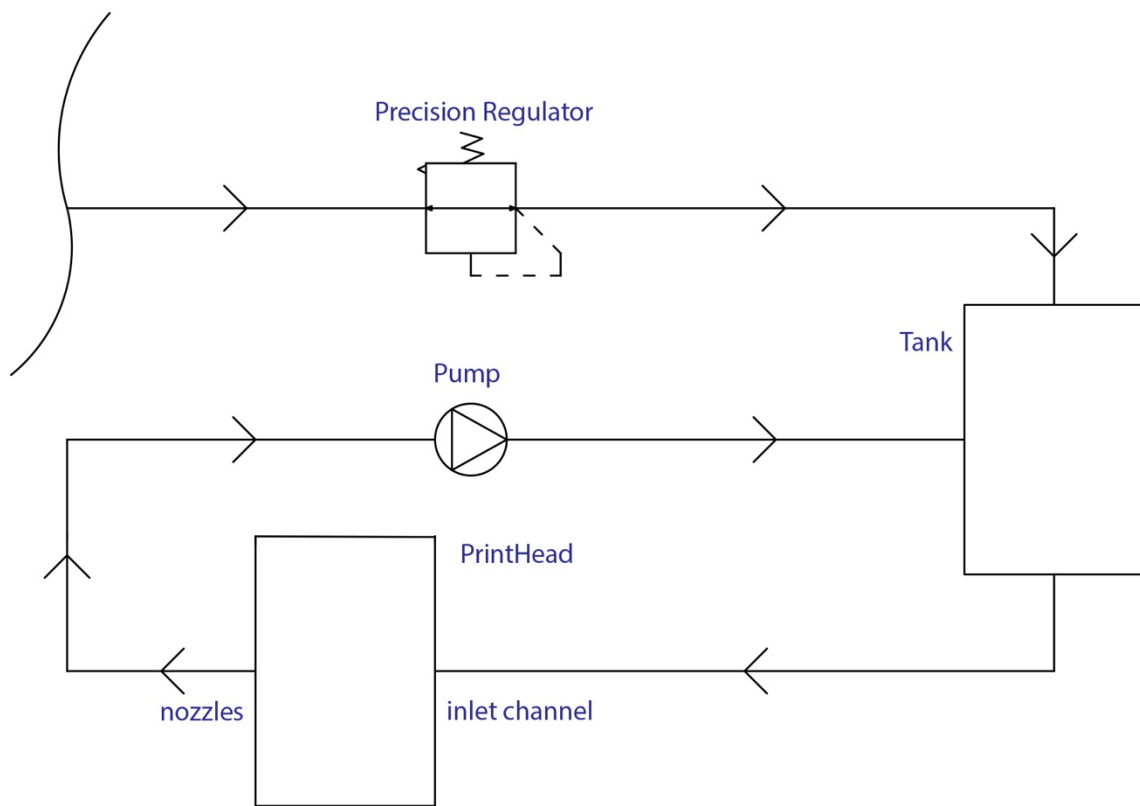


*Figure 65: Recirculation Printhead System Scheme [36]*

## 4.2 Automatic Pressure Regulation

The automatic pressure regulator was designed and built on Biowatcher to have the possibility to adjust automatically pressure inside the printhead, setting the desired value using appropriate codes in Arduino, *10.1 Pressure Regulation Arduino*, and Matlab, *10.2 Final Code with Pressure Regulation Matlab*, software. Since technology, on which printhead is based, is piezoelectric, it is necessary that the pressure between the inlet channel and the nozzles remain negative all the time. Otherwise the surface tension, that would be created outside nozzles, would give problems to the printing process, not letting the drops of the right size come out and creating a large uneven drop in the not-desired place on the substrate. Without a negative pressure within the printhead, the printing process would not be possible. The vacuum is necessary to compensate the column of liquid from the tank to the nozzles:  $p(\text{nozzle}) = \rho \cdot g \cdot \Delta z - p(\text{vacuum})$ .

This pressure value changes, however, depending on the type of bioink and its morphology, but once identified, it is very simple to set it for each print with the same bioink, making the printing process simple, effective and repeatable by any operator.

Without this automatic pressure regulation, the printing process is still possible, applying the Stevino's Law ( $p = \rho \cdot g \cdot \Delta z$ , with  $p$  the pressure,  $\rho$  the fluid density and  $\Delta z$  the difference between the bioink level and the nozzles level) and positioning the tank in the way that the bioink level is under the nozzles level, to have a negative pressure at the end.

The electro-mechanical operation is controlled by the ATmega32U4 microcontroller present in the Arduino Micro<sup>®</sup>. Arduino Micro<sup>®</sup> is the smallest board of the Arduino family. This board is easy to integrate with electro-mechanical objects in order to be able to project them into what everyone wants to build. The Micro board is a microcontroller board based on the ATmega32U4, developed in conjunction with Adafruit [57].

It has:

- 20 input/output digital pins:
  - 7 of them can be used as PWM outputs;
  - 12 of them can be used as analog inputs;
- a 16 MHz crystal oscillator;
- a micro USB connection;
- an ICSP header;
- a reset button.

Contains all the cycle necessary for the ATmega32U4 microcontroller operations; it is possible to program it quickly and easily by connecting it to a computer with a micro USB cable. It has been designed and built using a form factor to easily place it on a breadboard [57].

The circuit, designed in **Figure 66**, has built, **Figure 67**, to function in this way:

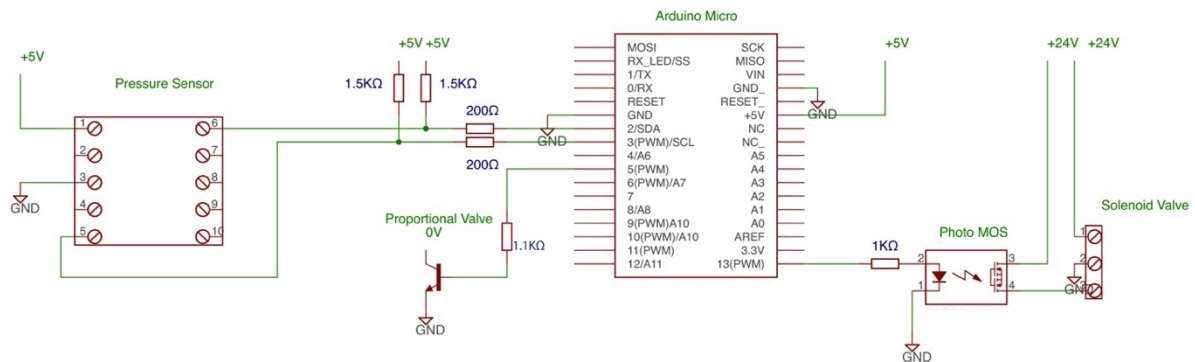


**Figure 66:** Pressure Regulation Circuit Scheme [36]

- The Pressure Sensor, DS Standard SSI-E-11671, measure the liquid pressure before coming into the printhead;
- If the pressure regulation is running, Arduino Micro give the command to the Proportional Valve (connected to Arduino Micro via a npn transistor, to control the current that goes to the Proportional Valve) to increase or decrease the vacuum: the vacuum has to be switched on before starting the regulation;
- The Proportional Valve (SMP PVQ13-5L-M5-A, in the centre of **Figure 66**) control the flow rate smoothly according to the current given by Arduino Micro;
- Then, if everything is running in the correct way, Arduino Micro give the command to the Solenoid Valve (SMC VX3110J-01F-05Z1, on the right of **Figure 66**) to switch the fluid flow in the direction of the Proportional Valve. In this way, the tank is connected to the Proportional Valve that regulate the flow rate and the vacuum regulation is running. In the same time, the Sensor Pressure gives a feedback to Arduino Micro on the pressure state and the microcontroller adjust the vacuum flow based on this data. The pressure coming into the printhead is set at a level, decided by the operator, and remain quite constant during all the time, thanks to this electro-mechanical system;

- If positive pressure is required to the printhead, i.e. to do the purge, Arduino Micro gives the command to the Solenoid Valve to switch to the positive pressure regulated manually by a manometer for a definite time, depending by operator's decision;
- The Photo MOS, DSX615, between the Arduino Micro and the Solenoid Valve control the low-level analog signals without distortions when another offset voltage is applied;
- Resistors values have been chosen and positioned in the circuit based on components datasheets.

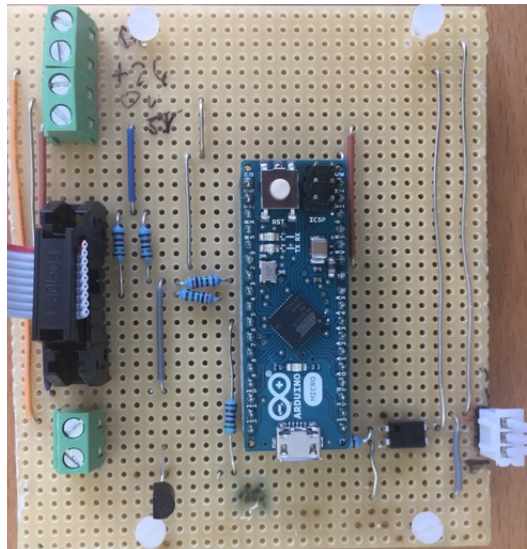


*Figure 67: Pressure Regulation Circuit [36]*

In parallel to the electric circuit, the fluidic circuit was designed and built. In addition to the electro-mechanical components explained previously, in the fluidic circuit there are purely mechanical elements, which do not require any electronic control via software, and, once set manually, do not require any further intervention by the operator.

In the fluidic circuit **Figure 68**, there are:

- Pressure sensor;
- 20  $\mu\text{m}$  filter to avoid particles larger than the nozzle diameter;
- 4-hole Tank that allows insertion of the bioink without having to interrupt the operation of the pressure regulator;
- Solenoid valve connected to a pressure gauge that regulates the positive pressure and the proportional valve for the vacuum;

- the pressure flow can be adjusted by Pressure Flow Valve. This component is a *continuous leakage* of air. Without it, the vacuum pressure cannot be reduced during the regulation;
- the Vacuum Ejector is a safety component connected to the proportional valve and the vacuum: if there was a leak and the liquid were to enter the proportional valve, this component would expel it, thus avoiding damaging the vacuum system.

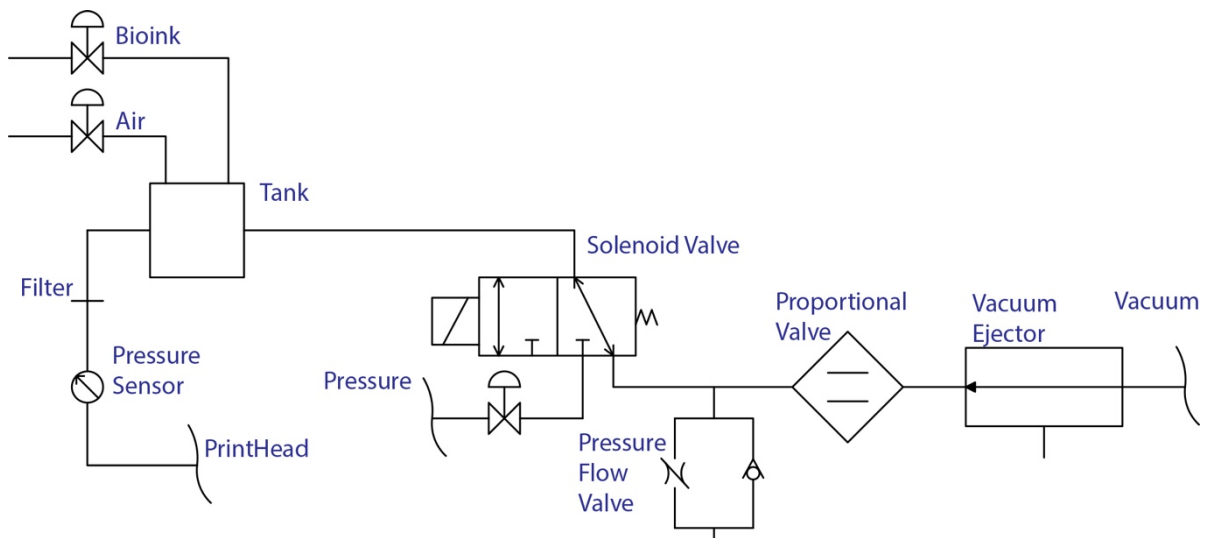


**Figure 68:** Fluidic Circuit [36]

The fluidic system described is shown in **Figure 69**:

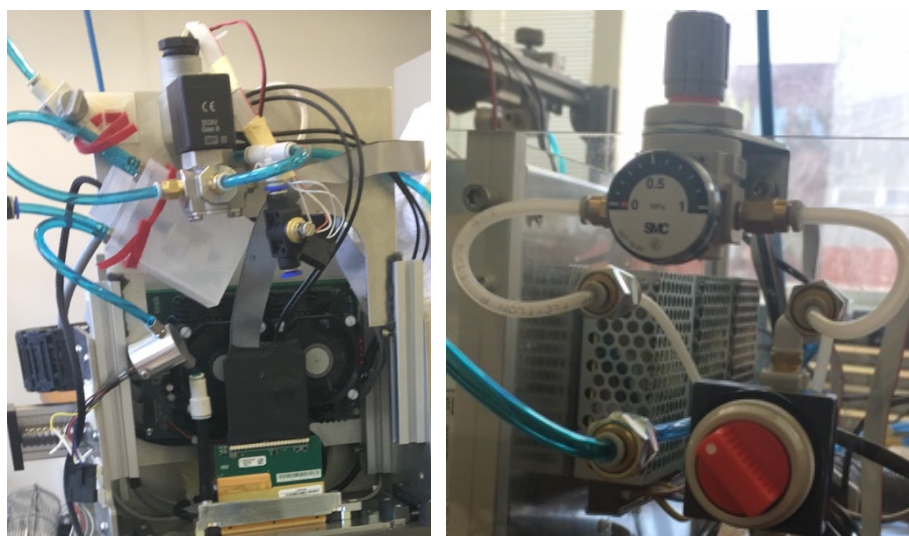


**Figure 69:** Fluidic System on the printer; manometer and pressure valve to activate the vacuum in the off position [36]

Values “Valve”, to regulate the pressure through the matlab code, chosen for the two liquids used in printing are respectively:

	DMEM 10% (FBS or CS)	3/4 N27 + 1/4 PBS/EDTA
Valve	25	27

### 4.3 Printing Procedure

A printing procedure was developed, after the investigation on the cleaning printhead procedure and several printing experiments. It describes which solution/solvents should be used in which order to keep the printhead in a working condition. Since the bioink consists of a PEG-Alginate hydrogel, organic solvents (ethanol and such) should be avoided. They would cause a cross-linking of the bioink, clogging the nozzle. Tri-Sodium Citrate/EDTA is the solvent to use after printing PEG-Alginate hydrogel based, for reasons explained in paragraph 4.1 *Cleaning Procedure of Printhead*.

Spitting is an operation which consists of printing a lot of big drops at high frequency. It allows to get liquid in the nozzle or unclog them.

Flushing or purging consists of applying a positive pressure on the ink, causing it to be forced out of the nozzles. This is used to get rid of air bubbles that might be present in the system.

Depending by the volume of the bioink to print, the operator can choose to use the automatic pressure regulation and fill the Tank with at least 20ml of bioink or to fill the small syringe (5ml) and print through bioink level adjustment.

The printing procedure is the following:

- filter the bioink at 20  $\mu$ m and fill the Tank or the syringe;
- switch on the vacuum for the pressure regulation and set it at the right number desired (on Matlab code) or adjust the bioink level in the syringe (it must be under the nozzles);
- flush and spit at least 2 seconds with pressure regulation code or push the syringe and then spit 60 seconds to avoid air bubbles in the system;



- start the printing process, *10.2 Final Code with Pressure Regulation Matlab* part 8;
- cover the printhead with the wet sponge between printing processes to let nozzles always wet (if they dry, then they could clog and it could be very difficult or impossible to unlock them);
- when printing processes are finished, put initially 20 ml of Tri-Sodium Citrate/EDTA in the Tank (or 5ml in the syringe) and purge, then the same quantity of demineralized water and purge again;
- set the printhead on the moist sponge covered with wipe (about 1cm compression).

#### 4.4 Stability Nozzle Process and Waveform Optimisation

DropWatching is the inkjet droplet analysis, a mandatory step to do whenever it is necessary to print a bioink with certain characteristics. It is a study on the shape and trajectory of the drops as soon as they come out from nozzles that can predict if it is possible to correctly carry out the printing process with certain parameters set. It is also used to check the state of nozzles, if they are clogged or dysfunctional, thanks to the high-resolution camera.

The shape of the drop must necessarily be spherical and must not form satellites, small drops that do not follow the trajectory perpendicular to the substrate, due to the presence of small air bubbles or particles in the bioink that slightly occlude the nozzle.

If these two characteristics are not respected, it is possible to change the waveform to get an optimal drop with as few satellites as possible, a high volume and speed.

These characteristics of the drop change according to the type of fluid and the electric waveform that is sent to the piezoelectric membrane. The membrane has the task of pushing the drops out from the nozzle and it can do this thanks to its property of changing shape following an electrical stress. Piezoelectricity is the property of some crystalline materials to deform in an elastic manner when they are traversed by current (a voltage difference is applied between the upper and lower part of the membrane). This deformation depends on the type of implied waveform sent and on its amplitude, voltage value in the wave peak.

The wavelet is designed like in **Figure 70** and the parameter changing by the operator are:

- rising time;
- dwell time;
- falling time;
- pulse interval, time between two consecutive pulses;
- voltage.

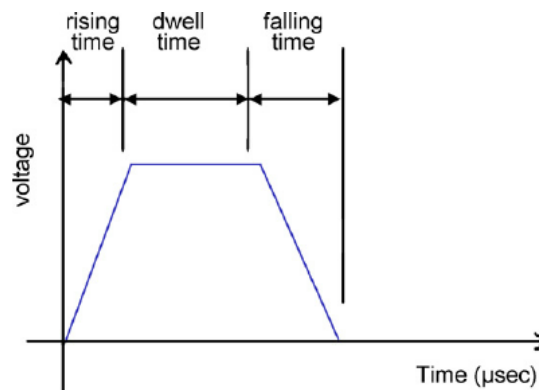


*Figure 70: Waveform Characteristics [36]*

The camera exposure and focus, droplet generator and flash diode are synched together using the FPGA-based controller. Inkjet drops have a velocity of approximately 1-20 m/s. For this reason, very short flash durations are required in order to capture the smallest high-speed drops with minimal motion distortion. With a flash duration of only a microsecond and a droplet speed of 10 m/s the droplet image is stretched to 10  $\mu\text{m}$ . By controlling the flash durations, several droplets can be stacked. By illuminating a droplet twice at different points during its flight, droplet speeds or flight angles can be determined independent of the background fluctuations influencing droplet velocity (jitter). [58]

An internally developed Matlab application *ITC-DropWatchingGUI*, shown in **Figure 71**, was used to easily display drops as the printing parameters would be adjusted in GIS, like the waveform shape and the voltage peak. The different times allow to tune the pulse shape while the voltage tunes its height. The waveform, sent to the piezoelectric membranes in the printhead, will cause their contraction, leading to a drop formation. If it is necessary, a double-pulse waveform can be generated and sent.

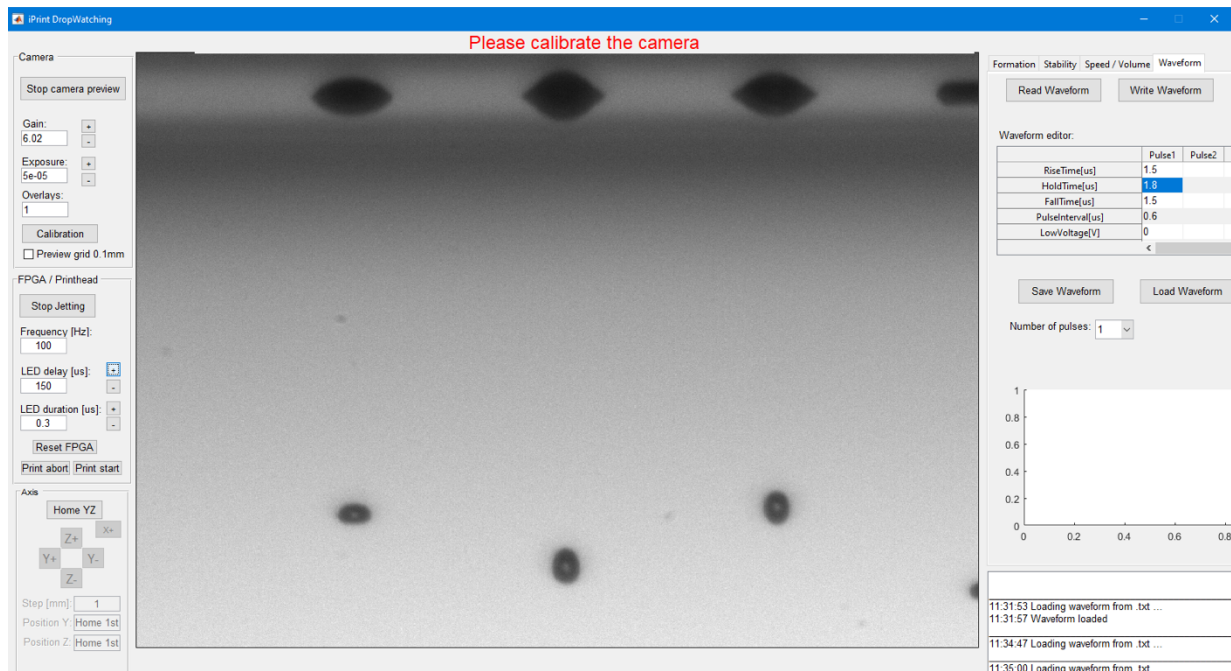


**Figure 71:** Example of hydrogel drops DropWatching after their expulsion from the printhead, in this case N27+PBS/EDTA is used [36]

The process already developed at the iPrint institute to asset the stability of the printing process over time was adjusted to work with the Automatic Pressure Regulation, part 7 (Measuring Loop) of *10.2 Final Code with Pressure Regulation Matlab*. It allows to check which nozzles on the printhead are clogged and to visualize drops shape.

First, images of drops over the whole printhead are acquired through dropwatching (initial part of the algorithm). Then, a home-made shape-recognition software is used to check where drops are present and their characteristics (speed, volume, satellite).

Two consecutive images have been processed, coloured red and green, and superimposed in a single image, shown in **Figure 72**, to help the operator to immediately visualize the trajectory of the drops.

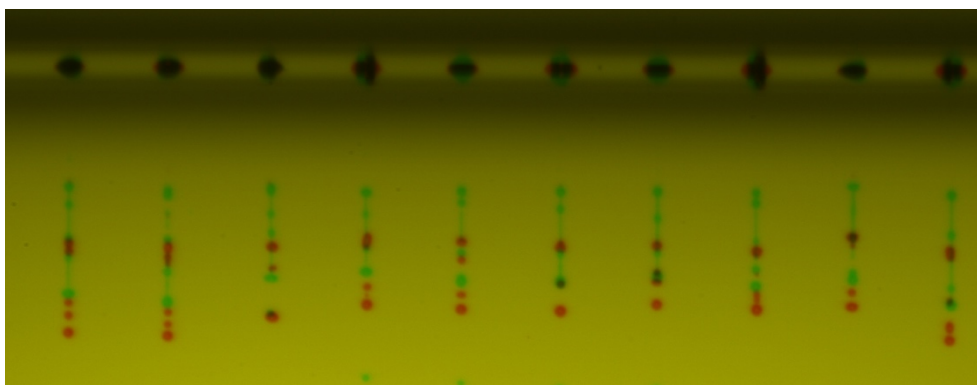


*Figure 72: Elaboration after Dropwatching of only hydrogel (N27 + PBS/EDTA) [36]*

An example of two non-functioning nozzles is given by the **Figure 73**. Several wavelets were tested before obtaining at least one working for each type of bioink tested. In fact, it was possible to collect images related to different wavelets. The "satellite" phenomenon was highlighted in red due to the possible presence of air bubbles inside the nozzle or to a partial occlusion of the same. In yellow instead, it is possible to see a nozzle blocked probably due to the not perfect cleaning of the printhead, from which no drop comes out. Satellites are also due to the waveform and the fact that the bioinks used are outside the optimal viscosity working range of the printhead (8 - 20mPa·s)

When these two phenomena occur, the following protocol is adopted:

- purge the bioink and then spitting to eliminate air bubble inside the printhead;
- in the meantime, clean nozzles with a wet tissue;
- if it does not work change the wavelet form.

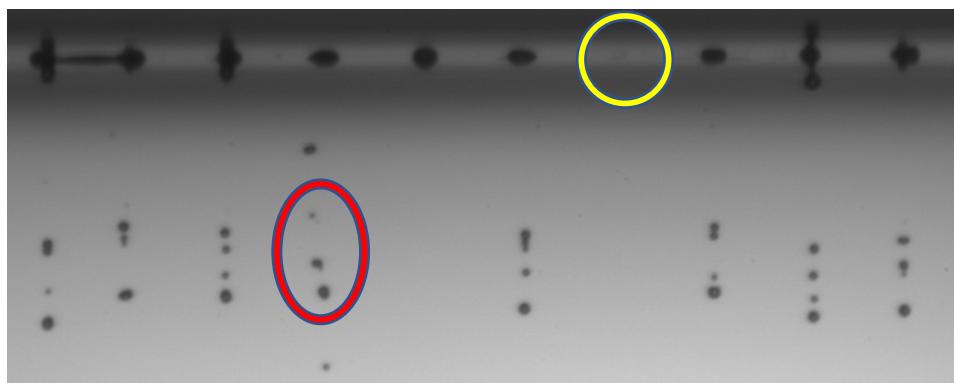


*Figure 73: Example of DropWatching not completely performed [36]*

Finally, these drops are mapped to the nozzles on the printhead. This information is plotted for a quickly overview, showed in **Figure 74**, of the situation and could also use to pay more attention to the cleaning procedure if too much nozzles are clogged. In this case, 11 nozzles are clogged and they don't eject drops.

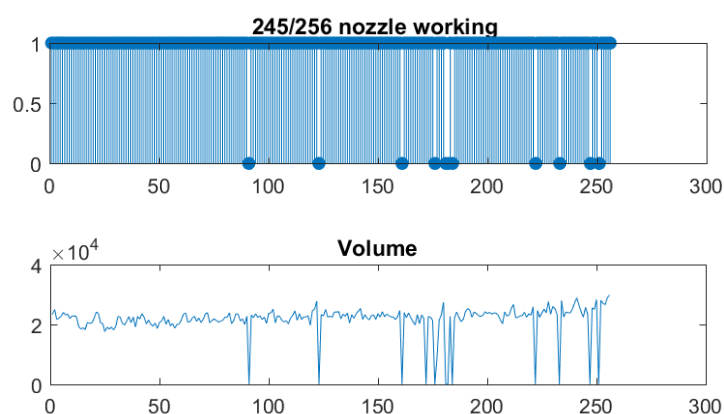


*Figure 74: Result of the nozzle check: nozzle working and volume printed per nozzle [36]*

This process runs every time you start a printing process to check if all the nozzles are working and unclogged. Then, between a process and another, it is necessary to put a wet sponge in contact with nozzles because they dry quickly and the drying causes clogging in a matter of minutes.

Parameters chosen for the wavelet after carrying out numerous DropWatching tests are:

Wavelet Parameters	DMEM 10% (FBS or CS)	3/4 N27 + 1/4 PBS/EDTA
Relax Time	5 $\mu$ s	5 $\mu$ s
Hold Time	2 $\mu$ s	3,5 $\mu$ s
Fall Time	2 $\mu$ s	2 $\mu$ s
Pulse Time	2 $\mu$ s	2 $\mu$ s
High Voltage	60 V	100 V

## 5 Preparation of Bioink

In this project, three different types of cells were used: Rat2, Fibroblast 3T3 and Lung Epithelial Cells A549.

The Rat2 cells have been used for tests concerning the bioink formulation compatible with both printhead and cell viability, this type of cells is easy to use and grows easily in cell culture.

Fibroblast 3T3 cells are easy to use, easy and fast growing, cells commonly used in research. As for the Lung Epithelial Cells A549, the idea in this project is not the only bioink, but in their DMEM on different substrates to show the viability results from the AMI labs [46].

The reference bioink type was taken from the previous project conducted at the iPrint Institute, i.e. the combination of N27 and PBS/EDTA (respectively 3/4 of the first and 1/4 of the second).

Rat2 cells were initially used because they were the cell types available for initial tests.

Bioink for Rat2 had already been formulated but not completely tested; the viability of these cells resulted to be less than 20% after the printing process.

To choose the perfect hydrogel based bioink for each Fibroblast 3T3 cells two tests were conducted:

- cell viability tests, that is the percentage of cells that managed to survive inside the bioink simulating by pipet the printing procedure, verifiable both with Trypan Blue and with the Fluorescence method;
- sedimentation tests to investigate the rate of cell sedimentation within the bioink and to be able to subsequently regulate the time to be dedicated to the printing process, once the bioink has been inserted.

Regarding Lung Epithelial A549 cells, only sedimentation was tested because it was decided, through a collaboration with the AMI Institute of the University of Fribourg, to print them in DMEM on different substrates and subsequently test their viability based on the substrate material used. Tests, already carried out by the AMI, which has been refurbished for the printing of this type of cells are described in the article by Barbara Rothen research group [46]. The aim of studying the printing process of this type of cells is to verify their viability after printing using the multi-nozzle printhead (Biowatcher) on different types of substrates. The main purpose of

printing the lung cells is to be able to create a uniform monolayer, through 3D printing, in which cells adhere efficiently to a cell-friendly or even non-toxic substrate.

Lung diseases are one of the third cause in the world of death. Being able to treat this type of cells as similar as possible to what happens inside the human lung is a point of strength on which the research must aim, and then get to engineer, print in a precise and repeatable way an entire lung.

### 5.1 Viability test with pipet and hydrogel for Rat2 with Trypan Blue method

Rat2 cells, **Figure 75**, are not cells from a well-defined cell line on the market, but they come from the differentiation of mouse-derived stem cells from the bone marrow, of fibroblastic-like morphology.

Being in an adult phase, this type of cell is not totipotent (that is the generator of all the cell lines of the body) but multiple/multipotent, i.e. it can only generate types of connective cells and no other tissues of different embryonic derivation (such as neurons or epithelium).

A cell can be called mesenchymal stem if it shows plastic adhesion properties under normal culture conditions, and if it has a fibroblastic-like morphology. Mesenchymal stem cells have a regenerative role of the tissues, they divide cyclically, and the newly formed cells replace those cells that show signs of aging by membrane receptors, or damaged cells. They can replicate and give rise to connective tissue cells, such as adipocytes, osteocytes, chondrocytes.

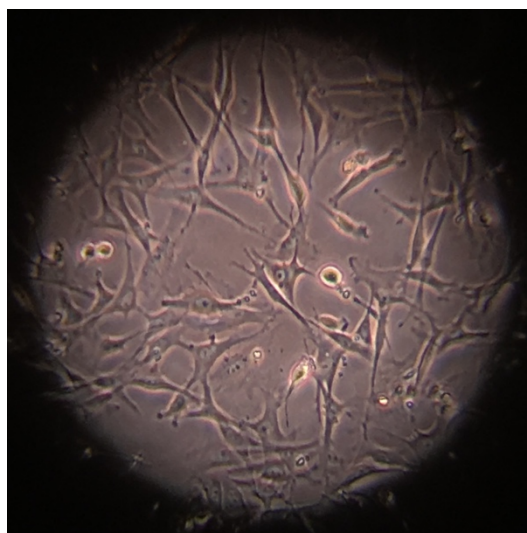


*Figure 75: Rat2 Cells [36]*



The viability of Rat2 cells was tested after a pipette simulation of what would happen with the printing process.

Three different viability tests were performed:

- the first viability test was performed comparing the hydrogels containing 1% Alginate and 2% Alginate;
- the second was done with the formula of the hydrogel 3/4 N27 and 1/4 PBS/EDTA to test, in addition to the viability of the cells, the concentration of solvent to be used in the test to dissolve the hydrogel and count the cells live/dead. If the hydrogel is not completely dissolved, cells may remain adherent to the same and not result in the final count;
- the third was conducted with the 3/4 N27 and 1/4 PBS/EDTA hydrogel using a method of hydrogel jellification different from that one used in previous tests.

### 5.1.1 First Viability Test for Rat2

The first test was carried out by counting cells in such a way as to obtain the  $3 \cdot 10^6$  cells/ml concentration. They were then separated into 4 tubes in order to test twice each type of hydrogel, and they were centrifuged at 12 RPMx100 for 7 minutes to separate the cells from the medium. Two types of hydrogels were tested: 1% and 2% Alginate, each in two different tubes. They were mixed with the cells and the printing process was simulated with pipettes trying to create an homogeneous layer of cells in hydrogel: the hydrogels with cells were placed on substrates based on the Agarose and calcium (through the calcium, the hydrogel creates crosslinks), after 5 minutes the DMEM 10% FBS was added in order to cover the entire hydrogel and penetrate the inside to bring the nutrients to the cells, then the samples were placed in the incubator for 4 hours before proceeding with the real viability test.

The preparation of the Agarose gel was carried out by placing 1,5g of Agarose and 0,28g of  $\text{CaCl}_2$  in 50 ml of deionized water, stirring the compound with a magnetic stirrer until boiling. Then the gel was placed quickly in the Petri Dish and cooled to 22°C, so that it could solidify. For sterilization, the Petri Dish containing the solidified gel was placed under UV light for 12 hours.

After 4 hours, the medium was collected in a tube. In the used Petri dish, the 0,015 M sodium citrate was added over the hydrogel to remove only the Alginate, not the Agarose. Then, tubes were taken in which samples of dissolved hydrogels were collected with the 4 Petri dish cells and centrifuged to separate the cells from the liquid.

Finally, to count cells, it was necessary to insert the DMEM 10% FBS of the same amount of hydrogel used in the process (1ml in this case). Cells were counted through the Trypan Blue dye solution and the results are in **Figure 76**.

## Rat2 Viability Tests: 3 Million of cells/ml

Trypan Blue Method with Confocal Microscope					
	Alive Cells (cells/ml)	Dead Cells (cells/ml)	Total Cells (cells/ml)	Alive Cells Percentage %	Dead Cells Percentage %
1% Alginate	370000	80000	450000	82,2	17,8
1% Alginate	490000	80000	570000	86,0	14,0
2% Alginate	190000	30000	220000	86,4	13,6
2% Alginate	230000	40000	270000	85,2	14,8

*Figure 76: First viability test for Rat2 [36]*

From this type of tests, the viability of the cells seems to be good, not optimal: a logical explanation of these results could be that the cell death is due to the fact that the Alginate in concentration above 1% creates very thick crosslink and the DMEM failed to penetrate inside very well and reach all cells. Unfortunately, however, the cells at the end of the count are fewer than the initial number; most likely because hydrogels with a high concentration of Alginate are more difficult to dissolve and cells could be trapped inside the 3D matrix.

### 5.1.2 Second Viability Test for Rat2

The second viability test for Rat2 cells was done using the same procedure and concentration of cells from the first test, but using the hydrogel 3/4 N27 and 1/4 PBS/EDTA like scaffold. Six

different tests were carried out to test six different amounts of solvent (from 1ml to 3,5 ml of sodium citrate) to dissolve the hydrogel before making the final count of cells for the viability test.

The **Figure 77** shows results of this experiment in terms of total cell count and percentage of live/dead cells.

These results represent the half-quantity of cells before doing the procedure with hydrogel. N27 and PBS/EDTA formula is too much liquid, in fact, when the DMEM was on the top of it, a piece of hydrogel migrated from the Agarose to the DMEM with crosslinking well with the substrate. For this reason, in the DMEM there are cells and hydrogel that do not result in the final counting. It is necessary to wait 10 minutes to let the hydrogel crosslink before adding the DMEM and put cells in the incubator.

From these results, it is not clear that too much sodium citrate, compared to hydrogel, make damage cells: it is preferable to use the minimum amount of sodium citrate to dissolve the hydrogel to avoid damaging the cells. The ideal procedure would be to dissolve the hydrogel with at most twice its amount (for example 1ml of sodium citrate to dissolve 0,5 ml of hydrogel). For this kind of hydrogel, 1 ml of sodium citrate is enough because it contains only 0,5% of Alginate HV and a large amount of solvent is not needed to dissolve it.

## Rat2 Viability Tests: 3 Million of cells/ml

Trypan Blue Method with Confocal Microscope					
3/4 N27 + 1/4 PBS/EDTA	Alive Cells (cells/ml)	Dead Cells (cells/ml)	Total Cells (cells/ml)	Alive Cells Percentage %	Dead Cells Percentage %
1ml sodium citrate	1320000	60000	1380000	95,7	4,3
1,5 ml sodium citrate	1660000	80000	1740000	95,4	4,6
2ml sodium citrate	1180000	100000	1280000	92,2	7,8
2,5ml sodium citrate	1340000	90000	1430000	93,7	6,3
3ml sodium citrate	1510000	80000	1590000	95,0	5,0
3,5ml sodium citrate	910000	50000	960000	94,8	5,2

Figure 77: Second viability test for Rat2 [36]

### 5.1.3 Third Viability Test for Rat2

The third viability test for Rat2 cells was done to verify the viability of cells, after the hydrogel, 3/4 N27 and 1/4 PBS/EDTA, was stained with a red food colourant and made crosslink with a solution liquid of  $\text{CaCl}_2$  50 mM.  $3 \cdot 10^6$  of cells/ml were prepared and placed in hydrogel. It was separated into two tubes, one of the two was coloured in red. The fact of colouring the hydrogel serves to the operator to better see the hydrogel, which would otherwise be transparent, when he needs to dissolve it in order to count the cells. Hydrogel drops through syringe were created, causing them to fall into the  $\text{CaCl}_2$  solution, as already done in the paragraph 4.1.3 *Recirculation*

*Test.* The Calcium solution was removed and replaced with DMEM; subsequently, the DMEM with the hydrogel spheres was placed in the incubator for 4 hours.

Hydrogel drops were collected with a spoon and dissolved with 0,055M Sodium Citrate. The solvent was removed after separating the cells from it by centrifugation; then the DMEM, of the same amount of hydrogel collected with the spoon, was added.

The viability test was done for the coloured hydrogel, the non-coloured one, and the one left in the DMEM that was not able to be taken because the spoon was too big.

**Figure 78** shows that all three results have a high level of viability, but the coloured hydrogel has a higher cell concentration because it was easier to collect most of the drops of hydrogel in the DMEM thanks to the greater visibility given by the colour.

### Rat2 Viability Tests: 3 Million of cells/ml

Trypan Blue Method with Confocal Microscope					
3/4 N27 + 1/4 PBS/EDTA	Alive Cells (cells/ml)	Dead Cells (cells/ml)	Total Cells (cells/ml)	Alive Cells Percentage %	Dead Cells Percentage %
hydrogel with food colour	2170000	60000	2230000	97,3	2,7
normal hydrogel	1690000	20000	1710000	98,8	1,2
remained hydrogel	1660000	100000	1760000	94,3	5,7

*Figure 78: Third viability test for Rat2 [36]*

In conclusion, given the results of the three viability tests for the Rat2 Cells, this type of mesenchymal cell of fibroblast-like behavior is able to remain alive if inserted into an Alginate-based hydrogel scaffold.

## 5.2 Test for different Types of Hydrogel remaining in Viscosity Range for Fibroblast 3T3

For Fibroblast 3T3, it was first necessary to find the correct bioink for the printing that would maintain the viability of cells because this type of cells had never been tested before with the Biowatcher and with these bioink formulas. The bioink already validated as working for Rat2 has been tested in comparison of other hydrogels and then the best in terms of cell viability has been chosen.

Cell Line Origin from Mouse Swiss NIH Embryo: they are embryonic fibroblast. They grow in adherent mode, with fibroblast morphology. The 3T3 cell line has become the standard fibroblast cell line. The “3T3” designation refers to the abbreviation of “3-day transfer, inoculum  $3 \cdot 10^5$  cells”. This cell line was originally established from the primary mouse embryonic fibroblast cells that were cultured by the designated protocol, so-called “3T3” protocol. The primary cells were transferred (the “T”) every 3 days (the first “3”), and inoculated at the rigid density of  $3 \cdot 10^5$  cells per 20cm<sup>2</sup> dish (the second “3”) continuously. The cells spontaneously stabilized in culture after 20 or 30 generations with a stable growth rate, and then named “3T3” cells [49].

For cell viability tests using pipets, it was decided to use these four hydrogels on two different substrates, Agarose with Calcium Chloride (solid) and a Calcium Chloride solution (liquid):

- N27,
- 3/4 N27 + 1/4 PBS/EDTA,
- 1% Alginate,
- 2% Alginate,

because the Biowatcher can print the hydrogel with the maximum concentration of 2% Alginate to still have alive cells (otherwise if the bioink is with more than the 2% of alginate, DMEM cannot reach cells and they die) after the printing process [59].

The test was performed with two different dye solutions: LIVE/DEAD ASSAY with Fluorescent Microscope and Trypan Blue.

### 5.2.1 Viability Tests with Fluorescent Microscope

Printing simulation with 3T3 cells was initially tested with pipetting and the Nikon Eclipse Ni fluorescence microscope. 3T3 Cells have been put inside four different hydrogels, on the solid surfaces made with Agarose and Calcium Chloride to let the hydrogels crosslink. After that the hydrogels became gel, the DMEM was added on each sample and all the samples have been put four hours in the incubator. After this printing simulation, it was possible to apply the procedure to establish, through a fluorescent microscope, how many cells are alive or dead.

The procedure for counting the live/dead cells occurred differently: it was not necessary to dissolve the hydrogels, so there was no cell death due to the abundance of sodium citrate, in fact it was used the LIVE/DEAD ASSAY KIT, inserting the dye solution directly on the crosslinked hydrogel and going to see with the fluorescence microscope the colour that the cells have taken.

Using NIS-Elements BR software, the samples were analysed with two focus modes, x4 and x20 respectively to do a better statistic in the cell counting with different microscope focusing. To visualize live cells, the lens with the green filter was used, while for the dead cells the red one. Examples of images of live and dead cells are shown in **Figure 79**.

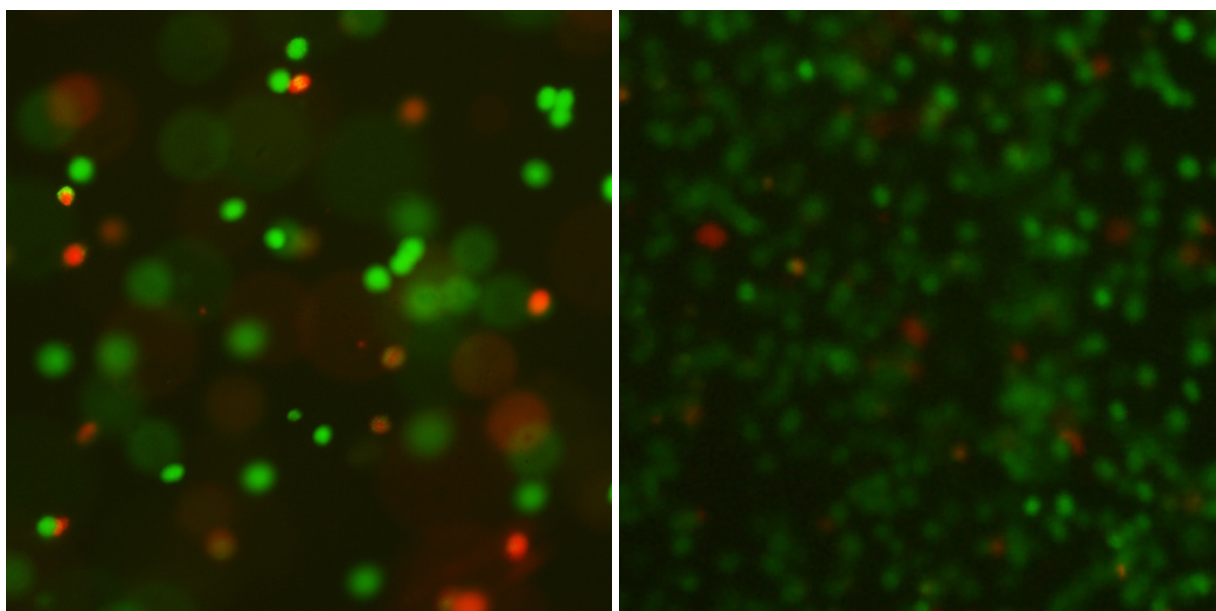


*Figure 79: Fluorescent Microscope Images: 2% Alginate x20 and 3/4 N27+1/4 PBS/EDTA x4 [60]*



All acquired images were analysed with the ImageJ software according to the following procedure:

1. Run ImageJ and load the picture:
2. Click on “image – colour – split channels” to get the red, blue and green decomposition of the main image. The images will be black and white picture but the name of the colour is in the name of the window, **Figure 80**.

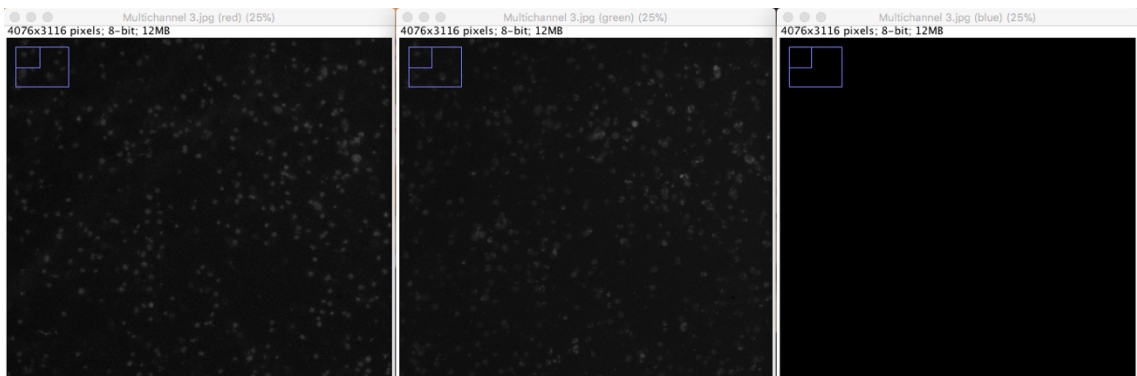


*Figure 80: Example of ImageJ Analysis [36]*

3. Close the blue (no dots on the window);
4. Select the green picture;
5. Press Ctrl+Shift+I to invert the image;
6. Press Ctrl+Shift+T to open the threshold command window;
7. Click on “auto” and adjust manually with the slider to have all the cells fill in red. Click on “apply”;
8. Close the threshold command window;
9. Click on “analyze–analyze particles”;
10. Set the option as **Figure 81**:

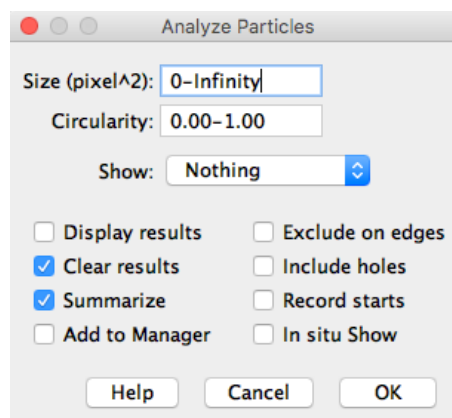


*Figure 81: Analyse Particles ImageJ Parameters [36]*

11. Click on “OK” to get the results;
12. Select the red picture and repeat the procedure from point 5 to 11.

Results obtained from the analysis of the green and red cells by ImageJ are reported in **Figure 82**.

Fibroblast 3T3 Viability Tests: 3 Million of cells/ml				
Live/Dead Assay with Fluorescent Microscope				
1% Alginate	Alive Cells	Dead Cells	Alive Cells Percentage	Dead Cells Percentage
x4 Objective Lens	215	40	84,3	15,7
x20 Objective Lens	86	47	64,7	35,3
x20 Objective Lens	35	10	77,8	22,2
2% Alginate	Alive Cells	Dead Cells	Alive Cells Percentage	Dead Cells Percentage
x4 Objective Lens	388	45	89,6	10,4
x20 Objective Lens	24	19	55,8	44,2
N27	Alive Cells	Dead Cells	Alive Cells Percentage	Dead Cells Percentage
x4 Objective Lens	192	120	61,5	38,5
x4 Objective Lens	180	74	70,9	29,1
x20 Objective Lens	293	77	79,2	20,8
3/4 N27 + 1/4 PBS/EDTA	Alive Cells	Dead Cells	Alive Cells Percentage	Dead Cells Percentage
x4 Objective Lens	605	26	95,9	4,1
x4 Objective Lens	210	31	87,1	12,9
x20 Objective Lens	134	40	77,0	23,0
Maximum Value				

*Figure 82: Viability test with Fluorescent Microscope for Fibroblast 3T3 [36]*

Cells within the 3/4 N27 and 1/4 PBS/EDTA hydrogel have significantly higher post-processing viability than other hydrogel combinations.

### 5.2.2 Viability Tests with Trypan Blue

To verify that the results obtained through the LIVE/DEAD ASSAY are effective, the Trypan Blue method has also been applied on two different substrates: Agarose with Calcium Chloride (solid) and a Calcium Chloride solution (liquid).

Printing-simulation was done:

- with the same modalities and hydrogels used with the LIVE/DEAD ASSAY to make a comparison between the two methods of verification of cell viability. For this method, the red food colour has been used, since it has already been verified to be non-toxic for the cells, to better visualize the hydrogel;
- by crosslinking the hydrogel in a  $\text{CaCl}_2$  solution by providing small spheres containing hydrogel and cells. This second method of testing was done because the Agarose is slightly toxic to the cells and the solvent sodium citrate 0,055M, in part, also dissolves the Agarose in addition to the Alginate, while in the 50mM  $\text{CaCl}_2$  solution it is not present.

Results obtained from this test, **Figure 83**, show the confirmation that the 3/4 N27 and 1/4 PBS/EDTA hydrogel is the best to use with Fibroblast 3T3 cells because it has good cell viability. The viability tested with the Agarose and  $\text{CaCl}_2$  substrate is lower because of osmotic pressure between Agarose and Alginate-based hydrogels. It would be advisable to increase the accuracy during the printing process regarding this gel which could be harmful to the cells.

### Fibroblast 3T3 Viability Tests: 3 Million of cells/ml

Trypan Blue Method with Confocal Microscope				
1% Alginate	Alive Cells (cells/ml)	Dead Cells (cells/ml)	Alive Cells Percentage	Dead Cells Percentage
CaCl <sub>2</sub>	90000	150000	37,5	62,5
Agarose	30000	50000	37,5	62,5
2% Alginate	Alive Cells (cells/ml)	Dead Cells (cells/ml)	Alive Cells Percentage	Dead Cells Percentage
CaCl <sub>2</sub>	70000	120000	36,8	63,2
Agarose	110000	90000	55,0	45,0
N27	Alive Cells (cells/ml)	Dead Cells (cells/ml)	Alive Cells Percentage	Dead Cells Percentage
CaCl <sub>2</sub>	350000	180000	66,0	34,0
Agarose	250000	200000	55,6	44,4
3/4 N27 + 1/4 PBS/EDTA	Alive Cells (cells/ml)	Dead Cells (cells/ml)	Alive Cells Percentage	Dead Cells Percentage
CaCl <sub>2</sub>	480000	150000	76,2	23,8
Agarose	20000	10000	66,7	33,3
Maximum Value				

*Figure 83: Viability test with Confocal Microscope for Fibroblast 3T3 in different hydrogels [36]*

Using the hydrogel that in previous printing simulations showed the highest value of cells viability, different simulation tests were decided to do.

Cells were counted to result in the concentration of  $3 \cdot 10^6$  cells/ml dissolved in the coloured hydrogel 3/4 N27 and 1/4 PBS/EDTA via a red food colour. Drops, of a total volume of 1 ml, were dropped from the syringe onto a substrate of Agarose and Calcium Chloride, in such a way as to make the hydrogel gel, procedure shown in **Figure 84**.

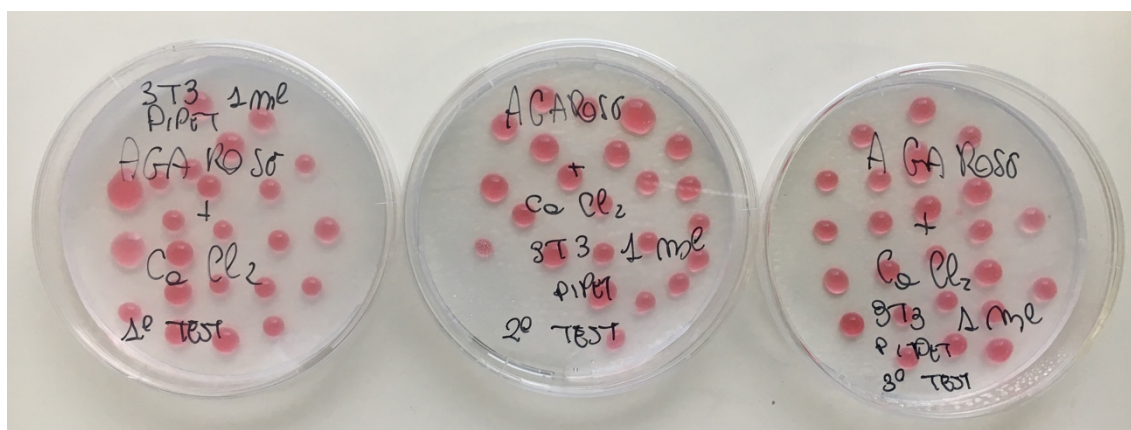


*Figure 84: Pipet Tests of Fibroblast 3T3 Cells [36]*

After confocal microscopy checking that cells were in the solidified hydrogel, first picture of **Figure 85**, 10 ml of DMEM 10% CS were added in each Petri Dish to allow cells to have necessary nutrients for their survival. The three Petri Dishes were placed in the incubator for 4 hours and then the viability test was carried out using Trypan Blue.

To perform this test, DMEM was removed, after that, the hydrogel drops were collected, placed in different tubes and dissolved with 2ml of Sodium Citrate Solution. Once the hydrogel was dissolved, the cells were separated from it by centrifugation at 1200 RMP x 7 minutes, the liquid compound was removed, and 1ml of DMEM 10% CS was added to bring the cells back to the same concentration initial they had in the hydrogel. At this point, the test was done and the results are shown in the figure. **Figure 85** part two shows an example of the live and dead cell count using the Trypan Blue.

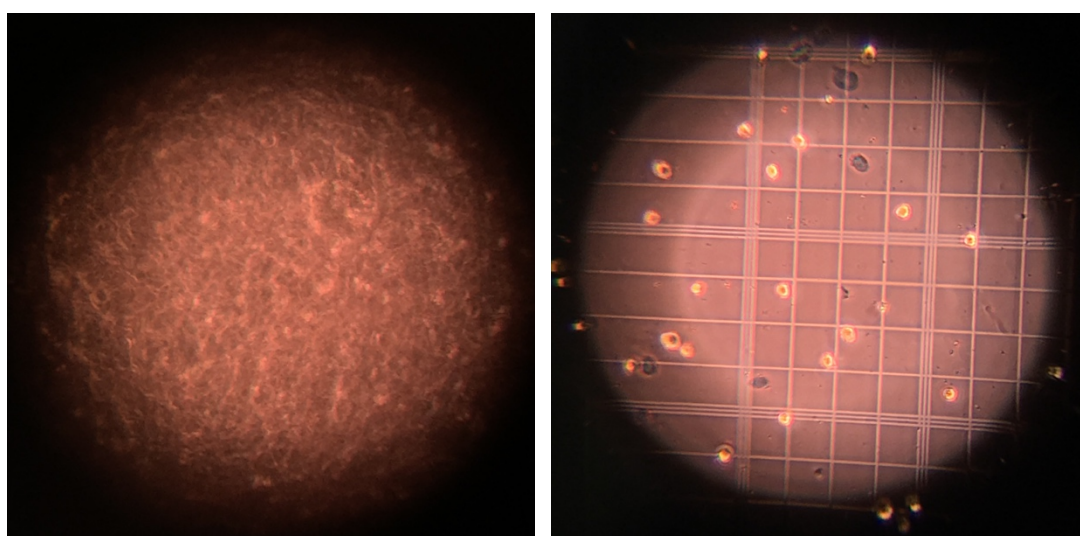


*Figure 85: Fibroblast 3T3 Cells in coloured hydrogel and with Trypan Blue under Confocal Microscope [36]*

## Fibroblast 3T3 Viability Test: 3 Million of cells/ml

### Trypan Blue Method and Confocal Microscope

in 3/4 N27 + 1/4 PBS/EDTA	Alive Cells (cells)	Dead Cells (cells)	Total Cells (cells)	Alive Cells Percentage %	Dead Cells Percentage %
1°Test on Agarose and CaCl <sub>2</sub>	2790000	130000	2920000	95,5	4,5
2°Test on Agarose and CaCl <sub>2</sub>	2260000	150000	2410000	93,8	6,2
3°Test on Agarose and CaCl <sub>2</sub>	1840000	70000	1910000	96,3	3,7

*Figure 86: Viability test with Confocal Microscope for Fibroblast 3T3 in 3/4 N27 and 1/4 PBS/EDTA [36]*

The results obtained from this simulation test, shown in the **Figure 86**, show an excellent cell viability after this treatment with 3/4 N27 and 1/4 PBS/EDTA on Agarose and Calcium Chloride: the mean value is 95,2% of alive cells with a standard deviation of 1,3%. Therefore, this hydrogel formulation is taken as a reference for the subsequent tests carried out on Fibroblast 3T3 cells.

### 5.3 Viability Tests for Lung Epithelial Cells A549 with Trypan Blue Method

Cell Line Origin from Human White lung carcinoma, derived from a 58-year-old Caucasian male. They grow in adherent mode, with epithelial morphology [50].

To simulate the printing process with pipet, shown in **Figure 87**, A549 cells were counted, centrifuged and placed in their DMEM in the  $3 \cdot 10^6$  cells/ml concentration. By pipet then, some drops were randomly dropped into the Petri Dish. After 30 minutes, thanks to the confocal microscope, cells were checked to see if they had adhered to the substrate where the drops of DMEM and cells had been dropped; subsequently another DMEM was added to the Petri Dish to allow cell growth and increased adhesion.



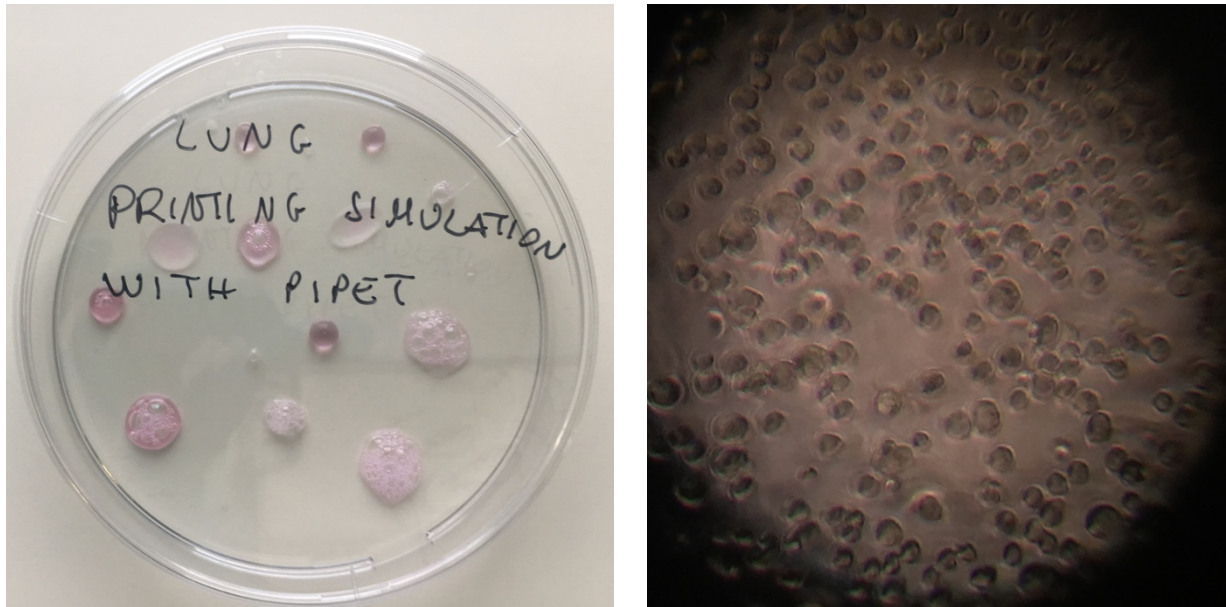


*Figure 87: Lung Epithelial Cells A549 Printing Simulation with Pipet [36]*

The viability test was performed using the Trypan Blue, going to detach the cells from the substrate through trypsinisation. Results are perfect, bringing back 100% of viability **Figure 88** and cells adhere well to the Petri Dish.

### A549 Viability Tests: 3 Million of cells/ml

Trypan Blue Method with Confocal Microscope					
DMEM 10% FBS	Alive Cells (cells/ml)	Dead Cells (cells/ml)	Total Cells (cells/ml)	Alive Cells Percentage %	Dead Cells Percentage %
Cells on Petri Dish	150000	0	150000	100,0	0,0

*Figure 88: Viability test with Confocal Microscope for Lung Epithelial Cells A549 [36]*



## 5.4 Sedimentation Tests for Cells

It is important to study the cells sedimentation in bioinks before to put them in print because, if the time that occurs to cells to sediment is too much short possible to print them in a specific bioink or the total process should be fast to avoid clogging.

### 5.4.1 Sedimentation Theory

When a particle is dispersed in a medium, three forces act on it; gravitational drag forces, **Figure 89**. The size of cell between 10-30  $\mu\text{m}$  brings them in colloidal particles. Depending on the properties of the particle and dispersion balance of forces will dictate whether a particle will cream, sediment, or remain [29]

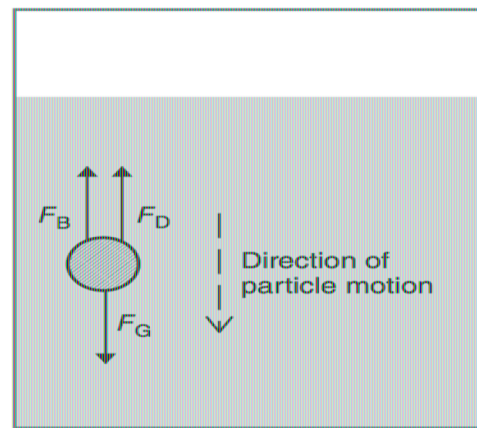


**Figure 89:** Schematic of forces acting on a dispersed particle [29]

For a colloidal stable dispersion, particles are to remain in suspension during the printing procedure in order to guarantee its quality.

The three forces acting on the dispersed particle are as follow:

1. Gravitational force,  $F_G$ , is due to the Earth's gravity, which acts on

Earth's surface.  $F_G = \frac{4}{3} \pi r^3 \rho_p g$  where  $r$  is the particle radius,  $\rho_p$  is the particle density, and  $g$  is the gravitational acceleration.

2. Buoyancy force,  $F_B$ , is the upward force exerted by the medium on a particle placed into it.  $F_B = \frac{4}{3} \pi r^3 \rho_m g$  where  $\rho_m$  is the density of the dispersion medium.
3. Drag force,  $F_D$ , is the frictional force experienced by a particle when it moves through a fluid. This force is due to the viscosity of the medium and is governed by Stokes' law. It follows:  $F_D = 6\pi r \mu v$  where  $\mu$  is the solvent viscosity and  $v$  is the particle velocity.

Therefore, as a particle is dispersed in a medium, it immediately experiences a downward gravitational force, which is balanced by the upward buoyancy force. By analogy, if a particle has a density greater than that of the medium, the particle will fall. As soon as it starts to move, the medium drag will impose an opposing force to the motion. In the case of a particle in a solution staying in a non-moving container, the gravitational forces become very small.

At some point, the particle reaches a terminal velocity,  $v_t$  called also sedimentation velocity, when the drag force balances the difference between gravitational and buoyancy forces:

$$F_G - F_B = F_D$$

$$\frac{4}{3} \pi r^3 (\rho_p - \rho_m) g = 6\pi r \mu v_t$$

$$v_t = \frac{2r^2(\rho_p - \rho_m)g}{9\mu}$$

Thus, this allows the colloidal stability of a particle dispersion to be predicted. In reality, this estimation will be affected by the wall effect and particle concentration [29]:

1. Wall effect considers additional retardation force on the falling particle due to the influence of the container walls. This influence can be compensated with a correction factor:  $f_w = \frac{v_t(b)}{v_t(\infty)}$  where  $f_w$  is the wall correction factor and  $v_t(b)$  and  $v_t(\infty)$  are the terminal velocities in a bounded and unbounded fluid, respectively. The wall correction factor is a function of the ratio of particle to container radius.

$2r/D_c$ . However, the wall correction factor becomes more complex as particle size and fluid type deviate from the ideal cases.

2. As the particle concentration increases, the settling behavior switches from single particle to batch settling. The inter-particle interaction induces a slower settling velocity. This is generally known as *hindered settling*, as governed by the equation  $v_t(1 - \phi)^n$  where  $v_{tc}$  is the terminal velocity of a uniformly sized particle at volume fraction  $\phi$  and  $n$  is a particle-specific empirically determined constant governed by the particle Reynolds number at  $v_{tc}$ .

If the sedimentation velocity is bigger than the theoretical results calculated with  $D_p = 2r$  is because clusters of 2 or 3 particles are formed. These clusters will have a bigger sedimentation velocity as the considered  $D_p = 2r$  is then too small. The sedimentation then has a lower sedimentation velocity as it gets smaller when the clusters have fallen at the bottom. It seems that the viable cell settling velocity varies significantly depending on the volume fraction of the cells in the solvent will also influence the viscosity and sedimentation velocity [29].

$$\mu_{eff} = \mu_0 e^{2,34\phi} \frac{1}{1 - \frac{\phi}{\phi_m}}$$

where  $\mu_{eff}$  is the effective viscosity of the solution,  $\mu_0$  is the viscosity of the solvent,  $\phi$  is the volume fraction.  $\phi_m$  is called the jamming volume fraction and it is the volume fraction is so big that operator always faces a situation with clogging. As the volume fraction increase as the volume fraction increase. The volume fraction can be calculated as  $\frac{4\pi R^3 N}{3V}$  where  $R$  is the particle radius,  $N$  is the number of particles and  $V$  is the total volume. that the maximum packing volume fraction for hard sphere is between  $\phi = 0,55 - 0,6$ . jamming volume fraction is reported to be between  $\phi_m = 0,2 - 0,6$ .

### 5.4.2 Aggregation

The aggregation is the self-assembly of colloidal particles. It is affected by diffusion and colloidal forces. The advection is the transportation of a substance and its effect is also called the hydrodynamic effect. The diffusion is due to the thermal energy. These effects are summarized by the Peclet number [29]:

$$Pe = \frac{6\pi D^2 U}{k_B T}$$

where  $U$  is the fluid velocity,  $D$  the diameter of the particle and  $T$  the absolute temperature. The diffusion due to the thermal energy follows the Einstein diffusion equation which is given by the Stokes-Einstein equation [29]:

$$D_{coeff} = \frac{k_B T}{6\pi\mu R}$$

where  $T$  is the absolute temperature,  $\mu$  is the viscosity and  $R$  is the radius of the particle. The aggregation is due to the short range attractive Van der Waals forces. It is understood through quantum physics. It is approximated by the Lennard-Jones potential, **Figure 90**.

$$V(r) = 4\varepsilon \left( \left( \frac{\sigma}{r} \right)^{12} - \left( \frac{\sigma}{r} \right)^6 \right)$$

where  $\sigma$  is the distance at which the inter-particle potential is known to be zero. Particles can reach the vicinity of another depending on the Peclet number.

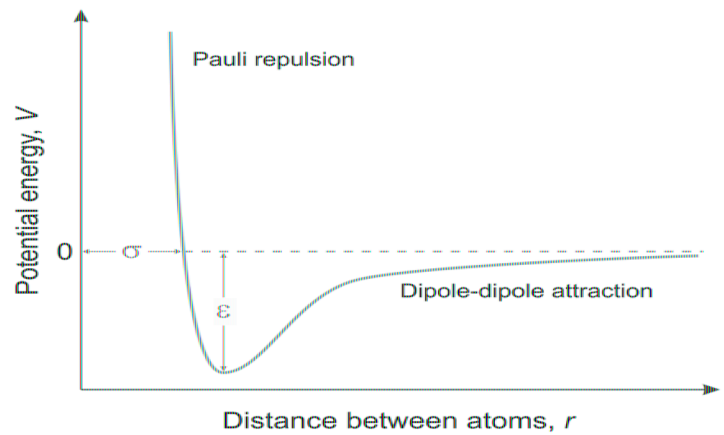


**Figure 90:** Graph of the Lennard-Jones interaction potential [29]

### 5.4.3 LDVO Theory

This theory is used to explain forces acting between interfaces and deposited particles on substrates. It uses the formula for the force between two colloidal particles at a distance  $r$  related to the free energy (statistical mechanics). It is assumed that the contributions are the Van der Waals and the double layer interactions (which are significant in charged cases).

The aim to avoid fast aggregation is to have a high-energy barrier. For instance, one can have a low salt level and the energy barrier develops due to the electric double layer interactions.

There are two regimes: fast aggregation or diffusion controlled aggregation (DLCA) and slow aggregation or reaction controlled aggregation (RLCA). The regime of the solution is determined by the aggregation rate coefficient  $W$  which gives the value of the ratio between the DLCA and RLCA aggregation. It is approximated using the Fuchs theory. [29]

$$W \approx \frac{1}{2\kappa R} e^{\left(\frac{V_{T,max}}{k_B T}\right)}$$

where  $1/\kappa$  is the Debye thickness of the diffusive layer,  $V_{T,max}$  is the maximum interaction potential,  $R$  is the particle radius and  $T$  is the absolute temperature. The aggregation rate is very sensitive to even small changes of the surface charge or potential, **Figure 91**

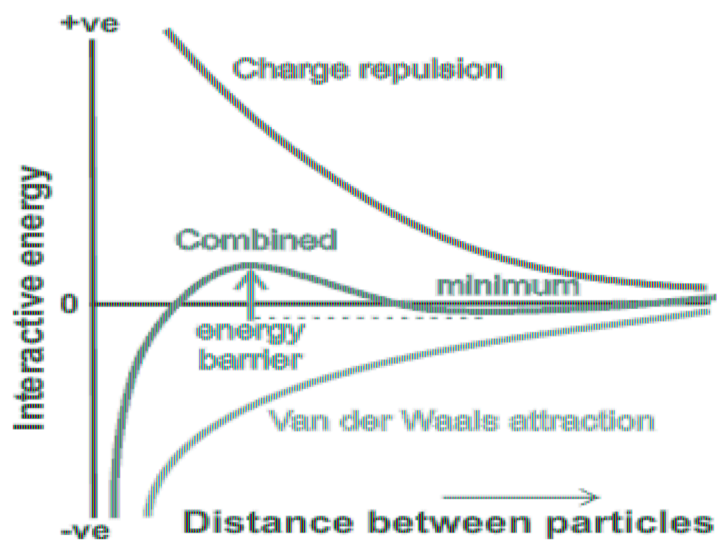


Figure 91: Graph of the DLVO interaction potential [29]

Clogging is described by the mean clogging time which is the time interval between the printer and when the flux is clogged.

$$\langle t_{clog} \rangle = \frac{1}{cQ}$$

where  $c$  is the concentration of the big particles and  $Q$  is the flow rate.

The clogging is determined by the flux deposition  $j_{dep}$  of particles on the surface. As the distance from the entrance of the channel, the Reynolds number decreases, the flux deposition increases. It is possible to modify the flux by varying the concentration of electrolyte salt.

#### 5.4.4 Sedimentation Velocity

The sedimentation velocity  $v$  is given by equation [29]:

$$v_t = \frac{2r^2(\rho_p - \rho_m)g}{9\mu}$$

The possibility to decrease the sedimentation velocity is to increase the viscosity of the range allowed by the system (piezo, printing). In the example given, the viscosity was  $\mu_{max} = 20mPas$ . As the viscosity has this relation with the volume fraction, it is also possible to increase the volume fraction in order to increase the viscosity.

#### 5.4.5 Neutral Buoyancy

The possibility to use Ficoll PM400 [61] to increase the neutral buoyancy when the density of the cells is higher than the density of the solution. A solution with the cells body density, that is close to the density of the solution is prepared. The physical effects on the solution is to have an "offset" of the gravity. Ficoll PM400 is used to increase the cell separation. It has the advantage to have a low osmotic pressure. It doesn't affect the viability and it doesn't change the results of the experiments where done with 0 – 20%w/v in the solvent. About 0.25% of Pluronic F127 reduce the surface tension.



Ficoll PM400% (w/v)	0	5	10	15
$v$ ( $\mu$ /s)	7,5	2,9	0,8	0,15

Other options to have neutral buoyancy is to use sucrose or dextran which also create density gradients for cell separation but they will make the osmotic pressure bigger. Ficoll PM400% was tested for the sedimentation rate for A549 cells but it did not give the same results as the cells sedimented at the same speed in DMEM without Ficoll PM400%.

#### 5.4.6 RLCA aggregation

To avoid aggregation, one solution would be to reduce the diffusion so the particle displacement is small. Knowing the diffusion coefficient from equation  $D_{coef}$  (eq. 1.10) decrease with the temperature or with an increasing viscosity.

Solutions can be made kinetically stable by building an energy barrier sufficient to overcome respect to the thermal energy of the particles. One stabilization mechanism is by using electrically charged particles.

The adsorption of ionic surfactants can increase the electrical charge on the surface of the particles. These can be salts which are fully dissociated or weak acids.

There is the possibility to stabilize particles when long term stability is required by coating of the particles with some material that prevents their close approach (e.g. silica).



#### 5.4.7 Algorithm Development and Test with PMMA and results

To study the sedimentation velocity and the initial and final number of cells within the bioink, both based on hydrogels and DMEM, a completely automatic way was studied that exploits the images collected by the cameras and automatically processes them on Matlab.

Bioink, in which cells in  $3 \cdot 10^6$  cells/ml concentration are present, is placed inside a glass tube in the focal position of the camera.

The algorithm, implemented in matlab and shown in paragraph *10.3 Sedimentation Test*, has been designed and structured to perform all operations automatically as soon as the operator decides to start the program.

First of all, initializations are performed to connect the FPGA and then synchronize the acquisition of the images with the light pulse provided by the LED. After that, it is possible to start a part in which the state of the camera is displayed, allowing the operator to check before starting the actual program, if the tube containing the bioink with the cells has been positioned in the focal position of the camera.

The operator is free to choose the total number of images to be scanned every 30 seconds. The algorithm then acquires the first image, calculates the average value (i.e. makes the sum of the values of each pixel and divides it by the total number of pixels) and automatically adjusts the duration of the LED if this value is outside the defined tolerance range.

It has been set as the average value of an 8-bit grayscale image, that is to 128 (since  $2^8 = 256$  corresponds to the maximum brightness value, white, and 0 corresponds to black) with a tolerance of 10.

This means that if the acquired image has a mean value outside the interval  $128 \pm 10$ , then the LED will increase its brightness, if the value is lower than 118, or it will decrease its brightness for values higher than 138.

As already anticipated, the camera is able to take a digital image. It is a numerical matrix,  $A[m,n]$ , formed by a certain number of lines ( $m$ ) and columns ( $n$ ).

Each element of the array of place  $[i, j]$  is called “pixel”; it is the smallest element of which a digital image is constituted. Each pixel has a colour and therefore only one numerical value.

Images that can be acquired from the camera installed on the Biowatcher are monochromatic 8-bit grayscale. This means that each pixel can assume a value between 0 and  $2^{(N_{bit}-1)}$ , in which  $N_{bit} = 8$  in this case ( $N_{bit}$  is the number of bit). In the standard encoding of digital images, the

number 0 corresponds to the black colour and the number  $2^{(N_{bit}-1)}$  to white (255 in this case); all the digits included between these two numbers correspond to shades of grey [62].

Knowing these parameters of digital images, it is easy to consider a monochromatic image as a two-dimensional numeric matrix that contains a certain number of values and implement an algorithm for processing it in matlab: doing operations on the images means working on matrices.

The algorithm created, after saving a copy of the image, processes it using the "adapthisteq" function that determines the threshold level to use in the binarization operation.

The thresholding is a particular method of segmentation (process aimed at identifying and delimiting in an image the areas occupied by the different types of objects present) that works mainly on grayscale images, and has the objective of drastically separating a category of object with respect to the rest. With this technique, a binary image is produced which represents the areas of interest with the white colour and with a black background the areas of non-interest (or vice versa); its operation consists in a selection based on all values (generally of brightness) above or below a certain threshold. The optimal threshold value is typically determined by the histogram relative to the image, identifying the valley zone between two peaks or between two main fashions [62].

The thresholding can be derived directly from the software on the basis of the histogram (automatic thresholding). Alternatively, the threshold can be set manually by the operator (manual thresholding) or by a combination between the threshold suggested by the software and the operator control (semi-automatic thresholding).

If the threshold can be considered constant throughout the image, it's about global thresholding; in the opposite case, it's instead of variable thresholding. The global thresholding is generally used when the image is characterized by homogeneous and well-defined colorations throughout its surface, as in this case the background colour is homogeneous and photographed cells are all the same colour and darker than the background.

On the other hand, when the image is characterized by a shaded hue (for example due to inhomogeneous lighting), the variable thresholding is used; in particular, the image is subdivided into smaller boxes within which there is a certain homogeneity of the colours, and a thresholding is applied separately on each frame, so as to select the best threshold value for each frame. For this purpose, there are also local thresholding algorithms, that use a variable threshold value (within a certain interval) locally inside the image so as to automatically compensate for the lack of homogeneity of lighting.

Another possible case consists in having a uniform background but with objects characterized by different brightness values. Also in this case a global thresholding cannot be applied, as some objects can be excluded or on the contrary a part of the background can be included. Adaptive thresholding algorithms have been developed to deal with such a situation, which allow us to identify the objects present with a good approximation. These algorithms are programmed to adapt the threshold value object by object, provided only that the average size of the objects is known to a certain extent [62].

The image is then converted into a binary format with the functions "adapthresh" and "imbinarize" specifying the threshold value, taking care to put the cells in white and the background in black (the function described works with these specifications). Then the perimeters of the objects are identified with the "bwboundaries" function and saved in a different vector for each acquired image. The number of elements in the vector corresponds to the total number of objects in the image.

With this algorithm, it was therefore possible to find the number of cells present in each image acquired at a temporal distance of 30 seconds, then, through appropriate calculations, also the speed of sedimentation of the same.

if the operator wants to view all the steps performed by the image processing algorithm, it is possible to use the "elaborate\_images" function and choose which image to re-analyse.

The algorithm has been tested each time with a tube containing Polymethyl methacrylate (PMMA) particles with a known diameter of 8  $\mu\text{m}$  suspended in demineralized water because the cells used in this Master Thesis have a diameter between 8 and 20  $\mu\text{m}$  and these PMMA particles were found to be very similar to them. Furthermore, it is not always possible to have live cells available for a long period of time. To test the algorithm, it was necessary to use a material that did not change morphology and properties in some hours. In fact, when cells die, even after 1 hour outside the conditions of sterility and incubation, they sediment faster because they change their morphology (apoptosis, cell membrane opening, lack of interaction with each other, etc).

An example of the test carried out using the algorithm over described on PMMA particles is shown in *Figure 92*.

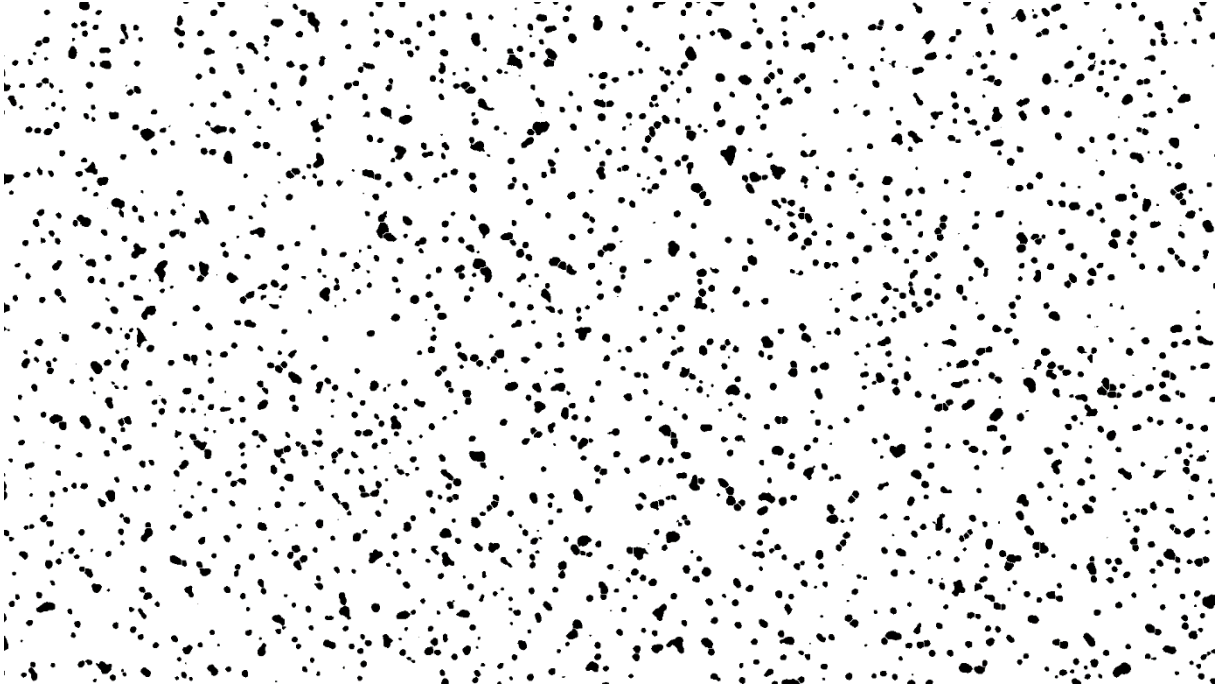


*Figure 92: Picture of PMMA elaborated with Sedimentation Algorithm [36]*

### 5.3.8 Sedimentation Tests with only DMEM and Hydrogel

Before carrying out the various sedimentation tests with cells, images were taken from the cameras relating to the suspension mediums used.

**Figure 93** and **Figure 94** show the images related to the DMEM and the hydrogel used respectively ( $\frac{3}{4}$  N27 +  $\frac{1}{4}$  PBS/EDTA): it is evident that no particles are present, or that the camera, thus set up, cannot detect particles smaller than the diameter of the cells.

In this way, it is certain that the created algorithm works correctly by intercepting and counting only the number of cells displayed, cause the "background" represented by the suspension medium is clearly without other particles.



*Figure 93: DMEM Picture [36]*

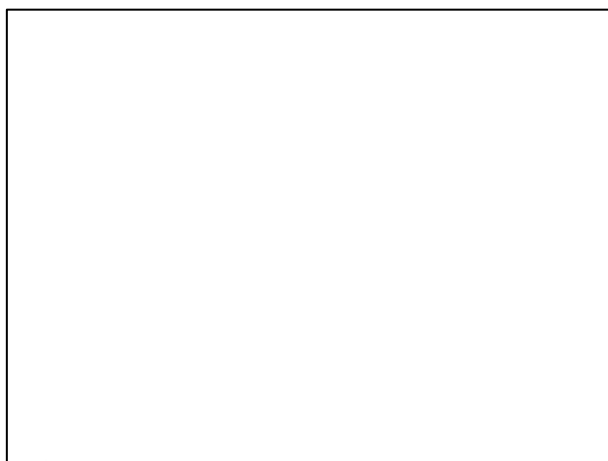


*Figure 94: 3/4 N27 + 1/4 PBS/EDTA Picture [36]*

#### 5.4.9 Sedimentation Test for Rat2

The sedimentation study for Rat2 cells was carried out in DMEM 10% FBS, that is the culture medium used for this type of cells and in the hydrogel obtained from the combination of the chemical formula N27 and PBS/EDTA.

The cell concentration used for both tests is  $3 \cdot 10^6$  cells/ml, reference in this Master Thesis as a standard concentration for the classic printing process, the one that has been used by AMI and others. This type of cell has the characteristic of being versatile, easily cultivable, of medium size, about 10 $\mu$ m diameter.

Tests were conducted over a period of 15 minutes because it is considered the maximum time in which cells can survive inside the cartridge and the printhead, under conditions of non-sterility, without causing damage or dying.

In this study, it is important to note the number of cells that the camera can display at the beginning and at the end of the past 15 minutes, and the slope of the curve in the graph that indicates the rate of cell decay at the bottom of the tube.

The chamber was positioned, in all experiments, to focus cells inside and in a central position of the tube in question. This position was chosen not to have the edge effects, cells near edges of the tube could aggregate with each other and on the wall, and to display exactly in the middle. In fact, initially cells are dispersed in the medium to analyse but, over time, they are moving towards the bottom, because of gravity force. For this reason, in order to calculate the sedimentation speed, the tube must not be focused on either the upper or lower part because in the first case, after few seconds, cells would no longer be visible; while in the second one the camera would see an agglomeration of cells and it would no longer be possible to count the number.

As cells sediment at the bottom of the tube, a higher initial number indicates a lower sedimentation velocity. In fact, from the **Figure 96**, it is possible to note the difference in the cell count between cells in DMEM and cells in hydrogel.

The hydrogel has a higher initial number, but it has a very steep course. If the operator wants to print this type of cells in the hydrogel, he must keep in mind that a good maximum time to carry out the printing process is about 5 minutes, in fact after this time interval, cells tend to sediment quickly. The hydrogel is denser and more viscous than DMEM and this helps to initially stabilize the cell suspension in it.

Cells in DMEM behave differently: the initial count turns out to be lower, but the trend in the time interval of 15 minutes turns out to be rather stable. This could mean an initial occlusion of the nozzle, but resolvable with a slight purge. The fact that the number of initial cells is so low means that many more cells, compared to those present in the hydrogel, have already precipitated at the bottom of the tube and in terms of printing this is related to the occlusion of nozzles.

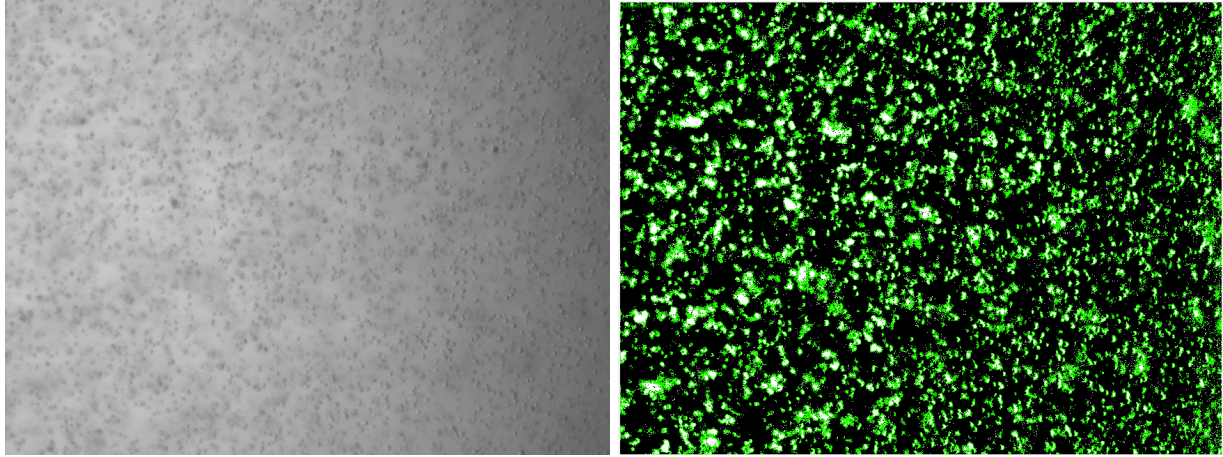


*Figure 95: Elaboration Image of Rat2 in DMEM 10%FBS [36]*

**Figure 95** shows cells processed by the sedimentation algorithm before and after the application of the thresholding, concerns cells in DMEM.

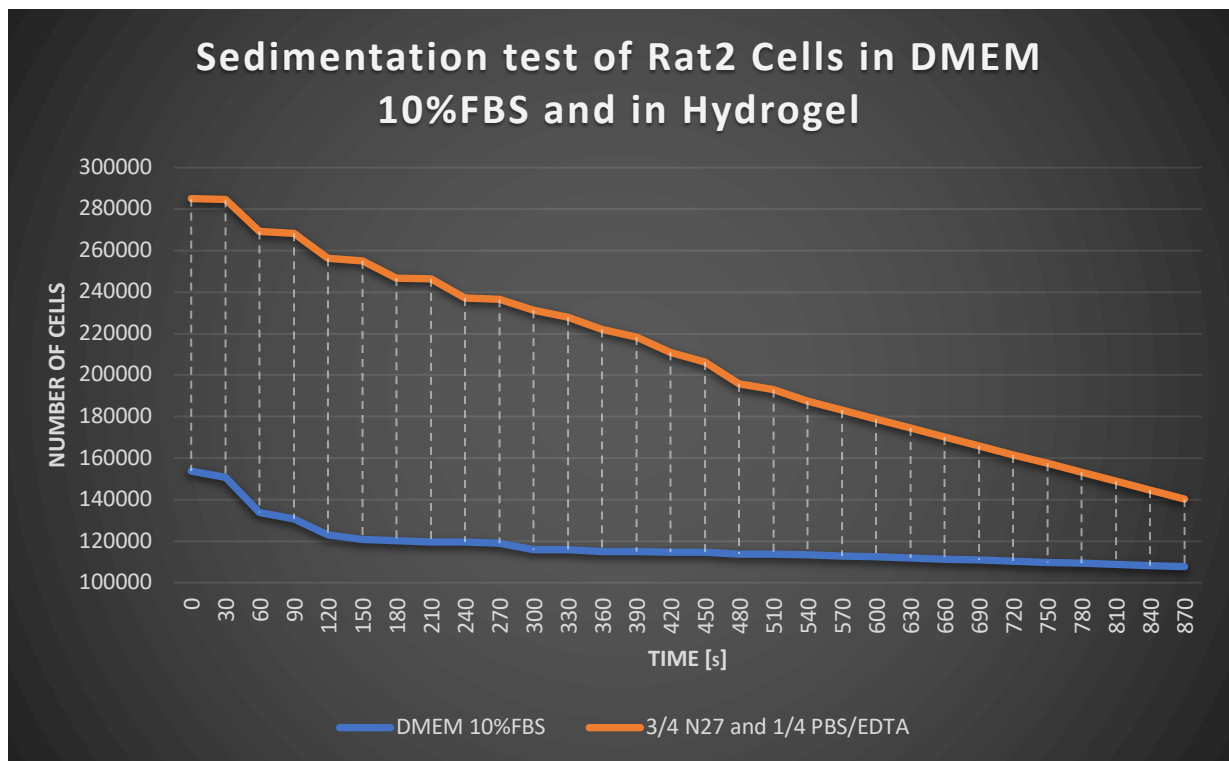


*Figure 96: Sedimentation tests of Rat2 Cells in DMEM 10%FBS and in Hydrogel [36]*

To calculate the sedimentation velocity of cells exploiting their number obtained by the automatic algorithm for the counting, it was decided to make the calculation making the



difference of the cells between the first and last counting and dividing by the total number of seconds passed. In this way, the unit of measurement obtained is Cells/second.

$$\text{sedimentation velocity} = \frac{\text{Initial Number of Cells} - \text{Final Number of Cells}}{\text{Total Time}}$$

It was not possible to double-check this value using the theoretical formula for the calculation of sedimentation velocity because the density of cells is not known (fundamental in the calculation by this method).

DMEM [cells/s]	3/4 N27 and 1/4 PBS/EDTA [cells/s]
52,81	166,34

#### 5.4.10 Sedimentation Test for Fibroblast 3T3

Regarding the sedimentation velocity study for Fibroblast 3T3 cells, it was decided to use and compare cell behavior both in their DMEM 10% CS and in hydrogels with which their viability was tested.

Hydrogels selected are N27, 3/4 N27 and 1/4 PBS/EDTA because the PBS/EDTA is useful to prevent cells adhesion to the walls of the tube, 1% Alginate and 2% Alginate.

The medium that initially has the highest cell count is N27, followed by 2% Alginate, DMEM, N27 and PBS / EDTA and for last the 1% Alginate, shown in **Figure 98**.

The number differences regarding this type of cells are not very large. The fibroblasts 3T3, being larger than the Rat2, about 15µm diameter, placed with the same concentration in the medium, are more subject to the thrust given by the speed force. Indeed, they sediment with a more or less uniform velocity, almost less than Rat2.

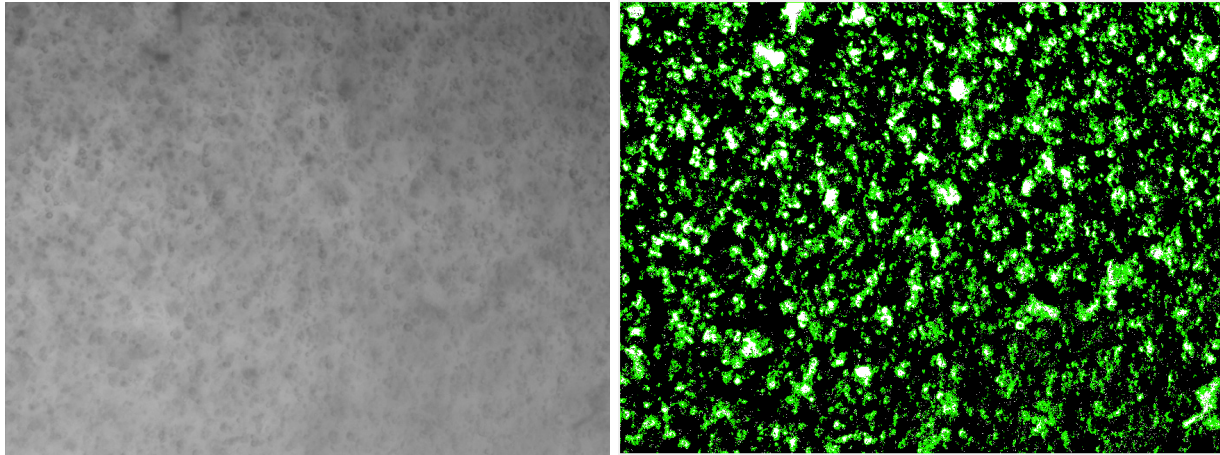


*Figure 97: Elaboration Image of Fibroblast 3T3 in 3/4 N27 and 1/4 PBS/EDTA [36]*

**Figure 97** shows cells processed by the sedimentation algorithm before and after the application of the thresholding, concerns cells in 3/4 N27 and 1/4 PBS/EDTA.

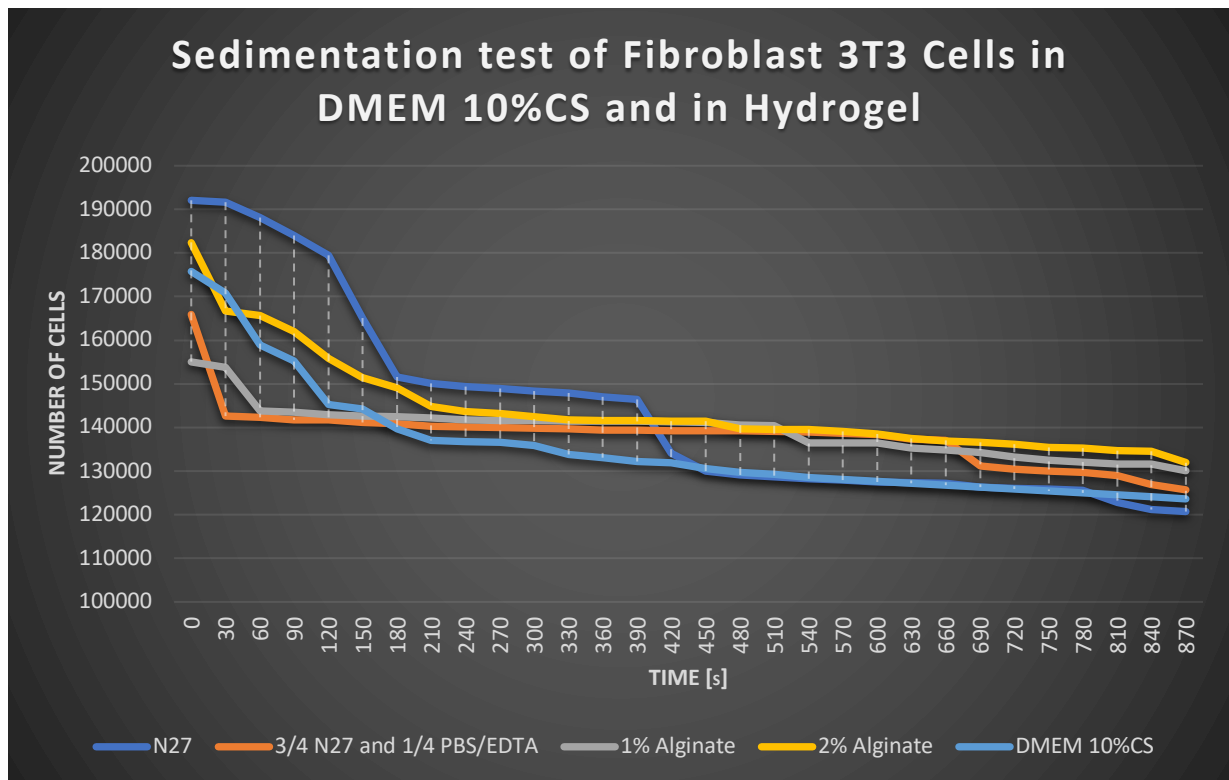


*Figure 98: Sedimentation tests of Fibroblast 3T3 Cells in DMEM 10%CS and in Hydrogels [36]*

The choice of the type of hydrogel was therefore made based on results obtained from the study of viability of the cells inside the polymer since the sedimentation study no longer prevails a material on the others in terms of the number of initial cells and lower sedimentation velocity.

DMEM [cells/s]	N27 [cells/s]	3/4 N27 and 1/4 PBS/EDTA [cells/s]	1% Alginate [cells/s]	2% Alginate [cells/s]
59,95	82,02	46,22	28,68	57,92

#### 5.4.11 Sedimentation Test for Lung Epithelial Cells A549

Because the Lung Epithelial cells A549 will only be printed suspended in their DMEM 10% FBS, it was decided to study sedimentation velocity only in DMEM, **Figure 100**. It is very high, 95,23 cells/s, so before performing the printing process, it is advisable to make the purge. Alternatively, it is possible to fill the cartridge with a few millilitres of DMEM and cells, print and clean the printhead before the next printing process. Cell sedimentation, being so fast, could block nozzles between a process and the other printing, so it would be better to clean the whole conduit.

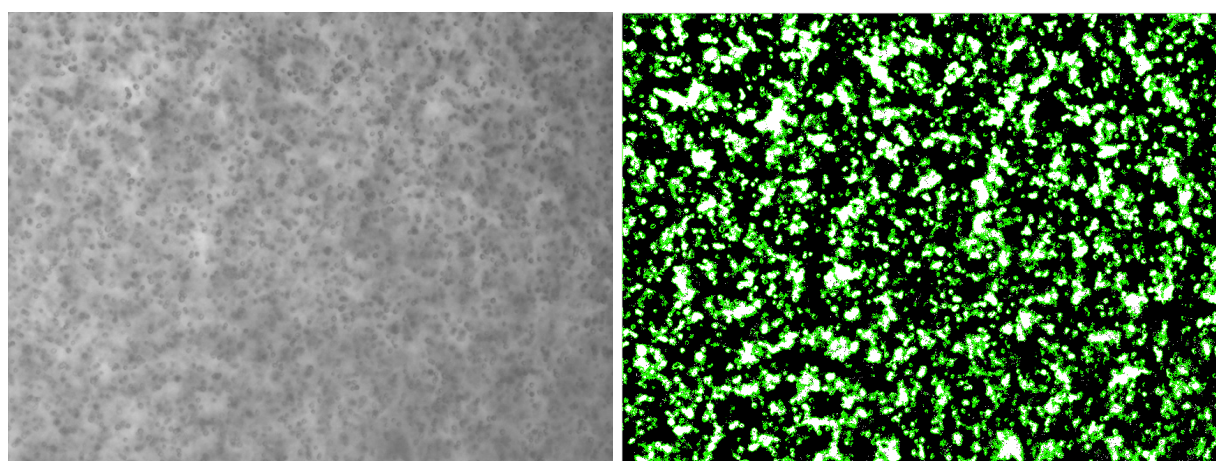


*Figure 99: Elaboration Image of Lung Epithelial Cells A549 in DMEM 10%FBS [36]*

**Figure 99** shows cells processed by the sedimentation algorithm before and after the application of the thresholding, concerns cells in DMEM.

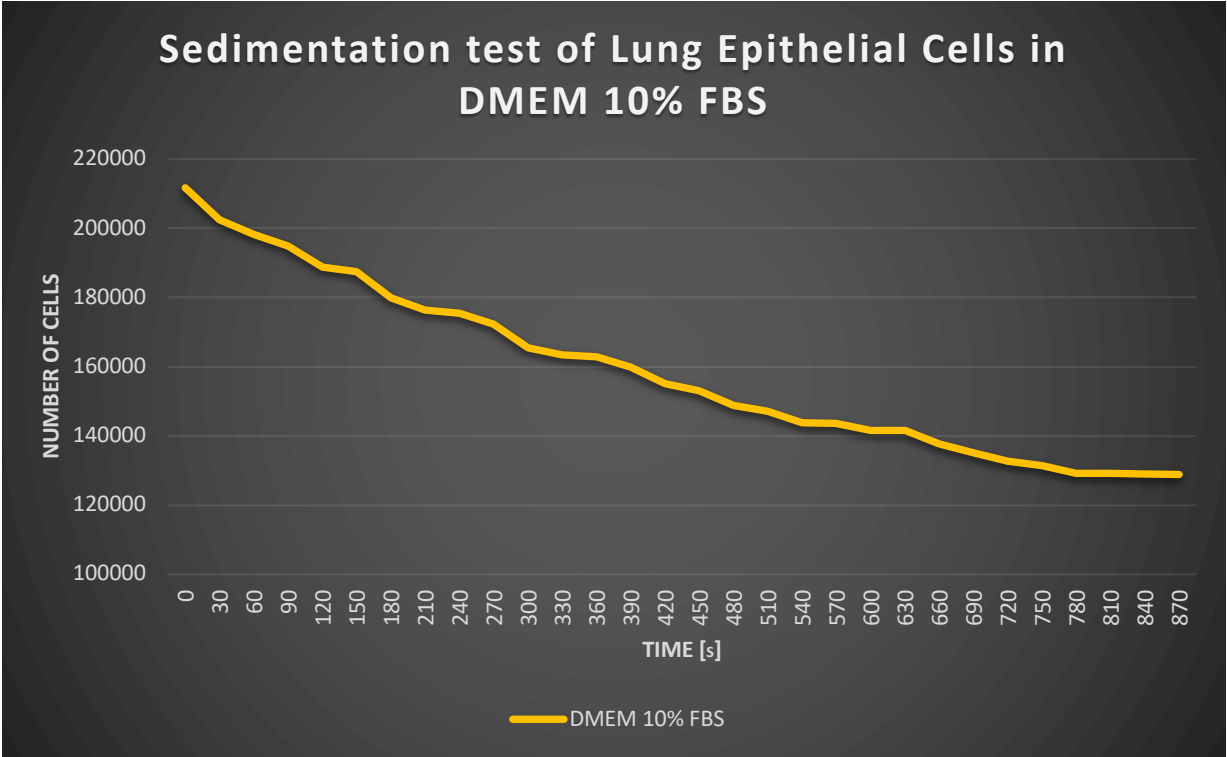


*Figure 100: Sedimentation tests of Lung Epithelial Cells A549 in DMEM 10%FBS [36]*

DMEM [cells/s]
95,23

5.5 Test and Optimization of the Best Printing Process for Cells

It has been decided to continue the Master Thesis work with the definition of printing process for only two types of cells: Fibroblast 3T3 and Lung Epithelial Cells A549. The cells called Rat2 have been excluded for printing because they have a behavior similar-fibroblast and are not a well-defined cell line, so they are not useful for research purposes.

Cells to be printed must be counted and centrifuged. The concentration of cells per millilitre was set as  $3 \cdot 10^6$  cells/ml; then, after the centrifugation process, cells are separated from the DMEM

in which they are located and the material, that will be used in the printing process, is added in the right quantity to obtain the desired cell concentration.

If there are any agglomerates of cells, the "Vortex" tool should be used to mix cells and the suspension medium. This tool mix the compound and does not damage cells.

After that, the printing process can be performed, inserting the compound to be printed in the syringe, if less than 5ml, or in the tank if greater, using the automatic pressure regulator. At this point it is possible to proceed with printing. The chosen geometry, to be set by matlab code, is rectangular, but the substrate has a circular shape; this means that in each printing process drops containing cells will be lost. After each printing process, the operator must put a wet sponge on the printhead to keep wet nozzles. In this way, all desirable prints can be made without worrying about the nozzles occlusion as long as the liquid to be printed remains.

3T3 fibroblast cells are printed in the 3/4 N27 and 1/4 PBS/EDTA hydrogel on a substrate based on Calcium and Agarose.

Lung Epithelial Cells, as in the experiment conducted by Barbara Rothen [46], are printed in DMEM 10%FBS forming a monolayer on different types of substrates, in order to test both the viability of the cells after the printing process and the contact with the substrate.

## 6 Results of Viability and Reliability

The BioPrinting process was performed in different ways for two types of cells: 3T3 and A549.

Initially their viability was tested after printing in their DMEM using the simple Petri Dish as a substrate. This viability test helps to understand how much the printhead can damage cells due to the thrust of piezoelectric nozzles and to the fact that Biowatcher is positioned in a laboratory where it is not working under sterile conditions, contrary to what it should have been done when working with cells.

Subsequently, other innovative methods of BioPrinting were tested for both cells, going to investigate the toxicity of two types of hydrogels, the Alginate and the Agarose, the first one used both as a scaffold and as a substrate, the second only as a substrate.

The aim of BioPrinting through a multi-nozzle printhead is to fill well plates or Petri Dishes of printed cells in the shortest possible time (a printing process takes place in 10 seconds) instead commercial Bioprinters on the market based on single nozzle (more time to print a monolayer or a 3D-structure) trying to damage the slightest number of cells.

Cell viability after these processes was tested with three methods:

- Trypan Blue Dye Assay, for both type of cells [43];
- LIVE/DEAD Assay with Fluorescent Microscope, only for Fibroblast 3T3 Cells [45];
- LDH Test, only for Lung Epithelial Cells A549 [63].

### 6.1 Printing Fibroblast 3T3 and Viability Tests

Fibroblast 3T3 cells are very large, compared to A549, cell agglomerations could be created within the nozzles for this reason. Therefore, the BioPrinting has been led, according to this problem: it is necessary to pay attention to the working and non-functioning nozzles. If there are problems related to the size of these cells, a 2-seconds purge is advisable to push cells out of the nozzles between one printing and another.

### 6.1.1 Print in DMEM

To test the process, particularly if the printing kills the cells, cells were counted and DMEM 10% CS was added after centrifugation in order to have a cell concentration in DMEM of  $3 \cdot 10^6$  cells/ml. The solution obtained was inserted into the Biowatcher cartridge and the printing process written on Matlab code has been started, 8) *Printing plane in 10.2 Final Code with Pressure Regulation Matlab*.

In parallel to this operation, as regards the 5% Alginate substrate, it was placed in the Petri Dish and crosslinked with 5ml of 50 mM  $\text{CaCl}_2$  placed above the Alginate layer for 10 minutes and placed at  $4^\circ \text{C}$ , after removing the 50 mM  $\text{CaCl}_2$ , until the printing process.

As soon as the solution is ready to be printed, all the substrates are prepared and placed one at a time below in nozzle. Between one printing and another, nozzles are cleaned by the operator and their occlusion status is controlled via the camera on the Biowatcher. It is important to remember to put a wet sponge between one operation and another because the nozzles should never become dry.

**Figure 101** and in **Figure 102** show the printed solutions immediately after BioPrinting in different Petri Dishes and the Alginate 5% respectively.

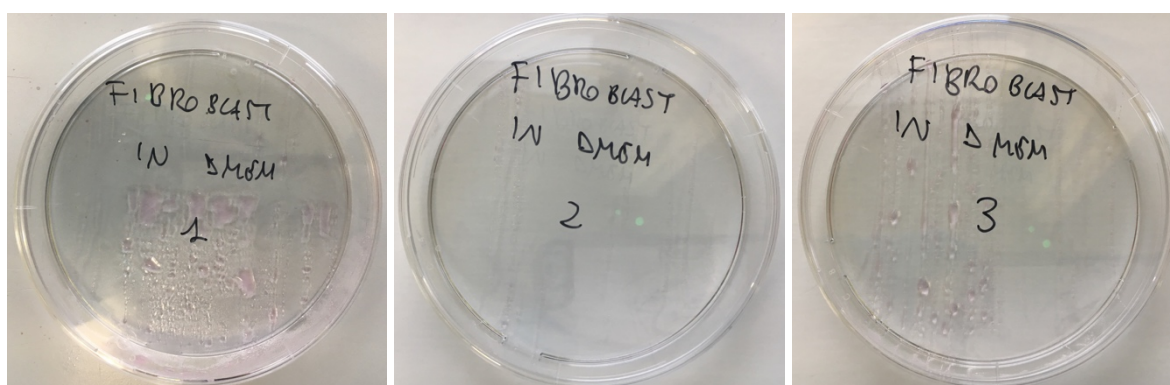


**Figure 101:** Fibroblast 3T3 after printing in DMEM 10%CS on Petri Dish [36]



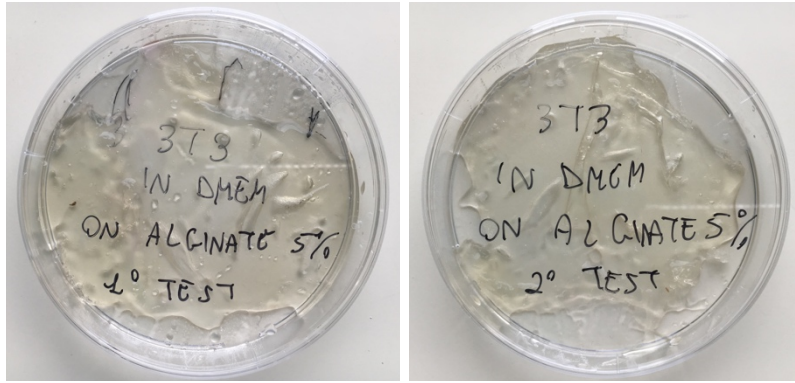


*Figure 102: Fibroblast 3T3 after printing in DMEM 10%CS on Alginate 5% [36]*

The cells were checked under a confocal microscope, shown in **Figure 103**, immediately after the printing, after 4 hours in the incubator and, only for those printed in the Petri Dish, after 24 hours in the incubator.

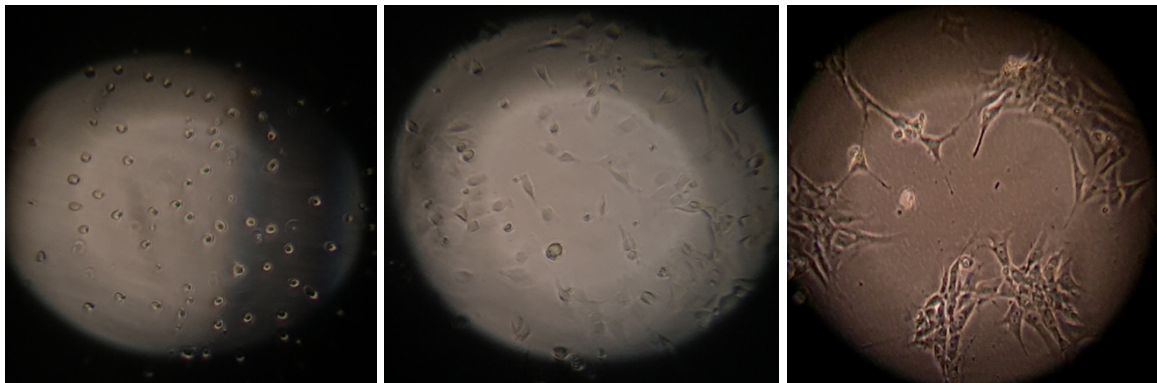


*Figure 103: Fibroblast 3T3 after printing in DMEM 10%CS, after 4 hours and after 24 hours on Petri Dish [36]*

It is possible to notice that, already after only 4 hours, cells are visibly alive because they started to adhere to the substrate. In fact, the cells that have not joined are roundish, but, without a viability test, it is not possible to be sure that they are alive/dead. Moreover, after 24 hours, cells started to replicate: this means that the printing process was not harmful for most of them.

After 4 hours, the viability test with Trypan Blue dye solution was done to printed cells on 5% Alginate. They were detached from the substrate by trypsinization and then the test was performed by counting the live cells, in white, and the dead cells, in blue.

After 24 hours, the cells printed in the Petri Dishes were checked, detached by trypsinization and the viability test was also done for them.

The results of the viability test have been reported in **Figure 104**, they have been obtained with the Trypan Blue method because it is easy and fast to use with the flat substrate of the Petri Dishes; cells can be detached and counted by trypsinization.

### Fibroblast 3T3 Printed: 3 Million of cells/ml

#### Viability Tests with Trypan Blue Method and Confocal Microscope

in DMEM 10%CS	Alive Cells (cells)	Dead Cells (cells)	Total Cells (cells)	Alive Cells Percentage %	Dead Cells Percentage %
1°Test on Petri Dish	300000	30000	330000	90,9	9,1
2°Test on Petri Dish	60000	20000	80000	75,0	25,0
3°Test on Petri Dish	240000	0	240000	100,0	0,0
4°Test on Petri Dish	70000	0	70000	100,0	0,0
5°Test on Petri Dish	80000	10000	90000	88,9	11,1
6°Test on Petri Dish	80000	0	80000	100,0	0,0
1°Test on Alginate 5%	820000	40000	860000	95,3	4,7
2°Test on Alginate 5%	940000	10000	950000	98,9	1,1

*Figure 104: Fibroblast 3T3 Cells Printed in DMEM 10%CS on Petri Dish and on Alginate 5% [36]*

From these results, it is clear that both substrates used are good, do not seem to be toxic for cells, in some cases even 100% of cell viability is reached.

The mean value of Fibroblast 3T3 alive after printing on Petri Dishes is 92,5% with a standard deviation of 9,9%. The mean value of Fibroblast 3T3 alive after printing on Alginate 5% is 93,2% with a standard deviation of 2,5%.

The 5% Alginate is an innovative substrate and its results are good, considering that a small percentage of cells could have died in the printing process and that the sterility conditions were not fully respected in Biowatcher.

A relatively low viability, 75%, is reported in one of the tests, it could be due to environmental conditions, i.e. lack of sterility and printing process in an environment where humidity cannot be controlled (DMEM could evaporate if the operator does not close the Petri Dish immediately after the printing process), but most of the experiments conducted show high cell viability.

### 6.1.2 Print in Hydrogel

To test bioink formulated at the iPrint Institute, the Alginate-based hydrogel has to be cross-linked on substrates contained Calcium Chloride.

Cells were counted and 3/4 N27 and 1/4 PBS/EDTA coloured hydrogel was added after centrifugation in order to have a cell concentration in DMEM of  $3 \cdot 10^6$  cells/ml. The solution obtained was inserted into the Biowatcher cartridge and the printing process written on Matlab code has been started as usual, with the same parameter for each printing process.

Cells were printed on different substrates containing Agarose and Calcium Chloride and printed:

- Agarose,  $\text{CaCl}_2$  and NaCl has been test but unsuccessfully for the presence of NaCl because, if it is not balanced with the exactly number of cells on it, it could be toxic and cells died;
- Agarose,  $\text{CaCl}_2$  and UV light to sterilize;
- Agarose and  $\text{CaCl}_2$ .

The hydrogel has been coloured with a food colorant to obtain greater visibility in the next phase concerning the viability test: for the operator, in this way it is easier to visibly identify a monolayer of cells (height of about 50  $\mu\text{m}$ ) compared to a pure hydrogel without any added colouring. It has already been tested in the paragraph

*5.2.2 Viability Tests with Trypan Blue* that the food colouring does not affect cell viability.

Immediately after printing, it was necessary to instantly cover the Petri Dish to prevent the hydrogel, which acts as a scaffold, to evaporate as it is water-based, in the absence of a humidity control in the room. The hydrogel thus formulated crosslinks in 10 minutes, so it is necessary to

wait 10 minutes before adding DMEM 10% CS, a fundamental element to keep the cells alive, and then insert all the samples into the incubator for 4 hours.

At this point it is possible to take samples, remove the DMEM 10% CS and finally carry out the viability test.

For Fibroblast 3T3 cells, the viability test was performed using two different methods:

- Trypan Blue Dye Assay and Confocal Microscope;
- LIVE/DEAD Assay and Fluorescent Microscope.

#### *6.1.2.1 Viability Tests with Trypan Blue and Confocal Microscope*

To be able to take the hydrogel, it was necessary to use a thin spatula, already prepared, of sterilized stainless steel with 70% ethanol and UV rays for 12 hours. The hydrogel taken was placed in a 15ml tube and the Sodium Citrate 0,055M solution was added in double the amount of the hydrogel taken from the Petri Dish (measurable by the numbered pipette) and it was centrifuged at 1200 RPM x 7 minutes. After this step, the fluid was removed, and the DMEM 10% CS was added in the same amount previously measured by hydrogel.

At this point, it was possible to carry out the Viability Test with Trypan Blue and Confocal Microscope.

**Figure 105** and **Figure 106** show pictures of solution with cells after printing, on different Petri Dishes with the same substrate (Agarose with Calcium Chloride), and cells at the Confocal Microscope after printing, after 4 hours in the incubation and in Trypan blue solution for the viability test counting.

Cells, after 4 hours in the incubation seems more spread and attached to the 3D hydrogel matrix, but only with the viability test it is possible to check if they are alive or dead.

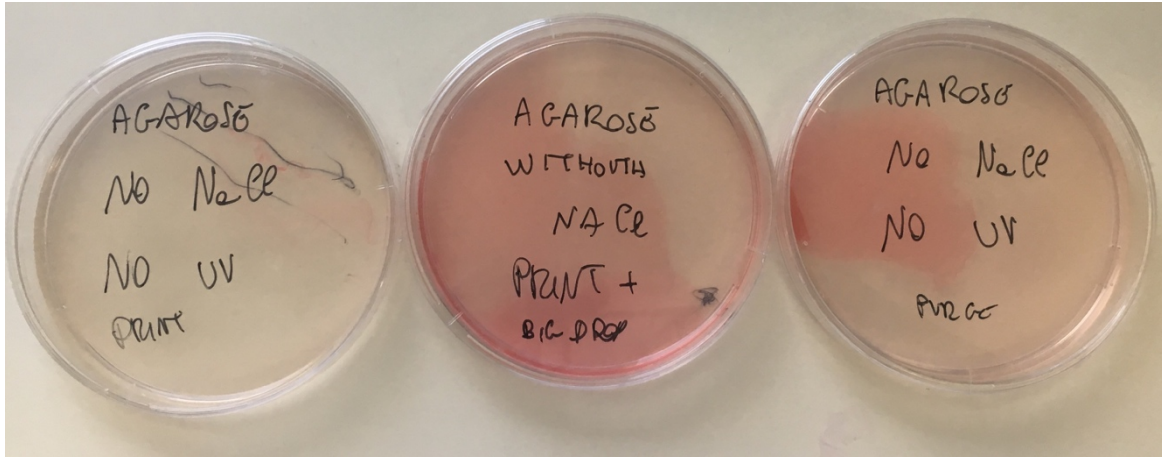


*Figure 105: Fibroblast 3T3 after printing in Hydrogel on Agarose [36]*

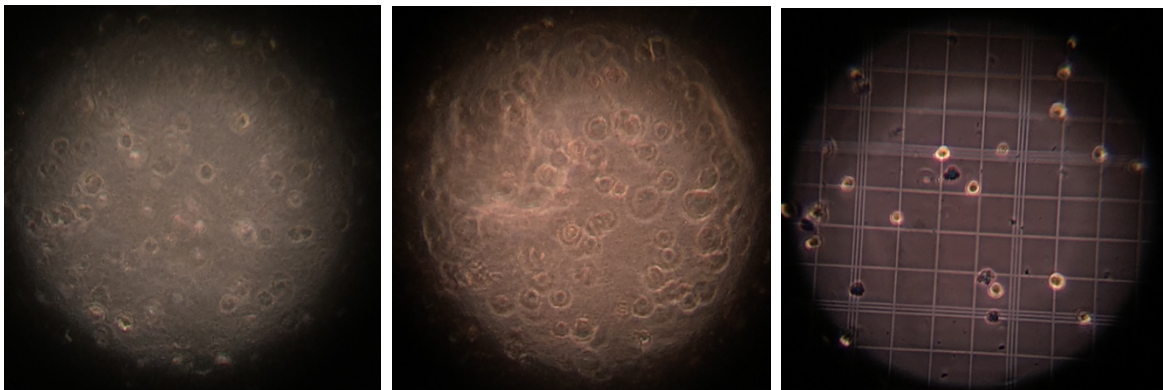


*Figure 106: Fibroblast 3T3 after printing in Hydrogel, after 4 hours and in Trypan Blue [36]*

Results, shown in **Figure 107**, obtained by the viability tests are lower, in terms of percentage of live cells, than those of the cells printed in DMEM 10% CS because the hydrogel matrix, creating crosslink with the calico, is not completely permeable to the passage of DMEM. The latter is indeed essential for cell viability as it contains the nutrients necessary to keep the cells alive and make them grow.

Lower values, below 50%, were obtained as a result of a failure of the room's climate system.

In fact, if the environment is too hot and dry, the printing process is hardly good because the hydrogel evaporates faster than expected and cells remain, in this way, exposed to the external environment.

To confirm or deny the results obtained, it was decided to carry out a second viability test using another method, i.e. via fluorescence.

### Fibroblast 3T3 Printed: 3 Million of cells/ml

#### Viability Tests with Trypan Blue Method and Confocal Microscope

in 3/4 N27 + 1/4 PBS/EDTA	Alive Cells (cells)	Dead Cells (cells)	Total Cells (cells)	Alive Cells Percentage %	Dead Cells Percentage %
1°Test on Agarose and CaCl <sub>2</sub>	1460000	230000	1690000	86,4	13,6
2°Test on Agarose and CaCl <sub>2</sub>	825000	105000	930000	88,7	11,3
3°Test on Agarose and CaCl <sub>2</sub>	550000	390000	940000	58,5	41,5
4°Test on Agarose and CaCl <sub>2</sub>	600000	710000	1310000	45,8	54,2
5°Test on Agarose and CaCl <sub>2</sub>	1060000	1190000	2250000	47,1	52,9
6°Test on Agarose and CaCl <sub>2</sub>	150000	140000	290000	51,7	48,3
7°Test on Agarose and CaCl <sub>2</sub>	700000	600000	1300000	53,8	46,2
8°Test on Agarose and CaCl <sub>2</sub>	2140000	470000	2610000	82,0	18,0

*Figure 107: Fibroblast 3T3 Cells Printed in 3/4 N27 and 1/4 PBS/EDTA Agarose and CaCl<sub>2</sub> [36]*

The mean value of Fibroblast 3T3 alive after printing on Agarose and CaCl<sub>2</sub> is 64,3% with a standard deviation of 18,3%.



#### 6.1.2.1 Viability Tests with LIVE/DEAD ASSAY and Fluorescent Microscope

To be able to compare the cell viability results obtained from the Trypan Blue analysis, a subsequent experiment was performed. Cells were printed in the same hydrogel and in the same density used in paragraph 6.1.2.1 *Viability Tests with Trypan Blue and Confocal Microscope* and viability tests were done via the LIVE/DEAD Assay and the Fluorescent Microscope, explained in 3.3 *Trypan Blue and Live/Dead Assay*.

The accuracy of this test should be better because the passage of hydrogel dissolution and centrifugation should not be done. This means that the percentage of dead cells is due exclusively to the materials used as scaffolds and as substrates and to the printing process.

The **Figure 108** shows Fibroblast 3T3 Cells after printing in 3/4 N27 and 1/4 PBS/EDTA on Agarose and CaCl<sub>2</sub> after 4 hours. Images, taken under the microscope, are not very clear because the food colour, added to make the hydrogel visible to the human eye, obscures vision by confocal microscope, but this is not important for cell count to establish the percentage of viability.

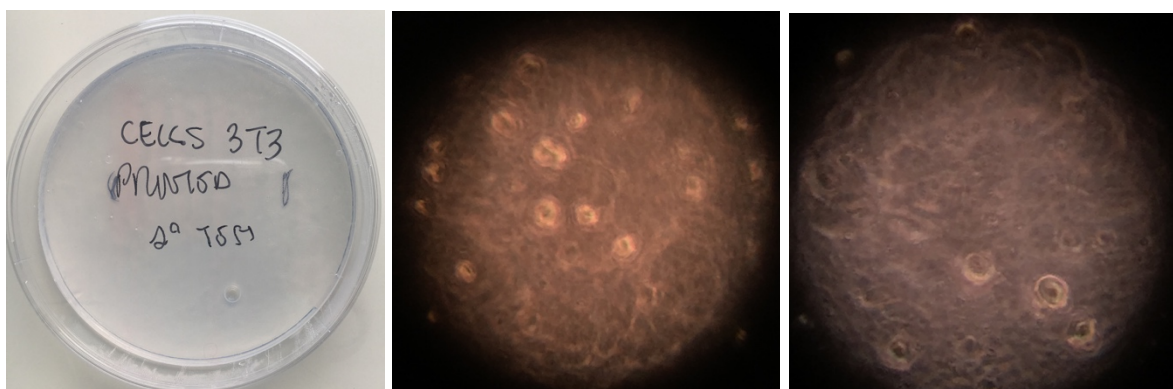


**Figure 108:** Fibroblast 3T3 Cells Printed in 3/4 N27 and 1/4 PBS/EDTA Agarose and CaCl<sub>2</sub>: after printing and after 4 hours (picture on the right) [36]

**Figure 109** shows two examples of live and dead cells. Pictures are taken using NIS-Elements BR software from the Fluorescent Microscope and samples were analysed with one focus mode, x4. To visualize live cells, the lens with the green filter was used for first and then for the dead cells the red one.



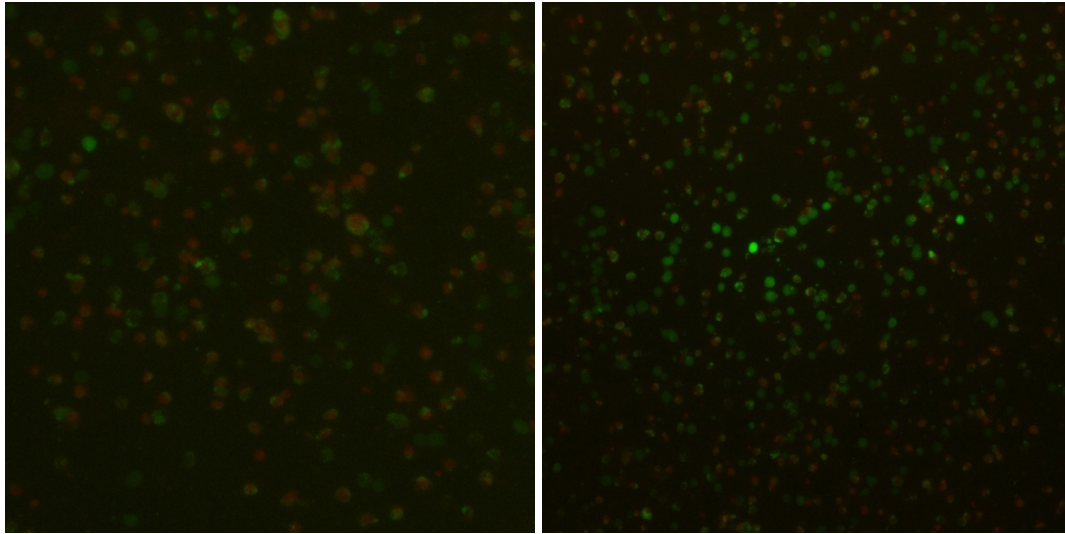


*Figure 109: Fibroblast 3T3 Cells Printed in 3/4 N27 and 1/4 PBS/EDTA Agarose and  $\text{CaCl}_2$  under Fluorescent Microscope [60]*

Results obtained with this viability test are reported in **Figure 110**.

It is possible to notice that both tests refer to the same percentage range of live and dead cells. In fact, the percentage of dead cells is high in both cases.

This phenomenon of cell death could be due to two factors:

- DMEM failed to properly penetrate the cell and hydrogel scaffold and therefore the nutrients necessary to keep cells alive were not provided to all cells. However, this is not very feasible because it would have expected to see the internal part with more dead cells and the external one, more in contact with DMEM, with more alive cells; instead the dead cells are physically positioned among the living ones, in the same plane.
- the gel based on Agarose and Calcium Chloride is semi-toxic to cells, due to the osmotic pressure. In fact, results obtained through pipet, were better because not all cells were in contact with the Agarose because the deposited layer had a thickness of about 2mm. On the other hand, in the printing procedure it was decided to print a homogeneous monolayer (thickness about 50  $\mu\text{m}$ ), so all the cells inside the hydrogel are very close to the Agarose gel and have a better chance of exchanging ions between the Alginate and the Agarose.

Agarose is not a toxic natural polymer for cells, but it could be no cell-friendly if it were to occur inside the Alginate-based hydrogel matrix. The Agarose hydrogel is necessary in these

experiments to create a solid substrate that could contains Calcium Chloride inside, the necessary chemical component to crosslink Alginate-based hydrogels.

Therefore, its use is not recommended if the operator deciders to print a monolayer of cells, but for a 3D structure, made up of several superimposed layers, it could be a good solution.

### Fibroblast 3T3 Printed: 3 Million of cells/ml

Live/Dead Assay with Fluorescent Microscope					
in 3/4 N27 + 1/4 PBS/EDTA	Alive Cells (cells)	Dead Cells (cells)	Total Cells (cells)	Alive Cells Percentage %	Dead Cells Percentage %
1°Test on Agarose and CaCl <sub>2</sub>	367	164	531	69,1	30,9
2°Test on Agarose and CaCl <sub>2</sub>	25	16	41	61,0	39,0
3°Test on Agarose and CaCl <sub>2</sub>	14	8	22	63,6	36,4
4°Test on Agarose and CaCl <sub>2</sub>	1420	978	2398	59,2	40,8
5°Test on Agarose and CaCl <sub>2</sub>	468	134	602	77,7	22,3
6°Test on Agarose and CaCl <sub>2</sub>	5681	3203	8884	63,9	36,1
7°Test on Agarose and CaCl <sub>2</sub>	3746	2826	6572	57,0	43,0

*Figure 110: Viability test with Fluorescent Microscope of Fibroblast 3T3 Cells Printed in 3/4 N27 and 1/4 PBS/EDTA Agarose and CaCl<sub>2</sub> [36]*

The mean value of Fibroblast 3T3 alive after printing on Agarose and CaCl<sub>2</sub> is 64,5% with a standard deviation of 7,0%.

## 6.2 Printing Lung Epithelial Cells A549 in DMEM and Viability Tests

Regarding the bioprinting of A549 cells, the solution used was the following for each process: cells were counted and DMEM 10% FBS was added after centrifugation in order to have a cell concentration in DMEM of  $3 \cdot 10^6$  cells/ml. The solution obtained was inserted into the Biowatcher cartridge and the printing process written on Matlab code has been started, 8) *Printing plane in 10.2 Final Code with Pressure Regulation Matlab*. When the solution is ready to be printed, all the substrates are prepared and placed in the right place to start the process. Between one printing and another, nozzles are cleaned by the operator and their occlusion status is controlled via the camera on the Biowatcher. It is important to remember to put a wet sponge between one operation and another because the nozzles should never become dry. It was decided to test the Petri Dish as substrates for this type of cells to verify the actual number of cells that could die in the printing process, the Agarose and the Alginate 5% to investigate whether these two materials are cell-friendly and if the cells adhere well to them.

### 6.2.1 Print in DMEM on Petri Dish

Lung Epithelial Cells A549 were printed in the Petri Dish 11 times. The **Figure 111** shows an example of cells printed in DMEM 10%FBS on the Petri Dish, an enlargement by confocal microscope (x10) of a strip of printed liquid captured after 4 hours from printing and finally an image of the cell count via Trypan Blue to verify the number of alive and dead cells.

The viability test with Trypan Blue was performed through the trypsinization procedure to detach the adherent cells to the substrate, keeping the DMEM in which they were about to make a double check. In fact, if there are dead cells, they would not stick to the substrate but they would fluctuate in DMEM, so it is important to analyse it otherwise all results would always give 100% alive cells.

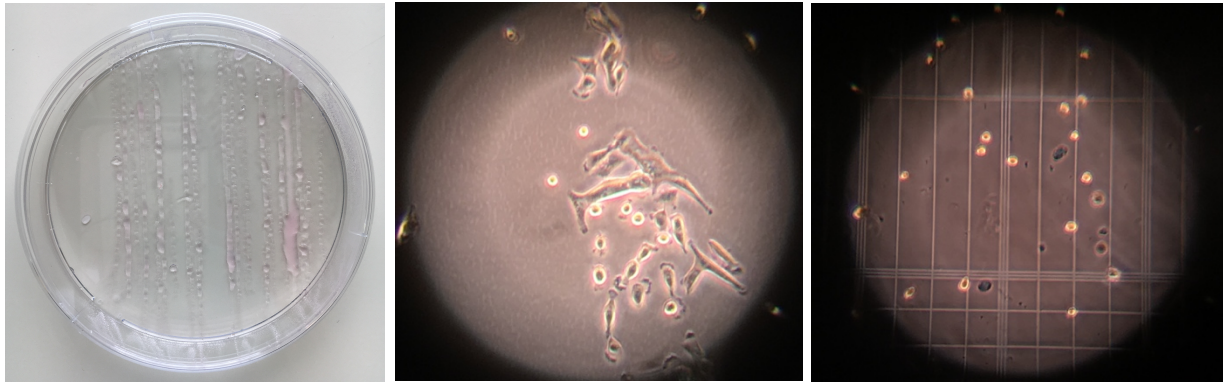


**Figure 111:** Lung Epithelial Cells A549 after printing in DMEM 10%FBS, after 4 hours and in Trypan Blue on Petri Dish [36]

Results of the viability test, shown in the **Figure 112**, show a very high percentage of live cells, 100%, on 9 samples of 11. The A549 cells, being smaller than 3T3, do not have any problem of agglomeration and occlusion of nozzles, therefore the thrust given by the piezoelectric crystal (actuator) did not significantly influence their viability.

They successfully survive the printing procedure, adhere to the Petri Dish substrate and begin to proliferate already after 24 hours. The two samples that show some dead cells are not very significant because in any case the percentage of living cells is much higher.

## Lung Epithelial Cells A549 Printed: 3 Million of cells/ml

### Viability Tests with Trypan Blue Method and Confocal Microscope

in DMEM 10%FBS	Alive Cells (cells)	Dead Cells (cells)	Total Cells (cells)	Alive Cells Percentage %	Dead Cells Percentage %
1°Test on Petri Dish	240000	0	240000	100,0	0,0
2°Test on Petri Dish	120000	0	120000	100,0	0,0
3°Test on Petri Dish	40000	0	40000	100,0	0,0
4°Test on Petri Dish	180000	0	180000	100,0	0,0
5°Test on Petri Dish	120000	0	120000	100,0	0,0
6°Test on Petri Dish	1260000	0	1260000	100,0	0,0
7°Test on Petri Dish	180000	0	180000	100,0	0,0
8°Test on Petri Dish	330000	0	330000	100,0	0,0
9°Test on Petri Dish	300000	0	300000	100,0	0,0
10°Test on Petri Dish	440000	30000	470000	93,6	6,4
11°Test on Petri Dish	390000	17000	407000	95,8	4,2

*Figure 112: Lung Epithelial Cells A549 Printed in DMEM 10%FBS on Petri Dish [36]*

The mean value of Lung Epithelial Cells A549 alive after printing in DMEM 10%FBS on Petri Dish is 99,0% with a standard deviation of 2,2%.

### 6.2.1 Print in DMEM on Different Substrates

Lung Epithelial Cells A549 were printed on two different types of substrates, both prepared as explained in paragraph 6.1 *Printing Fibroblast 3T3 and Viability Test*: Agarose without Calcium Chloride and Alginate 5%. Cell viability, on these substrates, was tested by two different tests: Trypan Blue and LDH after 24 and 48 hours.



### 6.2.1.1 Viability Tests with Trypan Blue and Confocal Microscope

**Figure 113** and **Figure 114** show respectively an example of cells just printed on the two different substrates (since the monolayer is very low, it is not possible to recognize the position of DMEM and cells drops without the microscope) and after 24 hours on the Alginate 5%.

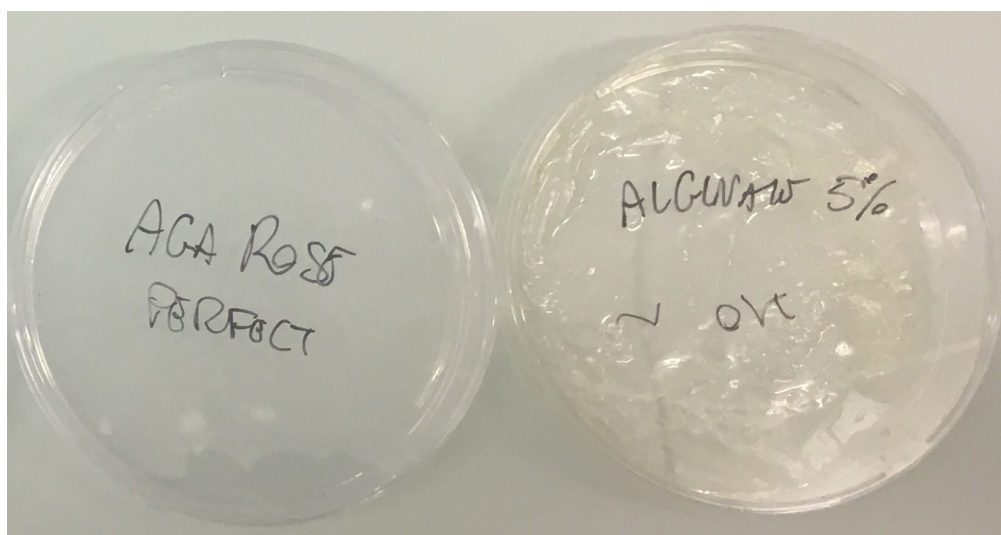


**Figure 113:** Lung Epithelial Cells A549 after printing in DMEM 10%FBS on Agarose and Alginate 5% [36]



**Figure 114:** Lung Epithelial Cells A549 after printing in DMEM 10%FBS on Alginate 5% after 24 hours [36]

**Figure 115** shows Cells under Confocal Microscope after printing on Agarose and on Alginate 5%, and finally an example of Trypan Blue test done after 24 hours from the printing process.

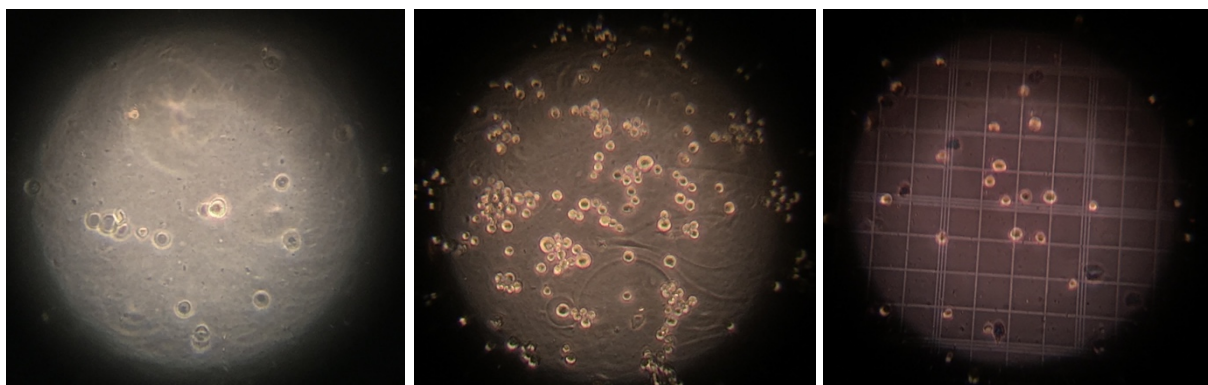


**Figure 115:** Lung Epithelial Cells A549 after printing in DMEM 10%FBS on Agarose, Alginate 5% and Trypan Blue of Lung on Alginate 5% [36]

The visible dots in the image of cells printed on Agarose, **Figure 115**, signify a negative reaction from the cells. In fact, in some previous experiments, these dots were present only after a cell death and represented fragments of dead cells. It is evident, however, from the image that some cells are intact, perhaps whole. For this reason, or to assess the level of cell death, to see how many cells actually, among those that can not be counted, are dead, it was decided to perform the LDH Test in which the amount of the LDH enzyme released is evaluated. from dead cells in DMEM, and it is possible to trace the percentage of dead cells in a given sample.

### Lung Epithelial Cells A549 Printed: 3 Million of cells/ml

#### Viability Tests with Trypan Blue Method and Confocal Microscope

in DMEM 10%FBS	Alive Cells (cells)	Dead Cells (cells)	Total Cells (cells)	Alive Cells Percentage %	Dead Cells Percentage %
1°Test on Agarose	180000	0	180000	100,0	0,0
1°Test on Alginate 5%	270000	0	270000	100,0	0,0
2°Test on Alginate 5% and algorithm performed	2320000	80000	2400000	96,7	3,3
3°Test on Alginate 5% and algorithm performed	1760000	80000	1840000	95,7	4,3
4°Test on Alginate 5% and algorithm performed	480000	0	480000	100,0	0,0

**Figure 116:** Lung Epithelial Cells A549 Printed in DMEM 10%FBS on Agarose and Alginate 5% [36]



Regarding the results of the viability test carried out with Trypan Blue, have been reported in **Figure 116** only those related to the test carried out after 24 hours from the printing process. In fact, both hydrogels used as substrates, after 48 hours, started the degradation process due to the constant temperature of 37 ° C and to the acid environment created due to the cellular metabolic activity.

The viability test with Trypan Blue was done by trypsinization, therefore the DMEM that was removed (remove the DMEM is a fundamental step for this procedure), was analysed through the LDH test. The mean value of Lung Epithelial Cells A549 alive after printing in DMEM 10%FBS on Alginate 5% is 98,1% with a standard deviation of 2,3%.

#### 6.2.1.2 LDH Tests

The LDH assay or cytotoxicity-fluorescence test is a cytotoxicity test that exploits a reaction that normally occurs within cells. The enzyme LACTATE DEHYDROGENASE (LDH) is an enzyme normally present in the cytoplasm of cells that catalyse the transformation reaction of lactate into pyruvate [63]. The reaction just described is represented in **Figure 117**.

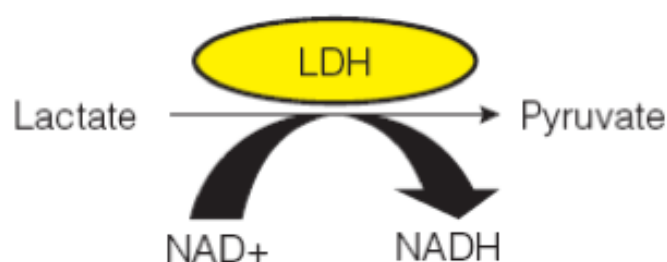


**Figure 117:** Reaction of transformation of Lactate into Pyruvate [63]

Following damage to the cell membrane, the LDH enzyme from the cytoplasm pours into the culture medium. The cytotoxicity test combines the reaction of the LDH enzyme with an opposite reaction where the substrate is a pro-fluorescent compound (the RESAZURIN) that is transformed by the enzyme DIAPHORASE into a fluorescent compound (the RESORUFIN) which emits at a wavelength of 490 nm. The reaction just described is represented in **Figure 118**.

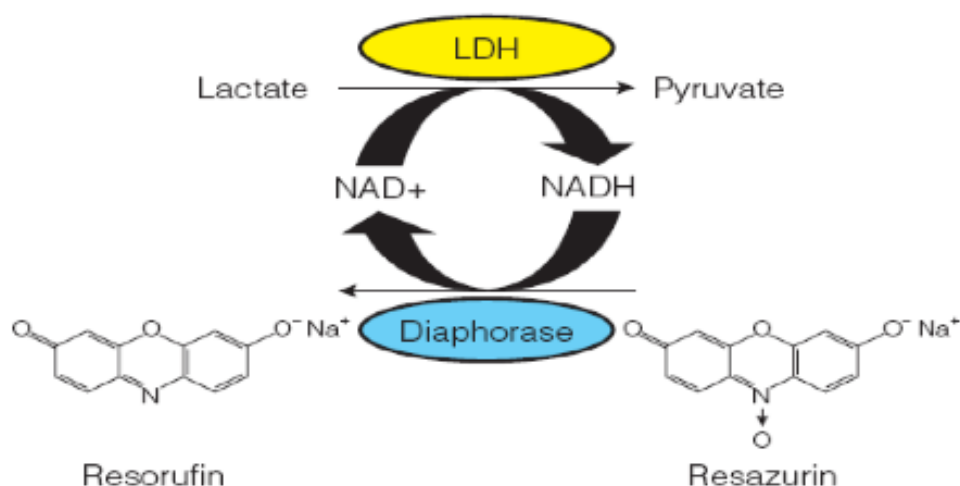


*Figure 118: Reaction of transformation of Resazurine into Resorufin [63]*

The opposite reaction mentioned above occurs only if the analysed cells are damaged because only in this case the LDH is poured into the substrate.

When cells are damaged or destroyed (death), the LDH enzyme is released into the liquid fraction of blood (serum or plasma), in addition to increasing its concentration in other biological fluids in the presence of certain diseases. The LDH represents, therefore, a general indicator of tissue and cellular damage.

The cell viability was assessed by Trypan Blue exclusion assay after 24 and 48 hours,

*6.2.1.1 Viability Tests with Trypan Blue and Confocal Microscope*, and by measuring the activity of lactate dehydrogenase (LDH) placed in the cell culture medium of the samples after 1 and 2 days obtained by printing on the conventional substrate, Petri Dish, and on substrates based on hydrogels on which it was decided to investigate.

For the quantification of cell death and cell lysis in printed samples on different substrates, a colorimetric assay was employed. It is based on the measurement of lactate dehydrogenase (LDH) activity released from the cytosol of damaged cells into their DMEM. For that assay, cell culture mediums were collected after 24 hours from printing and after 48 hours and stored at 4°C until analysis for each type of sample. The LDH cytotoxicity detection kit (Roche Applied Science, Mannheim, Germany) was used according to the supplier's manual. LDH was quantified photometrically by measuring at 490 nm, with 630 nm as reference wavelength. Each sample was assessed in with 630 nm as reference wavelength, in triplicate to have a better statistic in the final cytotoxicity calculation [63]. For positive controls A549, after printing in

DMEM 10%FBS on Petri Dish, were exposed to 2% Triton X-100 detergent in DMEM 10%FBS for 10 minutes at 37°C and checked with Trypan Blue Dye solution if they were dead.

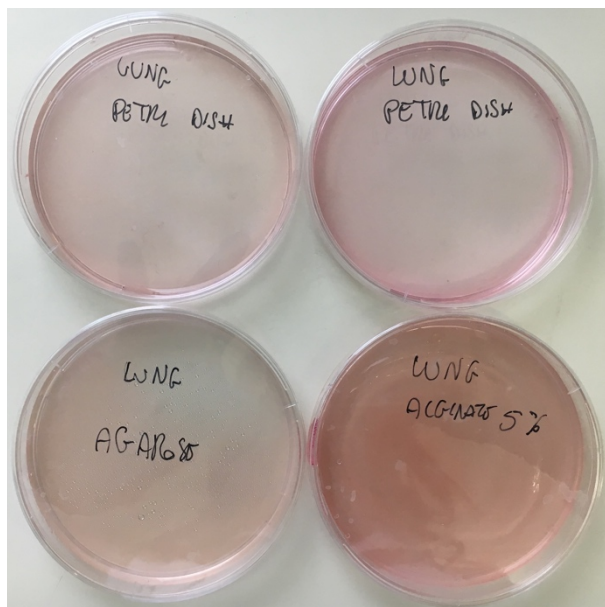


*Figure 119: Lung Epithelial Cells A549 Printed in DMEM 10%FBS on Petri Dish, Agarose and Alginate 5% [36]*

**Figure 119** shows Lung Epithelial Cells A549 printed in DMEM 10%FBS on Petri Dish, Agarose and Alginate 5%.

Cells were printed in 16 different Petri Dishes on three different substrates. After printing, a time of 30 minutes has been waited, letting samples in the incubator, to be able to add another 5ml of DMEM 10% FBS without changing cells positions on substrates. After 24 hours, the DMEMs related to the cells printed in 2 Petri Dishes without additional substrates, 2 Petri Dishes with Agarose and Petri Dishes with 5% Alginate were collected in different tubes for LDH tests. In these samples, the LDH enzyme is present in relation to the number of dead cells.

In order to evaluate the percentage of LDH released from the dead cells compared to the amount of enzyme that the same number of cells could have released, two samples of cells printed in Petri Dishes without additional substrate were subjected to 2% diluted Triton-X in DMEM. This component, in fact, kills cells damaging the cell membrane, all the cells contained in the sample release the enzyme LDH present in them.

In parallel to this procedure, the substrates were subjected to trypsinization and, through Trypan Blue, the live and dead cells were counted after 24 hours from the printing process.

The same procedure, carried out after 24 hours from the printing process, was repeated on the remaining 8 samples after 48 hours. Results obtained from Trypan Blue were shown in **Figure 120**.

### Lung Epithelial Cells A549 Printed: 3 Million of cells/ml

Viability Tests with Trypan Blue Method and Confocal Microscope					
in DMEM 10%FBS	Alive Cells (cells)	Dead Cells (cells)	Total Cells (cells)	Alive Cells Percentage %	Dead Cells Percentage %
1°Test on Agarose after 24h	180000	0	180000	100,0	0,0
2°Test on Agarose after 24h	130000	10000	140000	92,9	7,1
1°Test on Agarose after 48h	40000	10000	50000	80,0	20,0
2°Test on Agarose after 48h	60000	10000	70000	85,7	14,3
1°Test on Alginate 5% after 24h	270000	0	270000	100,0	0,0
2°Test on Alginate 5% after 24h	2320000	80000	2400000	96,7	3,3
1°Test on Alginate 5% after 48h	1760000	80000	1840000	95,7	4,3
2°Test on Alginate 5% after 48h	480000	0	480000	100,0	0,0
1°Test on Petri Dish after 24h	180000	0	180000	100,0	0,0
2°Test on Petri Dish after 24h	930000	40000	970000	95,9	4,1
1°Test on Petri Dish after 48h	450000	30000	480000	93,8	6,3
1°Test on Petri Dish after 48h	250000	0	250000	100,0	0,0

*Figure 120: Viability Tests of Lung Epithelial Cells A549 Printed in DMEM 10%FBS on Petri Dish, Agarose and Alginate 5% [36]*

From the percentages obtained from living cells, it is possible to notice that the viability remains stable, between 90 and 100%, in the substrates of Alginate 5% and in the Petri Dishes without the addition of materials in the space of 40 hours. As for the Agarose, the cells show a good percentage of viability within the 24 hours passed by the printing process, while they start to die in greater numbers after 40 hours, the viability is between 80 and 86%.

The mean value of Lung Epithelial Cells A549 alive after printing in DMEM 10%FBS on Petri Dish is 97,4% with a standard deviation of 3,1%. The mean value of Lung Epithelial Cells A549 alive after printing in DMEM 10%FBS on Alginate 5% is 98,1% with a standard deviation of 2,3%. The mean value of Lung Epithelial Cells A549 alive after printing in DMEM 10%FBS on Agarose is 89,6% with a standard deviation of 8,7%.

To perform LDH Tests on samples collected after 24 and 48 hours, 50  $\mu$ l were taken from each sample and inserted triplicates (putting the same sample into three different wells) to obtain better statistics.

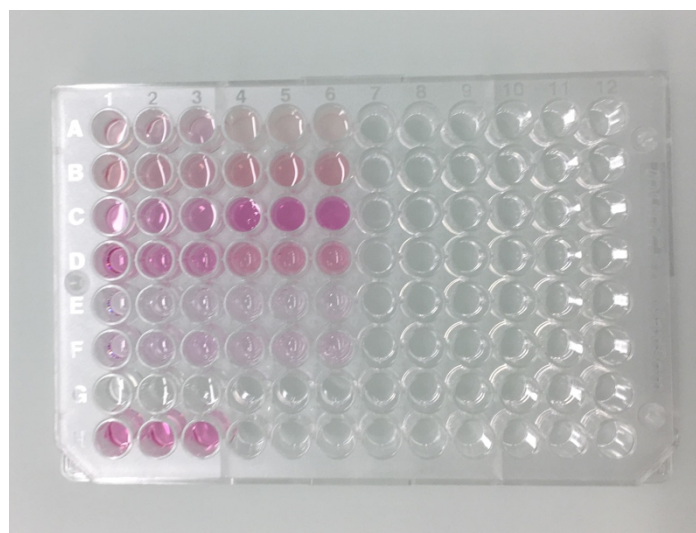


*Figure 121: Samples Preparation for LDH Tests [64]*

The **Figure 121** shows the first 96-well plate on which the colorimetric test has been done.

Samples have been selected and put in each well following the table below.

	1	2	3	4	5	6
A	Cells on Agarose after 24h			Cells on Agarose after 48h		
B	Cells on Alginate 5% after 24h			Cells on Alginate 5% after 48h		
C	Negative Control after 24h			Negative Control after 48h		
D	Positive Control after 24h			Positive Control after 48h		
E	Positive Control after 24h diluted 1:10			Positive Control after 48h diluted 1:10		
F	Positive Control after 24h diluted 1:5			Positive Control after 48h diluted 1:5		
G	Demineralized Water					
H	DMEM 10%FBS					

In each well the Catalyst and the Dye Solution (make the sample coloured) present in the Cytotoxicity Detection Kit have been added, according to the values of these two components described in it [63].

The values obtained from the colorimetric analysis, based on the difference in absorbance obtained at wavelengths 490 and 630nm, represent the slope of the line of absorbance of the LDH measured every 30 seconds for 5 minutes using an ELISA reader at AMI Institute [65]. It was necessary to process the obtained data as the values of the absorbance are not exempt from the noise. At each value obtained, the absorbance value of pure DMEM was subtracted as its colour increased the peak in the wavelength of 490nm.

All the values obtained from the same sample tripled in 3 well were averaged to have better statistics.

To calculate the cytotoxicity percentage of the samples related to the 5% Agarose and Alginate substrates, the following formula, of the Cytotoxicity Detection Kit [63], was used:

$$Cytotoxicity (\%) = \frac{exp.value - low\ control}{high\ control - low\ control} \times 100$$

in which *exp.value* is the obtained value of the sample to be used, *low control* represents the value related to DMEM with the cells printed in the Petri Dish without addition of substrate and *high control* represents the value relative to DMEM with the cells printed in the Petri Dish without addition of substrate killed by Triton-X 2% in DMEM 10% FBS.

The results of the cytotoxicity obtained are shown in the table below.

	Cytotoxicity % after 24 hours	Cytotoxicity % after 48 hours
1° Test Cells on Agarose	-1,57%	-4,76%
2° Test Cells on Agarose	6,11%	-2,02%
1° Test Cells on Alginate 5%	3,84%	-0,56%
2° Test Cells on Alginate 5%	-5,04%	9,94%

The negative percentages are correct and indicate a good result because, from the formula applied, it is shown that the cells adhered to the analysed substrate have a percentage of LDH released in the DMEM lower than those applied to the Petri Dish without adding material. This means that the cells that are found on these types of substrates prefer this type of material to adhere, stay alive and proliferate. As for the positive percentages, however, these results are good because the released LDH values are low compared to the measured total LDH. Obviously, some cells are dead, but the results are still good.

## 7 Conclusions and Future Perspectives

The results of viability test carried out through pipetting showed a percentage of live cells of  $79,4\% \pm 15,8\%$  for Fibroblast 3T3 in 3/4 N27 and 1/4 PBS/EDTA on the substrate of Agarose and Calcium Chloride in the Trypan Blue test. Instead, the results obtained from the same cells using the fluorescence microscope test show a cellular viability of  $86,6\% \pm 9,6\%$ .

The simulation of printing performed on Lung Epithelial Cells showed a 100% cellular viability: this result indicates that the gold standard substrate, the Petri Dish, is suitable for this type of cell culture and that in the printing the greatest incidence factor for cellular mortality it is the printing process, not this type of substrate.

Concerning the study of cell sedimentation within different bioinks, it can be concluded that when they are included in DMEM, it is advisable to print within 5 minutes, otherwise they would deposit on nozzles occluding them. While, when cells are suspended in the hydrogel formulated with 3/4 N27 and 1/4 PBS/EDTA, they sediment more slowly and they can be printed even for 10 minutes. In any case it is fundamental to pay attention to the possible occlusion of nozzles (through the camera used for the Dropwatching that focuses nozzles).

The results obtained by printing cells using the Biowatcher multi-nozzle inkjet are quite good for both types of cells used.

Considering that Fibroblast 3T3 are considerably larger than Lung Epithelial Cells A549, the viability of both types is very high when they are printed in their DMEM, noting a better viability of A549.

The mean value of alive cells is  $92,5\% \pm 9,9\%$  for Fibroblast 3T3 printed on Petri Dishes and  $93,2\% \pm 2,5\%$  when printed on Alginate 5%. Lung Epithelial Cells A549 present a viability of  $99,0\% \pm 2,2\%$  when printed on Petri Dishes,  $98,1\% \pm 2,3\%$  when printed on Alginate 5% and  $89,6\% \pm 8,7\%$  when printed on Agarose.

In fact, with this procedure, the results are better because in DMEM there are no particles of similar size to the cells, or that would result in an increase in the size of the cells themselves.

The printing procedure, performed by placing  $3 \cdot 10^6$  cell/ml in DMEM, can be considered good, reproducible and industrialized, with regard to a future tissue engineering approach in which many monolayers of cells printed in DMEM were to be produced.



A possible future approach of this method could be the use of more stable materials as substrates that are biocompatible and bioactive, engineered specifically for cell culture and for future transplants in the living organism, for example, Collagen type I could be a good solution.

Regarding the printing procedure used exclusively for Fibroblast 3T3 which provides as scaffold the use of a combination of hydrogels (Alginate and PEG) and as a substrate the Agarose combined with Calcium Chloride, the results of viability are lower than those obtained printing the cells inside the DMEM with an average of  $64,5\% \pm 7,0\%$ . This may be due to several factors such as the chemical interaction caused by the Alginate-Agarose coupling, the overly thick structure of the solidified scaffold does not allow a homogeneous diffusion of DMEM for cell viability and culture, the conditions of poor sterility in which it is found the printer, the fact that it is not possible to control the humidity of the room... etc. It is also possible that the Alginate and PEG gel contains particles inside which can join the cells, increasing the diameter, and the thrust given by the piezoelectric crystal would be harmful because it would forcefully push the compound out of the nozzle.

A solution to increase cell viability after the printing process could be to integrate a percentage of DMEM into the hydrogel solution and cells, ensuring at all times the nutrients necessary for cell viability; or it could be possible to investigate a different substrate to be used without the Agarose but which contains in any case the right amount of calcium needed to crosslink the hydrogel based on Alginate.

## 8 Figure Index

<b>Figure 1: Tissue Engineering Concept:</b> The classic TE approach (1) harvests cells from the patient and (2) expand them in-vitro. Upon sufficient expansion (3) cells are seeded on a scaffold contingently with growth factors. (4) The construct is then matured in-vitro before (5) being implanted in the patient. [3].....	9
<b>Figure 2:</b> Schematic of various components of ECM. [6].....	13
<b>Figure 3:</b> Collagen chain [3] .....	14
<b>Figure 4:</b> Proteoglycans [3] .....	16
<b>Figure 5:</b> Alginate models [9] .....	19
<b>Figure 6:</b> Alginate components [13].....	21
<b>Figure 7:</b> Polyethylene glycol [3].....	22
<b>Figure 8:</b> Process scheme of engineered tissue using layer by layer method [15] .....	24
<b>Figure 9:</b> (A) Resistive heater and (B) Piezoelectric actuator [29].....	28
<b>Figure 10:</b> Solenoid Valve Based BioPrinting Single Nozzle [29].....	29
<b>Figure 11:</b> Illustration of a viscosity measurement showing a cross section of a thin layer of fluid subjected to a shear stress between two plates that are in relative linear motion [29].....	32
<b>Figure 12:</b> Non-Newtonian Liquids [29] .....	33
<b>Figure 13:</b> Geometry used to define (a) shear flow and (b) extensional flow [29].....	34
<b>Figure 14:</b> Graph of different non-Newtonian fluid categories and illustration of intermolecular forces related to surface tension [29] .....	36
<b>Figure 15:</b> Schematic diagram showing the operating regime for stable operation of drop-on-demand inkjet printing, in terms of the Ohnesorge and Reynolds numbers [29] .....	40
<b>Figure 16:</b> Inkjet printing methods: (a) continuous inkjet and (b) drop-on-demand inkjet [29] .....	41
<b>Figure 17:</b> Piezoelectric actuator [31] .....	43
<b>Figure 18:</b> Thermal Ink Jet [31] .....	44
<b>Figure 19:</b> Different types of polymers [29].....	46
<b>Figure 20:</b> Different polymer architectures [29] .....	47
<b>Figure 21:</b> Illustration of (a) a number-fraction distribution and (b) the equivalent weight fraction distribution [29].....	48

<b>Figure 22:</b> Representative molecular weight distribution showing the most probable distribution with the different molecular weight averages shown [29] .....	48
<b>Figure 23:</b> Schematic of DLVO interactions experienced by two approaching colloidal particles [29] .....	52
<b>Figure 24:</b> Schematic of electrical double layer of a charged particle [29].....	54
<b>Figure 25:</b> Petri Dish and 40ml Flask. Image taken from the laboratory [36].....	57
<b>Figure 26:</b> Biological Safety Cabinet: Class I, Class II and Class III [37].....	58
<b>Figure 27:</b> Biological Safety Cabinet Class II [36].....	59
<b>Figure 28:</b> Schematic of Horizontal Biological Safety Cabinet [38] .....	59
<b>Figure 29:</b> Incubator [36].....	60
<b>Figure 30:</b> Centrifuge [36].....	61
<b>Figure 31:</b> Centrifugation Test with Fibroblast 3T3 Cells [36].....	62
<b>Figure 32:</b> Lung Epithelial Cells A549 separated from the DMEM 10%FBS .....	62
<b>Figure 33:</b> Confocal Microscope [36] .....	63
<b>Figure 34:</b> Schematic of essential structure of a confocal microscope [40].....	64
<b>Figure 35:</b> Fibroblast 3T3 and Lung Epithelial cells A549 [36].....	65
<b>Figure 36:</b> Fungi and Bacteria (40x) [36].....	67
<b>Figure 37:</b> Trypan Blue Solution [36] .....	68
<b>Figure 38:</b> Haemocytometer [36].....	69
<b>Figure 39:</b> Burke Chamber [42].....	69
<b>Figure 40:</b> Trypan Blue [44] .....	70
<b>Figure 41:</b> Back View of the Printing Process [36] .....	72
<b>Figure 42:</b> Biowatcher scheme components [36].....	74
<b>Figure 43:</b> Biowatcher: front and side views [36].....	75
<b>Figure 44:</b> Calcium EDTA complex [56].....	79
<b>Figure 45:</b> Creation of the Calcium Chloride Solution [36].....	80
<b>Figure 46:</b> 2% Alginate HV [36].....	80
<b>Figure 47:</b> 2% Alginate HV with Calcium Chloride Solution [36] .....	81
<b>Figure 48:</b> Trisodium Citrate and EDTA measured and put in demineralized water [36] .....	81
<b>Figure 49:</b> 2% Alginate HV already crosslinked and without demineralized water [36] .....	82
<b>Figure 50:</b> 15ml of Solvent added to the crosslinked hydrogel [36].....	82
<b>Figure 51:</b> 2ml of hydrogel and 2ml of Calcium Chloride Solution [36].....	83
<b>Figure 52:</b> Addition of the Solvent to the mixture [36].....	83

<b>Figure 53:</b> First and second solutions checked after 15 and 10 minutes respectively [36].....	84
<b>Figure 54:</b> 1ml of hydrogel and Calcium Chloride Solution, without water [36].....	84
<b>Figure 55:</b> Addition of 20ml of Solvent [36].....	85
<b>Figure 56:</b> Dissolution of the hydrogel [36] .....	85
<b>Figure 57:</b> 5ml, 2ml and 1 ml of hydrogel respectively after 30 minutes [36].....	86
<b>Figure 58:</b> 5ml, 2ml and 1 ml of hydrogel respectively after 45 minutes [36].....	86
<b>Figure 59:</b> 1ml of Alginate and 1ml of Alginate with Calcium Chloride Solution [36] .....	87
<b>Figure 60:</b> Addition of the solvent [36].....	88
<b>Figure 61:</b> Capillarity test after 30 and 60 minutes and then after 17 hours [36] .....	88
<b>Figure 62:</b> Final check [36].....	89
<b>Figure 63:</b> Creation of Recirculation System [36] .....	90
<b>Figure 64:</b> Recirculation System Scheme [36] .....	91
<b>Figure 65:</b> Recirculation Printhead System Scheme [36].....	92
<b>Figure 66:</b> Pressure Regulation Circuit Scheme [36].....	94
<b>Figure 67:</b> Pressure Regulation Circuit [36].....	95
<b>Figure 68:</b> Fluidic Circuit [36].....	96
<b>Figure 69:</b> Fluidic System on the printer; manometer and pressure valve to activate the vacuum in the off position [36].....	96
<b>Figure 70:</b> Waveform Characteristics [36] .....	99
<b>Figure 71:</b> Example of hydrogel drops DropWatching after their expulsion from the printhead, in this case N27+PBS/EDTA is used [36].....	100
<b>Figure 72:</b> Elaboration after Dropwatching of only hydrogel (N27 + PBS/EDTA) [36].....	101
<b>Figure 73:</b> Expample of DropWatching not completely performed [36].....	101
<b>Figure 74:</b> Result of the nozzle check: nozzle working and volume printed per nozzle [36] .	102
<b>Figure 75:</b> Rat2 Cells [36] .....	104
<b>Figure 76:</b> First viability test for Rat2 [36].....	106
<b>Figure 77:</b> Second viability test for Rat2 [36] .....	108
<b>Figure 78:</b> Third viability test for Rat2 [36] .....	109
<b>Figure 79:</b> Fluorescent Microscope Images: 2% Alginate x20 and 3/4 N27+1/4 PBS/EDTA x4 [60] .....	111
<b>Figure 80:</b> Example of ImageJ Analysis [36] .....	112
<b>Figure 81:</b> Analyse Particles ImageJ Parameters [36] .....	112
<b>Figure 82:</b> Viability test with Fluorescent Microscope for Fibroblast 3T3 [36] .....	113

<b>Figure 83:</b> Viability test with Confocal Microscope for Fibroblast 3T3 in different hydrogels [36] .....	115
<b>Figure 84:</b> Pipet Tests of Fibroblast 3T3 Cells [36] .....	116
<b>Figure 85:</b> Fibroblast 3T3 Cells in coloured hydrogel and with Trypan Blue under Confocal Microscope [36] .....	116
<b>Figure 86:</b> Viability test with Confocal Microscope for Fibroblast 3T3 in 3/4 N27 and 1/4 PBS/EDTA [36] .....	117
<b>Figure 87:</b> Lung Epithelial Cells A549 Printing Simulation with Pipet [36] .....	118
<b>Figure 88:</b> Viability test with Confocal Microscope for Lung Epithelial Cells A549 [36] .....	118
<b>Figure 89:</b> Schematic of forces acting on a dispersed particle [29] .....	119
<b>Figure 90:</b> Graph of the Lennard-Jones interaction potential [29] .....	122
<b>Figure 91:</b> Graph of the DLVO interaction potential [29] .....	123
<b>Figure 92:</b> Picture of PMMA elaborated with Sedimentation Algorithm [36] .....	129
<b>Figure 93:</b> DMEM Picture [36] .....	130
<b>Figure 94:</b> 3/4 N27 + 1/4 PBS/EDTA Picture [36] .....	130
<b>Figure 95:</b> Elaboration Image of Rat2 in DMEM 10%FBS [36] .....	132
<b>Figure 96:</b> Sedimentation tests of Rat2 Cells in DMEM 10%FBS and in Hydrogel [36] .....	132
<b>Figure 97:</b> Elaboration Image of Fibroblast 3T3 in 3/4 N27 and 1/4 PBS/EDTA [36] .....	134
<b>Figure 98:</b> Sedimentation tests of Fibroblast 3T3 Cells in DMEM 10%CS and in Hydrogels [36] .....	134
<b>Figure 99:</b> Elaboration Image of Lung Epithelial Cells A549 in DMEM 10%FBS [36] .....	135
<b>Figure 100:</b> Sedimentation tests of Lung Epithelial Cells A549 in DMEM 10%FBS [36] ....	136
<b>Figure 101:</b> Fibroblast 3T3 after printing in DMEM 10%CS on Petri Dish [36] .....	139
<b>Figure 102:</b> Fibroblast 3T3 after printing in DMEM 10%CS on Alginate 5% [36] .....	140
<b>Figure 103:</b> Fibroblast 3T3 after printing in DMEM 10%CS, after 4 hours and after 24 hours on Petri Dish [36] .....	140
<b>Figure 104:</b> Fibroblast 3T3 Cells Printed in DMEM 10%CS on Petri Dish and on Alginate 5% [36] .....	141
<b>Figure 105:</b> Fibroblast 3T3 after printing in Hydrogel on Agarose [36] .....	144
<b>Figure 106:</b> Fibroblast 3T3 after printing in Hydrogel, after 4 hours and in Trypan Blue [36] .....	144
<b>Figure 107:</b> Fibroblast 3T3 Cells Printed in 3/4 N27 and 1/4 PBS/EDTA Agarose and CaCl <sub>2</sub> [36] .....	145

<b>Figure 108:</b> Fibroblast 3T3 Cells Printed in 3/4 N27 and 1/4 PBS/EDTA Agarose and CaCl <sub>2</sub> : after printing and after 4 hours (picture on the right) [36] .....	146
<b>Figure 109:</b> Fibroblast 3T3 Cells Printed in 3/4 N27 and 1/4 PBS/EDTA Agarose and CaCl <sub>2</sub> under Fluorescent Microscope [60] .....	147
<b>Figure 110:</b> Viability test with Fluorescent Microscope of Fibroblast 3T3 Cells Printed in 3/4 N27 and 1/4 PBS/EDTA Agarose and CaCl <sub>2</sub> [36].....	148
<b>Figure 111:</b> Lung Epithelial Cells A549 after printing in DMEM 10%FBS, after 4 hours and in Trypan Blue on Petri Dish [36].....	150
<b>Figure 112:</b> Lung Epithelial Cells A549 Printed in DMEM 10%FBS on Petri Dish [36] .....	151
<b>Figure 113:</b> Lung Epithelial Cells A549 after printing in DMEM 10%FBS on Agarose and Alginate 5% [36].....	152
<b>Figure 114:</b> Lung Epithelial Cells A549 after printing in DMEM 10%FBS on Alginate 5% after 24 hours [36].....	152
<b>Figure 115:</b> Lung Epithelial Cells A549 after printing in DMEM 10%FBS on Agarose, Alginate 5% and Trypan Blue of Lung on Alginate 5% [36].....	153
<b>Figure 116:</b> Lung Epithelial Cells A549 Printed in DMEM 10%FBS on Agarose and Alginate 5% [36] .....	153
<b>Figure 117:</b> Reaction of transformation of Lactate into Pyruvate [63] .....	154
<b>Figure 118:</b> Reaction of transformation of Resazurine into Resorufin [63].....	155
<b>Figure 119:</b> Lung Epithelial Cells A549 Printed in DMEM 10%FBS on Petri Dish, Agarose and Alginate 5% [36].....	156
<b>Figure 120:</b> Viability Tests of Lung Epithelial Cells A549 Printed in DMEM 10%FBS on Petri Dish, Agarose and Alginate 5% [36] .....	157
<b>Figure 121:</b> Samples Preparation for LDH Tests [64] .....	158

## 9 Bibliography

1. Mano JF, Silva GA, Azevedo HS, Malafaya PB, Sousa RA, Silva SS, et al. Natural origin biodegradable systems in tissue engineering and regenerative medicine: present status and some moving trends. *J R Soc Interface*. 2007;4:999–1030.
2. Research: Bioactive Scaffolds and Tissue Engineering | The Stevens Group [Internet]. [cited 2017 Oct 18]. Available from: <http://www.stevensgroup.org/index.php/research/bioactive>
3. Course of “Engineering for Regenerative Medicine”, Valeria Chiono, Master’s Degree Course in Biomedical Engineering 2016/17, Torino.
4. Boccaccini AR, Blaker JJ. Bioactive composite materials for tissue engineering scaffolds. *Expert Rev Med Devices*. 2005;2:303–17.
5. O’Brien FJ. Biomaterials & scaffolds for tissue engineering. *Mater Today*. 2011;14:88–95.
6. 3D Cell Culture 101: An Introduction to 3D Cell Culture Tools and Techniques | Sigma-Aldrich [Internet]. [cited 2017 Oct 23]. Available from: <http://www.sigmaaldrich.com/technical-documents/articles/biology/3d-biomatrix-white-paper-3d-cell-culture-101.html>
7. Hodde J. EXTRACELLULAR MATRIX AS A BIOACTIVE MATERIAL FOR SOFT TISSUE RECONSTRUCTION. *ANZ J Surg*. 2006;76:1096–100.
8. fibrillina nell’Enciclopedia Treccani [Internet]. [cited 2017 Oct 26]. Available from: <http://www.treccani.it/enciclopedia/fibrillina>
9. Course of “Bionanotechnologies”, Gianuca Ciardelli, Master’s Degree Course in Biomedical Engineering 2015/16, Torino.
10. Kleinman HK, Martin GR. Matrigel: Basement membrane matrix with biological activity. *Semin Cancer Biol*. 2005;15:378–86.
11. Kibbey MC. Maintenance of the EHS sarcoma and Matrigel preparation. *J Tissue Cult Methods*. 1994;16:227–30.
12. Caliri SR, Burdick JA. A practical guide to hydrogels for cell culture. *Nat Methods*. 2016;13:405–14.
13. Chemical Structure « Alginate « KIMICA corporation | manufacturer and world-wide supplier of “Alginate / Alginic acid” Alginic Acid, Propylene Glycol Alginate, Calcium Alginate [Internet]. [cited 2018 Jan 23]. Available from: [http://www.kimica-alginate.com/alginate/chemical\\_structure.html](http://www.kimica-alginate.com/alginate/chemical_structure.html)



14. Bioprinting is coming of age: report from the International Conference on Bioprinting and Biofabrication in Bordeaux (3B'09) - IOPscience [Internet]. [cited 2018 Jan 22]. Available from: <http://iopscience.iop.org/article/10.1088/1758-5082/2/1/010201/meta>
15. Christopher Barnatt. 3D Printing Third Edition.
16. Atala A. Anthony Atala | Speaker | TED [Internet]. [cited 2018 Jan 22]. Available from: [https://www.ted.com/speakers/anthony\\_atala](https://www.ted.com/speakers/anthony_atala)
17. Nakamura M, Nishlyama Y, Henmi C, Yamaguchi K, Mochizuki S, Koki T, et al. InkJet bioprinting as an effective tool for tissue fabrication. Digit Fabr 2006 - Final Program Proc. 2006;2006:89–92.
18. Mironov V, Boland T, Trusk T, Forgacs G, Markwald RR. Organ printing: computer-aided jet-based 3D tissue engineering. Trends Biotechnol. 2003;21:157–61.
19. Wake Forest Institute for Regenerative Medicine (WFIRM) - Wake Forest School of Medicine [Internet]. [cited 2018 Jan 22]. Available from: <http://www.wakehealth.edu/WFIRM/>
20. Researchers print 3D human cells. BBC News [Internet]. 2015 Oct 21 [cited 2018 Jan 22]; Available from: <http://www.bbc.com/news/uk-scotland-edinburgh-east-fife-34586972>
21. Dr. Ozbolat [Internet]. [cited 2018 Jan 22]. Available from: <http://www.personal.psu.edu/ito1/>
22. Regenovo Biotechnology Co., Ltd. [Internet]. [cited 2018 Jan 22]. Available from: <http://regenovo.com/english/>
23. regenHU – Bioprinting solutions | 3D Bioprinters and Biomaterials [Internet]. [cited 2018 Jan 22]. Available from: <https://www.regenhu.com/>
24. 3D Printers | Desktop, Professional and Industrial | EnvisionTEC [Internet]. [cited 2018 Jan 22]. Available from: <https://envisiontec.com/>
25. Organovo - Bioprinting functional human tissue [Internet]. Organovo. [cited 2018 Jan 22]. Available from: <http://organovo.com/>
26. Zavyalova V, RBTH. Russian scientists successfully implant the first 3D-printed thyroid gland [Internet]. 2015 [cited 2018 Jan 22]. Available from: [https://www.rbth.com/science\\_and\\_tech/2015/11/02/rusian-scientists-succesfully-implant-the-first-3d-printed-thyroid-gland\\_536205](https://www.rbth.com/science_and_tech/2015/11/02/rusian-scientists-succesfully-implant-the-first-3d-printed-thyroid-gland_536205)
27. Aspect Biosystems Partners with InSCREENeX and Fraunhofer ITEM [Internet]. [cited 2018 Jan 22]. Available from: <https://www.aspectbiosystems.com/news/partners-inscreenex-fraunhofer-item>
28. 3D Bioprinting: Technologies, Products and Key Application Areas, (2nd Edition), 2018-

- 2035 [Internet]. [cited 2018 Jan 22]. Available from:  
[https://www.rootsanalysis.com/reports/view\\_document/3d-bioprinting-technologies-products-and-key-application-areas-2nd-edition-2018-2035/182.html](https://www.rootsanalysis.com/reports/view_document/3d-bioprinting-technologies-products-and-key-application-areas-2nd-edition-2018-2035/182.html)
29. Hoath SD, editor. Fundamentals of inkjet printing: the science of inkjet and droplets. Weinheim: Wiley-VCH Verlag GmbH & Co. KGaA; 2016.
30. Cui X, Boland T, D’Lima DD, Lotz MK. Thermal Inkjet Printing in Tissue Engineering and Regenerative Medicine. Recent Pat Drug Deliv Formul. 2012;6:149–55.
31. The Inkjet Training, iPrint Institute for printing, 27 November - 1 December 2017.
32. Coll K. 1885 - Roux maintains embryonic chick cells in saline solution [Internet]. FRAME. [cited 2018 Jan 22]. Available from: <http://www.frame.org.uk/1885-roux-maintains-embryonic-chick-cells-in-saline-solution/>
33. EBSS-sol-J-of-National-Cancer-Institute-1943-Vol4-Iss2-pp165-212.pdf [Internet]. [cited 2018 Jan 22]. Available from: <http://www.cuneyttas.com/EBSS-sol-J-of-National-Cancer-Institute-1943-Vol4-Iss2-pp165-212.pdf>
34. Scherer WF, Syverton JT, Gey GO. STUDIES ON THE PROPAGATION IN VITRO OF POLIOMYELITIS VIRUSES. J Exp Med. 1953;97:695–710.
35. Primary Cells vs. Cell Lines [Internet]. [cited 2018 Jan 23]. Available from:  
<https://www.lonza.com/products-services/bio-research/primary-cells/primary-cells-vs-cell-lines.aspx>
36. Image taken from the Bioprinting lab in the iPrint Institute for Printing.
37. Design and Equipment for the Cell Culture Laboratory [Internet]. Sigma-Aldrich. [cited 2018 Jan 23]. Available from: <https://www.sigmaaldrich.com/technical-documents/protocols/biology/design-and-equipment.html>
38. EdgeGARD® HF | The Baker Company [Internet]. [cited 2018 Jan 23]. Available from:  
<https://www.bakerco.com/products/edgegard-hf>
39. Confocal microscopy [Internet]. Wikipedia. 2018 [cited 2018 Jan 23]. Available from:  
[https://en.wikipedia.org/w/index.php?title=Confocal\\_microscopy&oldid=821028042](https://en.wikipedia.org/w/index.php?title=Confocal_microscopy&oldid=821028042)
40. Confocal microscopy - WikiLectures [Internet]. [cited 2018 Jan 23]. Available from:  
[https://www.wikilectures.eu/w/Confocal\\_microscopy](https://www.wikilectures.eu/w/Confocal_microscopy)
41. Introduction to Cell Culture [Internet]. [cited 2018 Jan 23]. Available from:  
<https://www.thermofisher.com/uk/en/home/references/gibco-cell-culture-basics/introduction-to-cell-culture.html>
42. MicrobeHunter Microscopy Magazine » Blog Archive » The hemocytometer (counting

- chamber) [Internet]. [cited 2018 Jan 23]. Available from: <http://www.microbehunter.com/the-hemocytometer-counting-chamber/>
43. W S. Trypan blue exclusion test of cell viability. - PubMed - NCBI [Internet]. [cited 2017 Dec 3]. Available from: <https://www.ncbi.nlm.nih.gov/pubmed/18432654>
  44. Lu B, Tarn M, Pamme N, Georgiou T. On-chip droplet polymerisation – Amphiphilic microgels from hydrophobic droplets. 2014.
  45. LIVE/DEAD® Viability/Cytotoxicity Kit \*for mammalian cells\*. 2005.
  46. Horváth L, Umehara Y, Jud C, Blank F, Petri-Fink A, Rothen-Rutishauser B. Engineering an in vitro air-blood barrier by 3D bioprinting. *Sci Rep*. 2015;5:7974.
  47. PDS00059.pdf [Internet]. [cited 2018 Jan 23]. Available from: <http://www.fujifilmusa.com/shared/bin/PDS00059.pdf>
  48. [cited 2018 Feb 3]. Available from: <http://www.unifr.ch/cardiology/en/team>
  49. NIH 3T3 Cell Line murine 93061524 [Internet]. Sigma-Aldrich. [cited 2018 Jan 15]. Available from: <https://www.sigmaaldrich.com/catalog/product/sigma/93061524>
  50. A549 Cell Line human 86012804 [Internet]. Sigma-Aldrich. [cited 2018 Jan 15]. Available from: <https://www.sigmaaldrich.com/catalog/product/sigma/86012804>
  51. Dulbecco's Modified Eagle's Medium - high glucose D5796 [Internet]. Sigma-Aldrich. [cited 2018 Feb 3]. Available from: <https://www.sigmaaldrich.com/catalog/product/sigma/d5796>
  52. Bovine Calf Serum 12133C [Internet]. Sigma-Aldrich. [cited 2018 Feb 3]. Available from: <https://www.sigmaaldrich.com/catalog/product/sigma/12133c>
  53. Fetal Bovine Serum F2442 [Internet]. Sigma-Aldrich. [cited 2018 Feb 3]. Available from: <https://www.sigmaaldrich.com/catalog/product/sigma/f2442>
  54. Pubchem. Sodium citrate [Internet]. [cited 2018 Jan 23]. Available from: <https://pubchem.ncbi.nlm.nih.gov/compound/6224>
  55. Pubchem. Calcium citrate [Internet]. [cited 2018 Jan 23]. Available from: <https://pubchem.ncbi.nlm.nih.gov/compound/13136>
  56. Calcium edta complex supplier | CasNO.12264-18-5 [Internet]. [cited 2017 Oct 26]. Available from: <http://www.lookchem.com/Calcium-edta-complex/>
  57. Arduino Micro [Internet]. [cited 2018 Jan 10]. Available from: <https://store.arduino.cc/arduino-micro>
  58. webmaster. The Inkjet Training course [Internet]. [cited 2018 Jan 11]. Available from: <http://www.theijc.com/about-event/the-inkjet-training-course>

59. Hu Y, Chen T, Dong X, Mei Z. Preparation and characterization of composite hydrogel beads based on sodium alginate. *Polym Bull.* 2015;72:2857–69.
60. Image taken from Université de Fribourg - Cardiologie.
61. GE Healthcare&trade;&nbsp;Ficoll PM400 - GE Healthcare&trade;&nbsp;Ficoll PM400 Dichtegradientenmedien [Internet]. [cited 2018 Jan 23]. Available from: <https://www.fishersci.ch/shop/products/ge-healthcare-ficoll-pm400-3/11580724>
62. Course of “Elaboration fo Medical Images”, Filippo Molinari, Master’s Degree Course in Biomedical Engineering 2016/17, Torino.
63. Cytotoxicity Detection Kit (LDH) 11644793001 [Internet]. Sigma-Aldrich. [cited 2018 Jan 23]. Available from: <https://www.sigmaaldrich.com/catalog/product/roche/11644793001>
64. Image taken from Adolphe Merkle Institute (A.M.I.) University of Fribourg.
65. Home | Adolphe Merkle Institute | Université de Fribourg [Internet]. [cited 2018 Feb 6]. Available from: <http://ami.swiss/en/>
66. Xu C, Chai W, Huang Y, Markwald RR. Scaffold-free inkjet printing of three-dimensional zigzag cellular tubes. *Biotechnol Bioeng.* 2012;109:3152–60.
67. Phosphate buffered saline 79383 [Internet]. Sigma-Aldrich. [cited 2018 Feb 6]. Available from: <https://www.sigmaaldrich.com/catalog/product/sigma/79383>
68. Trypsin-EDTA solution T6689 [Internet]. Sigma-Aldrich. [cited 2018 Feb 6]. Available from: <https://www.sigmaaldrich.com/catalog/product/sigma/t6689>
69. Trisodium citrate dihydrate meets USP testing specifications | Sigma-Aldrich [Internet]. [cited 2018 Feb 6]. Available from: <https://www.sigmaaldrich.com/catalog/product/sial/s1804?lang=en&region=GB>

## 10 Appendix

### 10.1 Pressure Regulation Arduino

```
#include <Wire.h>
// Constant for pressure sensor
#define OUT_MAX 29490
#define OUT_MIN 3277
#define P_MAX 200
#define P_MIN 0
// PWM output
#define PWM 5
// Average filter
#define NBRMES 20
// Constant for pressure calculating
const double S_VALUE = (OUT_MAX - OUT_MIN) / (P_MAX - P_MIN);
// Command variables
boolean start = false;
double mes[NBRMES] = {0};
double mesure = 0;
double lastmesure = 0;
int k = 0; // N measure
double setpoint = 0; // Pressure we want to achieve
double command = 0; // 0-255 signal sent to the pressure regulator
int tpurge = 0; // Purge time in ms
String cmd = String("");
boolean valve = false; // State of the valve
boolean purge = false; // State of purging
// Regulator variables
double kp = 1;
double ki = 0;
double minValue = 0;
double maxValue = 255;
double integrateValue = 0;
unsigned long beforeTime = 0;
unsigned long startedMillis = 0;
// Initialisation
void setup() {
  TCCR3B = TCCR3B & B11111000 | B00000001;
  startedMillis = millis();
  start = false;
  mesure = 0;
  setpoint = 0;
  command = 0;
  tpurge = 0;
  kp = 1;
  ki = 0;
  minValue = 0;
  maxValue = 255;
  integrateValue = 0;
  beforeTime = 0;
  pinMode(13, OUTPUT);
  valve = false;
  purge = false;
  analogWrite(PWM, minValue);
  //digitalWrite(PWM, 0); ///
  Wire.begin();
  Serial.begin(9600);
  Serial.flush();
}
//
// Main loop
void loop() {
  // Read serial command
  commandRead();
  // Read pressure
  mes[k] = pressureMesure(); // measure the pressure from the pressure sensor
  lastmesure = mes[k];
  k++;
  if (k >= NBRMES) {
    k = 0;
  }
}
```

```

double j = 0;
for (int i = 0; i < NBRMES; i++) {
    j += mes[i];
}
mesure = j / NBRMES;
// if regulation is running
if (start == true) {
    // Pump command
    regulator();
    analogWrite(PWM, command);
}
else {
    // Stop pump
    command = 0;
    integrateValue = 0;
    analogWrite(PWM, minValue);
}
// Turn on/off the valve
if (valve == true) {
    digitalWrite(13, HIGH);
}
if (valve == false){
    digitalWrite(13, LOW);
}
// Turn on the purge for a give time
if (purge == true){
    purgeON();
    // If there was a time set
    if (tpurge != 0 && millis()-startedMillis > tpurge){
        purgeOFF();
        purge = false;
        tpurge = 0;
    }
    // In case no time was given, it remains on
}
// Turn off the purge. Only useable when the purge was turned on without a given time
}
// Reading serial-data
void commandRead() {
    if (Serial.available() > 0) {
        char SerialByte;
        SerialByte = Serial.read();
        // if command is ended
        if (SerialByte == 10) {
            commandProcess();
        }
        // continue to read data
        else {
            cmd += String(SerialByte);
        }
    }
}
// Analyse the different commands
void commandProcess() {
    // Start regulation
    if (cmd.equals("Start")) {
        start = true;
        Serial.println(0);
    }
    // Stop regulation
    else if (cmd.equals("Stop")) {
        start = false;
        Serial.println(0);
    }
    // Give back the pressure mesure
    else if (cmd.equals("Mesure")) {
        Serial.println(mesure);
    }
    // Give back the last unprocessed pressure mesure
    else if (cmd.equals("Last")) {
        Serial.println(lastmesure);
    }
    // Give back the output signal to the pressure regulator (0 - 255)
    else if (cmd.equals("Command")) {
        Serial.println(command);
    }
    // Change the setpoint pressure
    else if (cmd.startsWith("Setpoint-")) {

```

```

String value = cmd.substring(9, cmd.length());
setpoint = value.toFloat();
Serial.println(setpoint);
}
// Change the Kp constant
else if (cmd.startsWith("KP-")) {
String value = cmd.substring(3, 9);
kp = value.toFloat();
Serial.println(kp);
}
// Change the Ki constant
else if (cmd.startsWith("KI-")) {
String value = cmd.substring(3, 9);
ki = value.toFloat();
Serial.println(ki);
}
// Change the min pump command value
else if (cmd.startsWith("MIN-")) {
String value = cmd.substring(4, 7);
int intValue = value.toInt();
// Check if the value is within the limits
if (intValue > maxValue) {
intValue = maxValue;
}
else if (intValue < 0) {
intValue = 0;
}
minValue = intValue;
Serial.println(minValue);
}
// Change the max pump command value
else if (cmd.startsWith("MAX-")) {
String value = cmd.substring(4, 7);
int intValue = value.toInt();
// Check if the value is within the limits
if (intValue > 255) {
intValue = 255;
}
else if (intValue < minValue) {
intValue = minValue;
}
maxValue = intValue;
Serial.println(maxValue);
}
// Turn ON the valve
else if (cmd.startsWith("valveON")) {
valve = true;
Serial.println("valve ON");
}
// Turn off the valve
else if (cmd.startsWith("valveOFF")) {
valve = false;
Serial.println("valve OFF");
}
// Do a purge with a given time in seconds (if no time, endless)
else if (cmd.startsWith("Purge-")) {
String value = cmd.substring(6, cmd.length());
unsigned long startedMillis = millis();
if (cmd.length() == 6){
String value = "0";
}
tpurge = value.toInt()*1000;
purge = true;
Serial.println("Purging");
}
else if (cmd.startsWith("PurgeOFF")) {
purgeOFF();
tpurge = 0;
purge = false;
Serial.println("Stopped purging");
}
// if unknown command
else {
Serial.println(-1);
}
// Reset command value
cmd = String("");
}

```



```

// Pressure aquisition and computation function
double pressureMeasure() {
  // Reading bytes from sensor
  Wire.requestFrom(byte(0x78), 2);
  byte msb = Wire.read();
  byte lsb = Wire.read();
  // Pressure calculating
  double Pcounts = (double)(((word)msb << 8) | lsb);
  return (Pcounts - OUT_MIN) / S_VALUE + P_MIN;
}
// Pressure regulation function
void regulator() {
  // calculating difference
  double difference = setpoint - mesure;
  // Delta time calculating
  unsigned long thisTime = micros();
  unsigned long deltaTime = thisTime - beforeTime;
  beforeTime = thisTime;
  // Integration
  integrateValue = integrateValue + ki * difference * (double)deltaTime * pow(10, -6);
  // Integrate value saturation
  if (integrateValue < minValue)
    integrateValue = minValue;
  else if (integrateValue > maxValue)
    integrateValue = maxValue;
  // Command calculating
  double result = kp * difference + integrateValue;
  // Command saturation
  if (result < minValue)
    result = minValue;
  else if (result > maxValue)
    result = maxValue;
  command = result;
}
//// Turn on/off the purge
void purgeON(){
  digitalWrite(13, HIGH);
  command = 255;
  integrateValue = 0;
  analogWrite(PWM, 0);
}
void purgeOFF(){
  digitalWrite(13, LOW);
}

```

## 10.2 Final Code with Pressure Regulation Matlab

```

%% Close the port if it needs
x=instrfind %;close the ports
fclose(x)
%% Initialize the platform
close all, clc;
fclose('all');
currentFolder = pwd; % Be sure to be where this file is located
addpath([currentFolder, '\Functions\noz']);
[paramMeasure,platform,FPGA,cameraPrgPath,dropwatchingPrgPath,imagesPath,printPath,imageName,cameraPrgName,dropwatchingPrgName,phDPI,
nbrNozzles]=Initialization_nozzle(currentFolder);

%% Homing all axis with the GCode command or with the jogging interface
f = figure;
settings.scale = 1.2;
motionGUI(f,10,10,settings) % Jogging interface (GUI)
str = marlinSend('G28 Z Y X'); % Homing all axis
nbrNozzlePerImage = 10; % Number of nozzles seen on one image
paramMeasure = loadjson('measureConfig.json');
% Focus linear interpolation, return the focus position for a given x-axis position
focus = @(x) paramMeasure.position.firstNozzleFocusX + (x-paramMeasure.position.firstNozzleY)*((paramMeasure.position.secondNozzleFocusX -
paramMeasure.position.firstNozzleFocusX)/(paramMeasure.position.secondNozzleY - paramMeasure.position.firstNozzleY));
% Height linear interpolation, return the printhead height position for a given x-axis position
height = @(x) paramMeasure.position.firstNozzleZ + (x-paramMeasure.position.firstNozzleY)*((paramMeasure.position.secondNozzleZ -
paramMeasure.position.firstNozzleZ)/(paramMeasure.position.secondNozzleY - paramMeasure.position.firstNozzleY));
%% Connecting FPGA
Connecting_FPGA(FPGA)
rmpath([currentFolder, '\Functions\noz']);

%% 6) Initiating the platform for measures. It is important to use the jogging interface to go to the first nozzles of the printhead (on the right of the
printhead) and write the coordinate in the "measureConfig.json" file (first...X, first...Z, first...Y). The nozzles should be centered in the picture.
% The user should go to the other end of the printhead (left end of the ph) and make sure that the height of the printhead stay the same and adjust the
% focus.
% The coordinate should be written in the same file as second...X, second...Y,... The program doesn't care about the alignment of the nozzles. There
% is just the height and the focus that are then used to interpolate the printhead position to maintain focus and constant height. The file should then be
% saved and read with the following command: (normally the file should not be changed for further experiences)

marlinmove(paramMeasure.position.firstNozzleY,platform.maxSpeed.Y/100,'Y');
marlinmove(paramMeasure.position.firstNozzleZ,platform.maxSpeed.Z/100,'Z');
marlinmove(paramMeasure.position.firstNozzleFocusX,platform.maxSpeed.X/50,'X');

%% Setpoint pressure for the regulation
% Switch the RED valve to open the VACUUM
value=23; %millibar vacuum pressure
PregSetSetting(value) %set the vacuum vpressure value to the system
PregSetKp(20) % Set the regulator parameters
PregSetKi(5)
PregStart()

%% Measure the value
PregGetMesure() %measure the pressure value, from the sensor pressure

%% Purge process: to give positive pressure to the system
% Regulate the positive pressure with the manometer
breakTime =2; %Time for the purge in seconds
% The solenoid valve opens for breaktime
fprintf(params.serial, 'Purge-');
ret=(fscanf(params.serial))
pause(breakTime)

fprintf(params.serial, 'PurgeOFF');
ret=(fscanf(params.serial))

%% Creation of the printed plane
im=ones(1024,nbrNozzles);
write4bitBitmap(im,[printPath,int2str(0),'_0.bmp']);
fullImgID = [printPath,int2str(0),'_0.bmp'];
nbrMeasures = ceil(nbrNozzles/nbrNozzlePerImage); % Number of measures along the printhead

% Empty cells for the path + names of the images
imgID=cell(nbrMeasures,2);

% Initialisation of the image
im=zeros(1024,nbrNozzles);

```

```

for i = 1:nbrMeasures
    % Index of the nozzles to be activated
    startNozzle=(i-1)*nbrNozzlePerImage+1;nozzleStep=1;nozzleEnd=i*nbrNozzlePerImage+1;

    % Prevent overflow at the end
    if nozzleEnd > nbrNozzles
        nozzleEnd = nbrNozzles;
    end

    imtmp = im;
    imtmp(:,startNozzle:nozzleStep:nozzleEnd)=1;
    imgID{i,1}=[printPath,int2str(i),'_b.bmp'];
    imgID{i,2}=[printPath,int2str(i),'_0_b.bmp'];
    write4bitBitmap(imtmp,imgID{i,2});
end

%% Spitting
spittingTime = 10;
spittingFrequ = 10000;
gisSend(['P,G,T,1000',int2str(spittingTime)],spittingFrequ)

%% Live preview
spittingTime = 1;
FPGAregisterWrite('c2',FPGA.ledDuration_ns); % Duration
id=gisPrintPlane(fullImgID) % Load spitting image
FPGAregisterWrite('20',1); % Encoder enable
pause(spittingTime); % End the spitting
FPGAregisterWrite('20',0); % Encoder disable
gisPrintAbort();
%% tmp
paramMeasure.position.firstNozzleZ= paramMeasure.position.firstNozzleZ-1

%% 7) Measuring loop. This loop capture all the images and therefore last a couple of minutes
% Temporary nrbmes
nbrMeasures = 26;
cam = Camera();
% Define the index of the test
if exist('ntest','var')
    ntest = ntest+1
else
    ntest=1
end

marlinmove(paramMeasure.position.firstNozzleY,platform.maxSpeed.Y/100,'Y');
marlinmove(paramMeasure.position.firstNozzleZ,platform.maxSpeed.Z/100,'Z');
marlinmove(paramMeasure.position.firstNozzleFocusX,platform.maxSpeed.X/50,'X');

% Set the LED duration
FPGAregisterWrite('c2',25); % Duration
FPGAregisterWrite('11',round(100e6/FPGA.frequency)); % Jetting frequency based on internal clock
% Set the folder where the images are to be saved
imageCurrentPath = [imagesPath, 'Images_', int2str(ntest), '\'];
mkdir(imagesPath, ['Images_', int2str(ntest)]);
nbrImagesPerMeasure = 2; % Two images at each position to later compute the speed
% Program's parameters
nbrImages = nbrImagesPerMeasure*nbrMeasures; % Number of images to be taken by the camera
nozzleSpacing = 25.4/phDPI;
measureSteps = nbrNozzlePerImage*nozzleSpacing;
mkdir(imageCurrentPath, 'Result'); % Create a "Result" directory with the new images
pos = zeros(nbrMeasures); % Save all the position where images were captured (mostly used for debug)

% Foreach position along the printhead
for i=1:nbrMeasures

    spittingTime = 1;
    spittingFrequ = 10000;

    gisSend(['P,G,T,1000',int2str(spittingTime)],spittingFrequ)%print
    pause(3.5);

    id=gisPrintPlane(imgID{i,1});
    waitForReadyToPrint(id);

    % Jetting
    h = waitbar(i/nbrMeasures); % Updating waiting bar to show progress
    % Capturing images and waiting until the end
    FPGAregisterWrite('c1',FPGA.ledDelay_us*100); % Delay first image
    FPGAregisterWrite('20',1); % Encoder enable

```

```

I = cam.capturePicture(); % Capture the picture inside a matrix
    pause(3.5);
finished = false;
%save the image in the folder
imwrite(I, horzcat(imageCurrentPath, 'Image_', num2str(i), 'a', '_ ', num2str(1), '.png'));
% Creating the output image which is the sum of the two originals ones
FPGAregisterWrite('c1', (FPGA.ledDelay_us+FPGA.ledDelayOffset_us)*100); % Delay second image

I2 = cam.capturePicture(); % capture the picture inside a matrix
imwrite(I2, horzcat(imageCurrentPath, 'Image_', num2str(i), 'b', '_ ', num2str(1), '.png'));
% Creating the output image which is the sum of the two originals ones
imgOut = zeros([size(I),3], 'uint8');
imgOut(:, :, 1) = I;
imgOut(:, :, 2) = I2;
imwrite(imgOut, horzcat(imageCurrentPath, 'Result', 'testFrame', num2str(i), '.bmp'));
% Creating the output image which is the sum of the two originals ones
% Disabling printing
FPGAregisterWrite('20',0); % Encoder disable
gisPrintAbort();
% Moving axis
yPos = paramMeasure.position.firstNozzleY+(i)*measureSteps;
pos(i) = yPos;
marlinmove(yPos, platform.maxSpeed.Y/140, 'Y'); % Moving to the next position
marlinmove(height(yPos), platform.maxSpeed.Z/200, 'Z'); % Correcting height

while(isempty(gisIsComplete(id)))
    pause(0.1);
end
pause(0.1);
end

close(h); % Close waiting bar
marlinmove(paramMeasure.position.firstNozzleY,platform.maxSpeed.Y/140,'Y');
marlinmove(paramMeasure.position.firstNozzleZ+2,platform.maxSpeed.Z/200,'Z');
marlinmove(paramMeasure.position.firstNozzleZ,platform.maxSpeed.Z/200,'Z');

% Image analyzing with the dropwatching program
system(horzcat(dropwatchingPrPath, dropwatchingPrName, '', imageCurrentPath, 'Result', '', imageCurrentPath, 'Result'));

% Reading images' results json file into the workspace
result = loadjson(horzcat(imageCurrentPath, 'Result', 'result.json'));

% Rearrange the file order of result according to the index of the cells
ResultsIntermediate = zeros(1,nbrImages/2);
resultsRearranged = cell (1, (nbrImages/2));

for n = 1:(nbrImages/2)
    ResultsIntermediate(1,n)=str2double(cell2mat(regexpi(result{1,n}.filename,'d*', 'Match')));
    resultsRearranged{1,ResultsIntermediate(n)} = result{1,n};
end

% Reading json result file. In this case a plot show the working nozzles
% nbrNozzles = 256; % Just for debug (doesn't need to redefine the variable)
% nbrNozzlePerImage = 10; % Just for debug (doesn't need to redefine the variable)
% nbrImages = 52; % Just for debug (doesn't need to redefine the variable)
% result = loadjson('result.json'); % Allready performed previously

% Creating drop pattern (some sort of comb filter)
startPosition = 145; % position in px of the first nozzle of an image
nozzleSpacing = 256; % Spacing between two nozzles in px
tolerance = 80; % tolerance in pixel of the nozzle position
% Creating the pattern
patern = zeros(1,nbrNozzlePerImage,'uint32');
for i=1:nbrNozzlePerImage
    patern(i) = startPosition + (i-1)*nozzleSpacing;
end
% Empty cells for the drop peroperties to be stored
dropProperties = cell(1,nbrNozzles);
% Analyzing the resultsRearrangeds
for i=1:(nbrImages/2)
    % Go through each detected drop
    for idx=1:resultsRearranged{1, i}.img.nbSilos
        pos = resultsRearranged{1, i}.img.silos{1, idx}.x; % Load the centre in x
        % compare the silo with all the position in the pattern
        for k=1:nbrNozzlePerImage
            % if the silo match a position in the pattern

```

```

        if (pos <= (patern(k)+tolerance)) & (pos >= (patern(k)-tolerance))
            index = (i-1)*nbrNozzlePerImage+k;
            if index < (nbrNozzles+1)
                dropProperties{1,index} = resultsRearranged{1,i}.img.silos{1,idx};
            end
        end
    end
end
end
end
% Create vectors with the properites
dropOnNozzle = zeros(1,nbrNozzles);
dropSpeed = zeros(1,nbrNozzles);
dropVolume = zeros(1,nbrNozzles);
for i=1:nbrNozzles
    if ~isempty(dropProperties{1,i})
        dropOnNozzle(i)=1;
        for j = 1:length(dropProperties{1,i}.red.elements)
            dropVolume(i) = dropVolume(i)+dropProperties{1,i}.red.elements{1,j}.volume_px3;
        end
    end
end
end
% Ploting the printhead working nozzles
figure(2)
subplot(3,1,1)
stem(dropOnNozzle,'filled');
title([int2str(sum(dropOnNozzle)), '/', int2str(nbrNozzles), ' nozzle working '])
subplot(3,1,2)
plot(dropSpeed)
title('Speed')
subplot(3,1,3)
plot(dropVolume)
title('Volume')
% Save the figure
saveas(gcf,[imageCurrentPath, 'Summary.png'])

%% 8) Printing plane
nLayers = 1;
nPrint=5;
% Start the printing process
for t=1:nPrint

    for i = 1:nLayers
        printSpeed = platform.maxSpeed.X/30;

        % Positions where the platforms starts / ends the printing movement
        startPosX = 150;
        endPosX = 50;
        printDir = sign(endPosX - startPosX);
        printPosX = 140; %Position where the printing starts
        printLengthX = 75; %Length of the printing
        % Time before starting and stopping the printing
        tPrintWait = abs(startPosX - printPosX) / printSpeed;
        tPrintOn = abs(printLengthX) / printSpeed;
        % Positions on the other axis for the printing
        printPosY = 120;
        printPosZ = 0;
        % Compute the printing frequency for the FPGA
        dropPerX = 400; % # drops per mm in the X direction (Y is given by the printhead)
        FPGAregisterWrite('11',round(100e6/(dropPerX*printSpeed)));%Jetting frequency based on internal clock

        % Go to starting position
        marlinmove(startPosX,printSpeed,'X');
        marlinmove(printPosY,printSpeed,'Y');
        marlinmove(printPosZ,printSpeed,'Z');
        % Start the movement
        id=gisPrintPlane(fullImgID) % Load full image
        marlinmove(endPosX,printSpeed,'X');
        a = 'down'
        % Pause until the position to start printing is reached
        pause(tPrintWait);
        FPGAregisterWrite('20',1); % Enable the encoder
        % Pause until the position to end the print is reached
        pause(tPrintOn);
        FPGAregisterWrite('20',0); % Disable the encoder
        %Go back to the starting position
        marlinmove(startPosX,printSpeed,'X');
        a = 'up'
        gisPrintAbort();
    end
end
end
end

```

```
rest(999)
end
pause(1)
end
```

```
%% 9) If needed, closing FPGA and RAMPS
%fclose(params.marlinComPort); % Closing RAMPS
fclose(params.marlin);
fclose(params.hsyncFPGA);
```

## 10.3 Sedimentation Test

```

%% Close the port if it needs
x=instrfind    %;close the ports
fclose(x)

%% Initialize the platform
close all, clc, clear all;
fclose('all');
currentFolder = pwd; % Be sure to be where this file is located
addpath([currentFolder, '\Functions\sed']);
[paramMeasure,platform,FPGA,cameraPrgPath,dropwatchingPrgPath,imagesPathSedimentation,printPath,imageName,cameraPrgName,dropwatchingPr
gName,phDPI,nbrNozzles,height]=Initialization_sedimentation(currentFolder);

%% Connecting FPGA
Sedimentation_FPGA(FPGA)
rmpath([currentFolder, '\Functions\sed']);

%% video preview
cam = Camera();
preview(cam.vid); % preview of the camera
%% If you want to capture the picture
im = cam.capturePicture(); % capture the picture inside a matrix
figure;
imshow(im)

%% Sedimentation rate measurement
%Definition of the picture number and the folder
Npictures=15; %Number of images in the folder
cam = Camera();
currentFolder = pwd;
addpath([currentFolder, '\Sedimentaion']);
currentLedDuration = 50; %nanoseconds
FPGAregisterWrite('c2',currentLedDuration); %Duration
FPGAregisterWrite('20',1); % Encoder enable
if exist('NFolder','var')
    NFolder = NFolder+1
else
    NFolder=1 %PAY ATTENTION to the folde number to not overwrite
end
imageCurrentPath = [imagesPathSedimentation, 'Images_', int2str(NFolder), '\'];
mkdir(imagesPathSedimentation, ['Images_', int2str(NFolder)]);
mkdir(imageCurrentPath, 'Result'); % Create a "Result" directory with the new images
% Set up path to the camera software
cameraPrgPath = [currentFolder, '\Camera\FramGrabber\FramGrabber\Debug\Framgrabber'];
%Take an image as sample
targetMean = 150; %mean value of the image to adjust the led duration: increase if the image is dark
%decrease if the image is bright
tolerance = 10; %tolerance of targetMean
lastImageGrayLvl = 128; % Mean value to start the led adjusting
addpath([horzcat('C:\temp\Sedimentation\Images_', int2str(NFolder))]);
%Initialize the results vector
results_d=zeros(Npictures,1);
%Calculate the time between the images acquisition and elaboration
t=zeros(Npictures,1);
valTime=zeros(Npictures+1,1);
tic;
im2=[]; %matrix to put all the images
B2=[];
for i=1:Npictures
    %Adjust the led duration
    if lastImageGrayLvl <= (targetMean - tolerance)
        currentLedDuration = currentLedDuration + 10;
        FPGAregisterWrite('c2',currentLedDuration); %Duration
    elseif lastImageGrayLvl > (targetMean + tolerance)
        currentLedDuration = currentLedDuration - 10;
        FPGAregisterWrite('c2',currentLedDuration); %Duration
    end

    %save the image in the folder
    I = cam.capturePicture(); % capture the picture inside a matrix
    imwrite(I, horzcat(imageCurrentPath, 'Image_', num2str(i), '.bmp'));
    % Creating the output image which is the sum of the two originals ones
    lastImageGrayLvl=mean(mean((flip(I,2))));

```



```

%Elaboration of image and counting of the particles
I = adapthisteq(I); %adjust the contrast
% Use [adaptthresh] to determine threshold to use in binarization operation.
%PAY ATTENTION: If the objects are dark and the background bright use 'dark'
%otherwise use 'bright'. This is the default.
T = adaptthresh(I, 0.4,'ForegroundPolarity','dark');
% Convert image to binary image, specifying the threshold value.
BW = imbinarize(I,T);
img=~BW;
B = bwboundaries(img);
num=length(B);
img2(:,i)= img;
B2=[B2; B];
%take an image every 30 seconds
t(i+1)=toc;
Time=30;
valTime(i)=(t(i+1)-(i-1)*Time);
if valTime(i)<=Time
    val=abs(Time-valTime(i));
    pause(val)
end
results_d(i)=num;
end
t=t(2:end);
D=figure('visible','off');
total_time=t(Npictures);
Time=(total_time-t(1))/(Npictures-1);
plot(t,results_d,'-o'),xlabel(['Time [s]']),ylabel(['Number of particles']),grid;
% Creating the output image which is the sum of the two originals ones
saveas(D, horzcat(imageCurrentPath, 'Result\','FinalResult', num2str(Npictures+1), '.bmp'));
filename = 'test.mat';
save(horzcat(imageCurrentPath, 'Result\','test.mat'));
FPGAregisterWrite('20',0); % Encoder disable

%% Elaboration of images to visualize the mask
imageCurrentPath = ['C:\temp\Sedimentation\Images_', int2str(NFolder), '.'];
load(horzcat(imageCurrentPath, 'Result\','test.mat'));
i=1; %Chose the image to analyze
elaborate_images(img2,i,Npictures,imageCurrentPath,B2 );
%% Remove the image folder from the path
rmpath([horzcat('C:\temp\Sedimentation\Images_', int2str(NFolder))]);

%% 12) If needed, closing FPGA and RAMPS
fclose(params.marlinComPort); % Closing RAMPS
fclose(params.marlin);
fclose(params.hsycFPGA);

```

## Function “elaborate images”:

```

function [ results_d ] = elaborate_images( img,i,Npictures,imageCurrentPath,B2 )

%INPUT: im1=matrix with all the images
%      Npictures=number of the pictures
% chose one image from the folder DMEM
I=img(:,i);
B=B2(:,i);
num=length(B);

f=figure('visible','off');
imshow(I);
text(10,10, strcat("\color{green} Objects Found:",num2str(length(B))));
hold on;

for k = 1:length(B)
    boundary = B {k};
    plot(boundary(:,2), boundary(:,1), 'g', 'LineWidth', 0.2)
end

saveas(f, horzcat(imageCurrentPath, 'Result\','FinalImage', num2str(Npictures), '.bmp'));
% Creating the output image which is the sum of the two originals ones
end

```

## 10.4 Sedimentation Test Tables

**TABLE 1:** Rat2,  $3 \cdot 10^6$  cells/ml: 1 ml of solution (DMEM\_10%FBS) and in Hydrogel 3/4 N27 and 1/4 PBS/EDTA,  $3 \cdot 10^6$  cells.

Number of Cells in DMEM	Number of Cells in Hydrogel	Time [s]
153734	285031	0
150845	284595	30
133778	269320	60
130767	268148	90
122971	256375	120
120830	254970	150
120137	246550	180
119754	246468	210
119728	237034	240
119141	236597	270
115955	231352	300
115846	227993	330
115106	221944	360
114871	218374	390
114749	211017	420
114672	206417	450
113861	195876	480
113794	193132	510
113529	187394	540
113007	183114	570

**TABLE 2:** FIBROBLAST 3T3,  $3 \cdot 10^6$  cell/ml in DMEM 10%CS and Hydrogels.

DMEM	N27	3/4 N27 and 1/4 PBS/EDTA	1% Alginate	2% Alginate	Time [s]
175767	192071	165900	155021	182358	0
170797	191598	142580	153803	166664	30
158893	188081	142300	143815	165618	60
155264	183941	141729	143537	161995	90
145306	179505	141701	142957	155784	120
144210	165046	141174	142673	151440	150
139679	151561	140845	142525	149029	180
137021	150149	140190	142187	144776	210
136806	149396	140050	141681	143600	240
136582	148954	139939	141622	143189	270
135867	148345	139863	141581	142441	300
133860	147857	139730	141481	141657	330
133007	146999	139384	141475	141645	360
132134	146395	139327	141393	141526	390
131833	134023	139293	141227	141471	420
130602	129928	139260	141132	141434	450
129651	129158	139198	140571	139686	480
129207	128639	139018	140422	139530	510
128552	128189	138894	136464	139460	540
128103	127988	138576	136416	139030	570
127654	127528	138341	136412	138514	600
127205	127357	137328	135300	137538	630
126756	127162	137097	134781	136825	660
126307	126364	131148	134256	136609	690
125858	126045	130483	133288	136222	720
125409	125805	130040	132469	135370	750
124960	125550	129636	132078	135200	780
124511	122815	128914	131667	134743	810
124062	121226	126937	131660	134528	840
123613	120712	125689	130067	131967	870

**TABLE 3:** LUNG EPITHELIAL CELLS A549,  $3 \cdot 10^6$  cell/ml: 0,4 ml of solution (DMEM\_10%FBS),  $1,2 \cdot 10^6$  cells in the tube.

Number of Cells	Time [s]
211720	0
202450	30
198278	60
194966	90
188704	120
187531	150
179923	180
176337	210
175510	240
172243	270
165493	300
163444	330
162968	360
159943	390
155154	420
152998	450
148874	480
147129	510
143792	540
143725	570
141616	600
141550	630
137736	660
135065	690
132686	720
131460	750
129201	780
129160	810
129021	840
128872	870

## 10.4 Materials used in This Master Thesis

The Material used in the iPrint Institute are:

- Deionized Water;
- PEG: Polyethylene glycol 8000, M=7300-9000g/mol, Roth 0263.2;
- Alginate HV: Alginic Acid Sodium Salt, 15-25cP at 1% in water, Sigma-Aldrich 180947;
- Alginate LV: Alginic Acid Sodium Salt from brown algae, 4-12CP at 1% in water, Sigma-Aldrich A0682;
- CaCl<sub>2</sub>: Calcium Chloride, Roth CN93.1;
- Agarose: Agarose standard, Roth 3810.2;
- PBS/EDTA: Roti-CELL PSB/EDTA, sterile, 0,046% EDTA, Roth 9152.1;
- Phosphate Buffered Saline (PBS) 1X [67];
- Trypsin/EDTA 0,25% T4049 Sigma-Aldrich [68];
- Rat2 [48];
- Fibroblast 3T3 [49];
- Lung Epithelial Cells A549 [50];
- DMEM [51] 10%CF [52];
- DMEM [51] 10%FBS [53];
- LIVE/DEAD assay: LIVE/DEAD viability/cytotoxicity kit for mammalian cells, Thermo Fischer L3224;
- Trypan Blue Dye Solution [43];
- Trisodium Citrate [69].

## 11 Acknowledgments

*I sincerely thank Professor Roseline Nussbaumer who has followed and supported me in every moment of my Master Thesis work and the members of the BioPrinting lab team for the availability and preparation that they have helped to provide me, Wenger Raphael, Mauron Muriel and Caldi Jonathan.*

*I thank Fritz Bircher, director of the iPrint Institute for Printing, for giving me the opportunity to work on my Final Project at his Institute.*

*I thank Professor Danilo Demarchi for his support in my thesis project.*

*I thank the team of Barbara Rothen and A.M.I. Institute for collaboration regarding the LDH test.*

*I would like to thank Marie-Noelle Giraud and her collaborators in the Department of Cardiology of the University of Fribourg for the collaboration and support given to me in tests done with the Fluorescent Microscope.*

*To my parents, Giacomo and Patrizia, who have always supported and encouraged me in my choices regarding my studies and my life.*

*To my grandparents Salvatore, Elena e Rosaria who, despite the distance in this period of study, have always loved me and they are touched for each of my goals achieved.*

*To my sister Tiziana, my friend of the university challenge*

*To my boyfriend Fabio, my happiness and my sun*

*To Flavia a special thank for the patience*

*To all the people who believe in me and to my friends...*

*Thanks to exist!!!*